

THE NUCLEAR ASPECTS  
Of The  
ACCIDENTAL CRITICALITY

At

Wood River Junction, Rhode Island

July 24, 1964

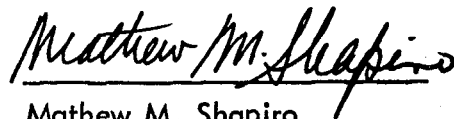
Work Performed By:

F. R. Nakache  
Mathew M. Shapiro  
H. Soodak  
C. Marotta  
R. Schamberger

Report Written By:

F. R. Nakache  
Mathew M. Shapiro

November 12, 1964



Mathew M. Shapiro  
Manager of Research



W. L. Allison  
Chairman of Investigation

This report supplements the United Nuclear Corporation report of August 21, 1964, "Nuclear Incident at United Nuclear Corporation, Wood River Junction, Rhode Island, July 24, 1964".

## TABLE OF CONTENTS

|   | <u>Page</u> |
|---|-------------|
| I. Summary  | 1           |
| II. Introduction  | 2           |
| III. Discussion of the Nuclear Aspects                                      | 6           |
| A. Reconstruction of the Incident   | 6           |
| B. Evidence of a Second Excursion   | 9           |
| C. Estimates of the Total Number of Fissions Which Occurred                 | 15          |
| D. Doses Received by the Superintendent and Supervisor                      | 20          |
| IV. Conclusions   | 41          |
| V. Appendix   | 42          |
| A. Experimental Data  | A-1         |
| A-1 Physical Measurements of the Accident Environment                       | A-1.1       |
| A-2 Radiation Readings in the Period Following the Incident                 | A-2.1       |
| A-3 Investigation of the Chemical Aspects Relating to the Incident          | A-3.1       |
| A-4 Sodium Activation Analysis for Supernatant Liquid Samples               | A-4.1       |
| A-5 Radiochemical Analysis of the Fission Products                          | A-5.1       |
| A-6 Determination of Uranium and Sodium Contents in Tank                    | A-6.1       |
| A-7 Activation Analysis of Metallic Samples                                 | A-7.1       |
| A-8 Hair Sulfur and Blood and Whole Body Sodium Activation Measurements     | A-8.1       |
| A-9 Spectrographic Analysis of Steel Samples                                | A-9.1       |
| A-10 Miscellaneous Measurements   | A-10.1      |
| B. Details of the Physics Calculations                                      | B-1         |
| B-1 Criticality Studies on the Rhode Island Incident                        | B-1.1       |
| B-2 Calculations of Neutron Leakage Spectra                                 | B-2.1       |
| B-3 Neutron Dose to Incident Neutron Flux Conversion Ratios                 | B-3.1       |
| B-4 Gamma Ray Dose and Gamma Ray-to-Neutron Dose Ratio Calculations         | B-4.1       |
| B-5 Conversion of Activation Measurements to Total Incident Current Density | B-5.1       |
| Section 1 General Relations   | B-5.1       |
| Section 2 Calculations of Various Factors                                   | B-5.8       |
| C. Bibliography   | C-1         |

## I SUMMARY

This report describes the results of various investigations made by United Nuclear Corporation into the nuclear physics aspects of the accidental criticality which occurred on July 24, 1964, at Wood River Junction, Rhode Island. This report is therefore a supplement to the earlier United Nuclear Corporation report dated August 21, 1964 which described the incident itself.

Total fissions which occurred are estimated to be  $1.3 \times 10^{17}$ . Evidence that a second excursion took place is described and the possible mechanisms are evaluated. Estimates of doses received by personnel are given and the methods of calculation are described. The postulated events leading to the criticality and the statement in the earlier report that the criticality occurred due to the accidental pouring of a concentrated solution of uranyl nitrate from safe to non-safe geometry are verified by the results of these subsequent investigations.

## II INTRODUCTION

### A. The Critical Incident

On July 24, 1964, at approximately 6:06 pm, an accidental nuclear excursion occurred at the Fuels Recovery Plant of the United Nuclear Corporation in Wood River Junction, Rhode Island. One employee was exposed to lethal radiation and died some 49 hours after the incident; five other personnel were exposed to radiation in excess of 1.25 rems. A description of the plant, the background to the incident and a qualitative description of what occurred are contained in a United Nuclear Corporation report dated August 21, 1964, entitled "Nuclear Incident at United Nuclear Corporation, Wood River Junction, Rhode Island, July 24, 1964".

### B. The Objective of the Nuclear Investigation

On July 27, 1964, the United Nuclear investigation task force was formalized. One important sector of the total investigation was the nuclear (or physics) aspects of the incident. The objectives of the nuclear aspects investigation included the following:

1. Reconstruction of the initial conditions surrounding the criticality and the nature of the system which went critical.
2. Determination of whether criticality continued after the initial excursion or if subsequent excursion occurred.
3. Estimate of the total number of fissions which occurred.
4. Estimates of the radiation doses received by exposed personnel.

This report contains the results of the nuclear physics investigation which continued through August, September and October 1964 following the incident. As such, this report is a supplement to the earlier United Nuclear Corporation report dated August 21, 1964.

### C. The Investigation

Prior to beginning the decontamination and cleanup, the investigating team made a very thorough survey of the entire plant to observe the conditions left by the incident. Many photographs were taken and samples were taken from all jars and bottles located in that portion of the plant where the incident occurred. Coins from the pockets of plant personnel, a watch and samples of metallic material from the room in which criticality occurred were collected for activation analysis. The decontamination effort was controlled so that no pertinent evidence was destroyed. No uranium bearing material was moved in the plant until its relevance to the incident had been established.

The conditions relating to the establishment of criticality were almost completely unknown. There were no records of the chemical composition and strengths of the solutions whose mixing led to the criticality. The data obtained subsequently were not all consistent. One objective of the physics investigation was to reconstruct a sequence of events which is consistent with most of the data. It will be useful to set forth here briefly the facts as they were known a few days after the incident occurred. The adequacy of any detailed reconstruction must be measured against its compatibility with these facts.

C. The Investigation - (Continued)

The Operator carried up to the third floor of the tower area an 11 liter polyethylene bottle which he believed to contain trichloroethane and which, in fact, contained a solution of enriched uranium. He started to pour the contents of the 11 liter bottle into a tank which is normally used for making up an aqueous sodium carbonate solution. The volume of carbonate solution and the strength of this solution in the tank at the time of the incident were unknown. The uranium in the 11 liter bottle was approximately 93% enriched. Neither its concentration nor its acidity were known. At the time of the pouring, the solution was being agitated by an electric stirrer. When the bottle was nearly empty, an excursion occurred. An unknown volume of solution was expelled from the tank and the nuclear alarm sounded.

The first radiation readings after the criticality alarm sounded were taken by the Supervisor at the emergency building. At Criticality plus 5 minutes, levels of 90-100 mr/hr were read; at Criticality plus 10 minutes, the level was 50-60 mr/hr. By Criticality plus 30 minutes, the level at the emergency building was 10-20 mr/hr and that level continued for the next two hours. The building is located approximately 450 feet from the vessel in which criticality occurred.

Approximately 1-3/4 hours later, the Plant Superintendent and the Supervisor entered the building in order to drain the solution remaining in the tank into a safe geometry. The Superintendent was wearing a regulation film badge, containing both a photographic film and an indium foil. The Supervisor had previously given his regular radiation badge to the health physicist and was now wearing a visitor's badge which contained only indium foil but no film. They proceeded together to the third floor of the tower. The Supervisor stayed at the door, about 15 feet from the stainless steel tank and the Superintendent entered the room. The polyethylene bottle was found mouth down, in the tank. The Superintendent removed the bottle and placed it on the floor, turned off the electric stirrer and immediately left the room. He and the Supervisor then went to the first floor and proceeded to drain the sodium carbonate solution from a 3" diameter glass column into jars which are 6.25" diameter and hold approximately 1 gallon. During the draining of this carbonate solution containing only a very small amount of uranium, the Superintendent unsuccessfully attempted to start the material draining down into the 3" diameter glass column. On the assumption that the uranium precipitate had settled into the drain-pipe at the bottom of the vessel and was thus preventing material from draining, the Superintendent went to the third floor and restarted the stirrer. He then assisted the Supervisor in filling the gallon jars on the first floor. The first few jars thus contained mainly sodium carbonate or a mixture of sodium carbonate and solution from the carbonate tank; the last jars filled contained only solution from the carbonate tank. In all, 12 gallon jars were filled.

During the draining operation, one gallon jar, 3/4 full (3 liters) was dropped and its contents spilled onto the floor. An additional 1-2 liters was spilled when the drain hose on the second floor slipped out of the funnel. This draining operation took approximately 20 minutes. The film badge worn by the Superintendent showed an exposure to 50 R of gamma rays. Silver coins which were in the pocket of the Superintendent and indium foils worn by both men indicated that they had been exposed to thermal neutrons.

### C. The Investigation - (Continued)

To achieve the aforementioned objectives of the physics investigation it was important to know the volumes of solutions involved and their concentrations. The strength of the uranium solution would provide information which would be helpful in determining the origin of the particular bottle which was used. The total volume in the system at the time criticality occurred affects both the fraction of neutrons which leaked from the system and the energy spectrum of the neutrons. The latter is needed to interpret the fast neutron activation data.

The yield (total number of fissions) is desired in order to determine the total energy release and to provide some insight into the quenching mechanism which terminated the excursion. In conjunction with a good model for a transient analysis, it can also aid in determining the initial excess reactivity.

The determination of the lethal dose which the victim received may shed some light on the biological effects of radiation. Accurate determinations of the dose may help in understanding the immediate cause of death. Correlation of the several methods of estimating whole body dose has already led to the refinement of one technique and may lead to others.

The determination of the dose received by the Superintendent and the Supervisor was the most difficult task. They were exposed to neutrons and gamma rays but only the gamma ray exposure of the Plant Superintendent was known. Both the neutron and the gamma ray doses of the Supervisor were unknown. In order to determine the total exposures of each man, it was necessary to establish the origin of these irradiations.

### D. Acknowledgments

Acknowledgments are due several organizations without whose contributions United Nuclear's job would have been far more difficult, if not impossible. We wish to acknowledge the assistance of:

Health and Safety Division of the U. S. Atomic Energy Commission at Idaho Falls for the analysis of fission products and certain of the activation analyses.

Health Physics Division of the Oak Ridge National Laboratory of the U. S. Atomic Energy Commission for analysis of fission products, other chemical analyses and for many helpful discussions.

Los Alamos Scientific Laboratory for the activation analyses of human hair and for the spot checking of United Nuclear's criticality calculations.

Personnel from the New York Operations Office of the Atomic Energy Commission.

Dr. John Stanbury of the Massachusetts General Hospital for providing blood sodium activation data on the deceased and for arranging for the collection of data at the Whole Body Counter at the Massachusetts Institute of Technology.

Nuclear Science and Engineering Corporation for fission product determinations and measurements of sodium activation.

D. Acknowledgements - (Continued)

The Rhode Island State Council of Defense for assistance during the emergency phase.

Special thanks are due Dr. Marvin M. Mann of the U. S. Atomic Energy Commission for his guidance and suggestions without which important sources of data might have been overlooked.

### III DISCUSSION OF THE NUCLEAR ASPECTS

#### A. Reconstruction of the Incident

On the basis of chemical data, analysis of activations, criticality and shielding calculations, a reasonable reconstruction of the incident has been prepared. Details of the arguments leading to this reconstruction will be found in later sections of this report.

The carbonate tank contained 41 liters of 0.54 molar sodium carbonate solution. The polyethylene bottle contained 11 liters of uranyl nitrate with a concentration of 256 grams per liter. While the Operator was pouring the uranium solution into the tank, an excursion of approximately  $1.0 \times 10^{17}$  fissions occurred. The radiolytic gas formed (probably enhanced by  $\text{CO}_2$  from a chemical reaction between the uranyl nitrate solution and the sodium carbonate solution) ejected 10 to 11 liters of solution from the tank and left 2 kgs. of uranium in the tank in 41 - 42 liters of liquid. Twenty to thirty seconds after the excursion, the solution reacted chemically in such a manner as to produce a large volume of  $\text{CO}_2$  gas bubbles with a subsequent rise in the liquid surface and formation of a precipitate containing the majority of uranium. After the gas left the system, the surface dropped leaving some uranium precipitate deposited on the wall of the tank. During the next hour and three-quarters, additional precipitate dropped into the drain line. During this period of time the tank was either subcritical or became so long before the re-entry of the Plant Superintendent and the Supervisor.

One and three-quarters hours after the incident the Plant Superintendent and the Supervisor entered the building and went to the third floor of the tower. The Supervisor stayed on the landing outside the door. The Plant Superintendent entered the room, removed the bottle from the tank and placed it on the floor. He turned off the electrical stirrer and immediately left. After he had passed the Supervisor and just as he started down the stairs, a second excursion resulted from the flattening of the top surface of the liquid in the tank. The reactivity associated with the surface distortion was 0.021 in k. This excursion was temporarily terminated by the formation of the bubbles of steam and radiolytic gas. The steam resulted from local boiling in the vicinity of the small precipitate particles which also served as nucleation sites for the radiolytic gas. The excursion was permanently terminated by settling of the precipitate to the bottom of the tank.

During this excursion, the Supervisor was subjected to the radiation resulting from  $2-3 \times 10^{16}$  fissions at a distance of 15 feet from the tank. The Plant Superintendent was at about the same distance but was shielded by a 12" hollow concrete block wall.

Both men returned to the first floor and attempted to drain the carbonate tank. Due to the precipitate clogging the  $1/2$ " drain pipe, only the material in the 3" diameter column could be drained. The Superintendent returned to the third floor and restarted the stirrer. This removed the block at the drain pipe. Because part of the uranium precipitate had entered the drain and more soon followed, and because the stirrer was operating, the tank did not go critical a third time. The Superintendent returned to the first floor and assisted the Supervisor in draining the remaining solution.



## A. Reconstruction of the Incident - (Continued)

### 1. Data on Uranium and Sodium Contents

Appendix A-6 presents the detailed data concerning the uranium and sodium contents of the 37 liters of material drained from the tank and of the spilled material. The conclusions from direct analyses are:

|                          |          |
|--------------------------|----------|
| Uranium in the 37 liters | 2000 gm. |
| Total uranium content    | 2820 gm. |
| Sodium in the 37 liters  | 715 gm.  |
| Total sodium content     | 1010 gm. |

Assuming that the container Y poured by the Operator contained 2820 gm. uranium in 11 liters gives a uranium concentration of 256 gm/liter which is not inconsistent with the information concerning the plugged evaporator which led to the production of highly concentrated material.

### 2. The Two Configurations in the Tank

The draining of the tank resulted in 37 liters of drained liquid and 4-5 liters of spilled liquid. One spill from a jar estimated to be three-fourths full was about 3 liters and the second spill of 1-2 liters occurred when the tygon tube slipped out of the second floor funnel. The 37 liters of drained liquid contained 2000 gms. of uranium or a concentration of 54 gms/liter. The first conclusion is that the final tank configuration, before draining, contained 41-42 liters with a uranium concentration of 54 gms/liter.

Using the 54 gms/liter concentration, it is found that 52 liters is the volume containing 2820 gms. Thus, the total volume was 52 liters. Subtracting from this total volume the 11 liter contents of the safe geometry container, there results the conclusion that the initial volume of the carbonate solution was 41 liters. This contained 1010 gms. of sodium carbonate or a molarity of 0.54. Into this was poured 11 liters of uranyl nitrate solution containing 2820 gms. of uranium at a concentration, then, of 256 gms/liter. Following the excursion, there remained 41-42 liters in the tank. Thus the spill from the first excursion contained 10-11 liters.

### 3. Mixing Experiments

Mixing experiments were performed in a glass tank of the same diameter (18") as the actual carbonate tank. Movies were taken of four mixing runs. In each, 10 liters of uranyl nitrate solution containing 230 gms. of uranium per liter were poured from the safe geometry container into the tank with the stirrer on. The tank contained successively,

1. 50 liters of 1 molar  $\text{Na}_2\text{CO}_3$
2. 50 liters of 1/2 molar  $\text{Na}_2\text{CO}_3$
3. 40 liters of 1/2 molar  $\text{Na}_2\text{CO}_3$
4. 33.7 liters of 1/2 molar  $\text{Na}_2\text{CO}_3$

A. Reconstruction of the Incident - (Continued)

3. Mixing Experiments - (Continued)

In all cases, a natural pouring took about 20 seconds with 10 and 30 seconds representing fast and slow pours. In all cases, it was clearly evident that the stirrer action produced an essentially homogeneous solution. The yellow color of the poured stream could be seen hitting the liquid in the tank and then spreading rapidly, within two seconds, to produce a uniform yellow color throughout the tank.

The effect of the stirrer on the shape of the liquid surface could be seen at volumes ranging from 33.7 liters to 60 liters. The distortion of the surface was clearly evident in all cases. The liquid was pulled down in the region above the stirrer blade and piled up in the diametrically opposite position in a non-stationary pattern which seemed to have a disturbing wave travelling around the circumference. At 44.7 liters, which was the volume some time after pour No. 4 (following the precipitate formation) and was also close to the volume of the final configuration in the accident, the surface was distorted with amplitudes of about 3 cms. Upon turning off the stirrer, there seemed to be an initial time lag following which the surface begins to flatten out; the total time to obtain a significantly flattened surface was several seconds.

In pours 1 and 2, the initially-clear carbonate solution was first somewhat clouded by air bubbles produced by the stirrer action. As the uranyl nitrate spread throughout, the solution became light yellow in color. After some seconds it became definitely darker, indicating the presence of gas evolution. At the end of the pour, the solution was again light yellow in color and fairly clear, showing no visible precipitate particles. Pour No. 3 followed the pattern of No. 1 and No. 2, becoming even darker until some 20 seconds after the pour, at which time the surface rose up and foamed for some 15 seconds before subsiding. The final solution again looked clear, but a sample drawn off showed a slowly-settling precipitate. In pour No. 4 even more violent foaming occurred, resulting in a 25% increase in volume. After the CO<sub>2</sub> had been expelled, a precipitate was seen sticking to the glass where the foaming took place, and the solution was thick with precipitate particles.

Bench scale experiments on the chemical aspects of the mixing are reported in Appendix A-3. The acidity considerations are consistent with the formation of precipitate in pours No. 3 and No. 4 and the non-formation in Pours No. 1 and No. 2. The foaming is the result of the evolution of large amounts of CO<sub>2</sub> in the reaction leading to the precipitate formation. As also reported in Appendix A-3, the precipitate particles formed during the foaming process are about one micron in size. When the solution is allowed to settle, there is agglomeration of particles into aggregates of about 20 microns in size.

## B. Evidence of a Second Excursion

The present evidence indicates that two (2) excursions took place. The fissions estimated are:

|                  |                              |
|------------------|------------------------------|
| First excursion  | $1.0 - 1.1 \times 10^{17}$   |
| Second excursion | $0.2 - 0.3 \times 10^{17}$   |
| Total fissions   | $1.3 \pm .25 \times 10^{17}$ |

### 1. The First Excursion

The first excursion took place while the Operator was pouring uranium solution into the tank. Owing to the absence of a neutron source, it is possible for the excursion to take place some time after criticality is achieved.

About  $10^{17}$  fissions occurred in the first excursion. The only feasible shut down mechanism is the formation of  $H_2$  and  $O_2$  bubbles (radiolytic gas) by the dissociation of water. Calculations based on experiments and analysis with KEWB (Appendix B-1) indicate such an energy release occurs with an excess reactivity of 1.7 dollars. This requires a critical mass of 2.0 kg. which was available. An inertial pressure of 30-50 psi was estimated. Pressures in excess of 10 psi have been observed to splash solutions out of the containers.

Chemical analyses indicate that 10-11 liters containing 500-600 gms. of U-235 were ejected. The remaining solution was found to be very nearly critical (Appendix B-1). Actually there is an uncertainty in the amount of uranium present in solution which reduces the estimate of reactivity. The force of the excursion and the violent frothing during the evolution of  $CO_2$  following the excursion tended to leave uranium above the liquid level on the tank wall. Precipitate was also likely to settle in the 1/2" diameter drain pipe below the tank (the drain valve was open). Uranium removed reduces the reactivity about 2¢/g.

It is likely that the system was left about one dollar below delayed critical. The shutting off of the stirrer increased the reactivity by about 2.5 dollars resulting in a second excursion. The KEWB experiments show that a step insertion of 1 dollar (100 milliseconds) would give about  $3 \times 10^{16}$  fissions. No ejection of solution would be expected. The precipitate particles serve as nucleation sites and the five (5) liters of radiolytic gas generated is more than enough to quench the reaction until the gas leaves the system. In addition, local boiling of the water near the precipitate particles can release large volumes of steam. Settling of the precipitate could account for the permanent shut down but no definitive calculations have been performed.

### 2. The Second Excursion

The most difficult part of this nuclear aspects investigation has been explaining how the Superintendent and Supervisor were exposed to neutrons. The primary evidence for an excursion, as opposed to operation at constant power, comes from the relative neutron exposures of the two (2) men.

## B. Evidence of a Second Excursion - (Continued)

### 2. The Second Excursion - (Continued)

At the time of his entry into the building, 1-3/4 hours after the initial burst, the Superintendent had in his pockets two dimes and a silver dollar which were examined for neutron induced activity. When positive indications of neutron exposure were found from these analyses, the indium foils on the badges which the two men wore into the building were located for further investigation. At the suggestion of Dr. Marvin Mann, samples of hair were sent to LASL for analysis. The USAEC arranged for the two men to be examined at the MIT Whole-Body Radiation Counter on July 30, 1964, before knowing of the coin activations.

The film badge of the Superintendent indicated a gamma dose of 50 R. The data concerning his neutron exposure are given in Table III-D-6 in Section III-D. The Supervisor did not wear a gamma film badge but only an indium badge; his gamma dose must, therefore, be estimated. The data concerning his exposure to neutrons is given in Table III-D-6 in Section III-D. The data in this table indicate the Supervisor was exposed to greater neutron fluxes than the Superintendent.

Three possible explanations for the source of neutrons were considered. These are:

- a. At the time of their entry the reactor was critical and operating at a low power in the neighborhood of 100 watts and they received their exposure while on the third floor of the tower.
- b. Either the reactor was critical at some low power or a second excursion occurred just prior to their draining the tank and they received their exposures from delayed neutrons while on the floor below.
- c. A second excursion took place while they were both on the third floor.

These three possibilities are discussed below.

### 3. Continued Criticality at Low Power

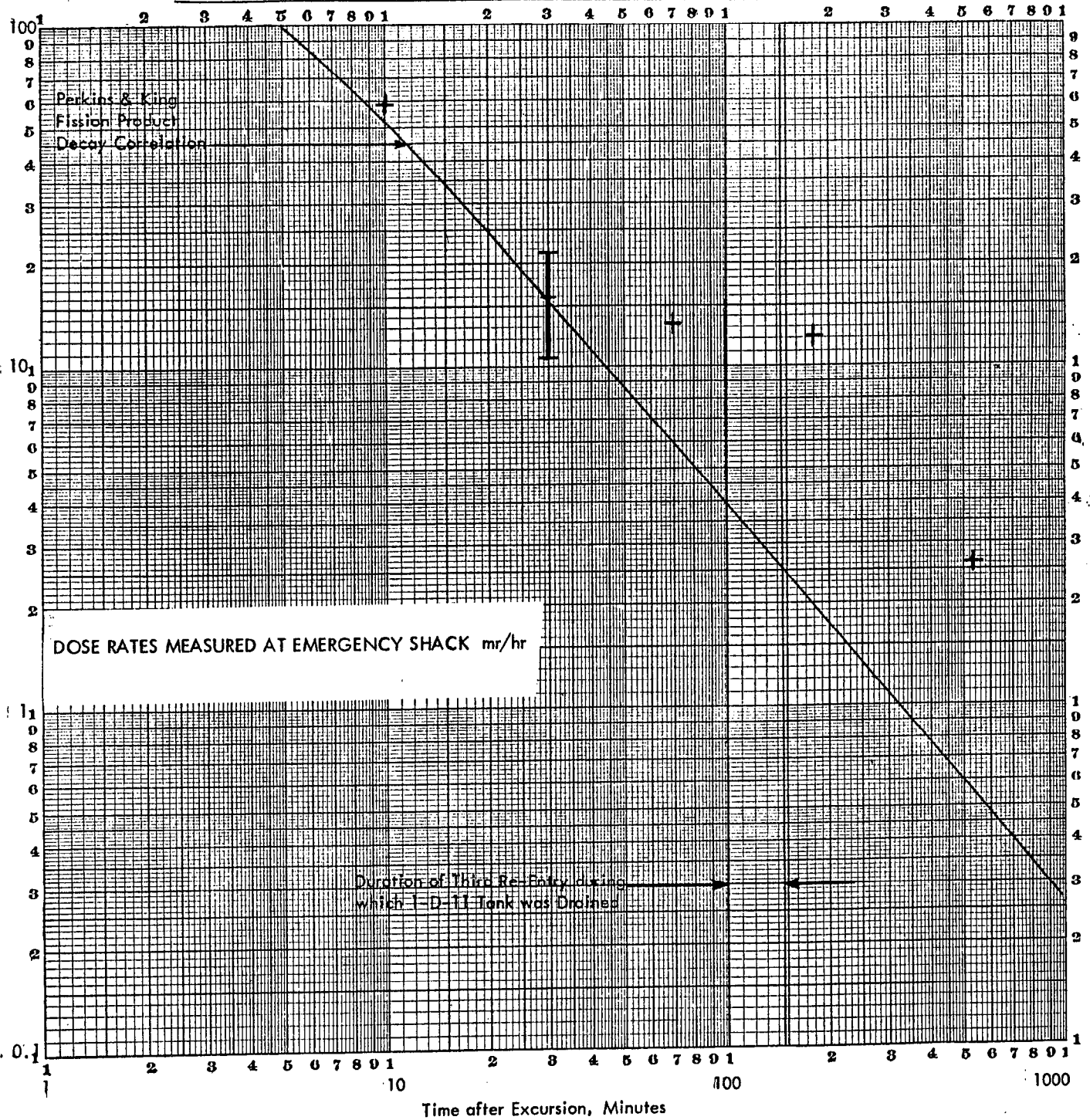
The only evidence to support this assumption is the radiation intensity measured at the emergency shack with a survey meter. These data are tabulated in Appendix A-2.

Figure III-B-A following shows the variation of dose rates at the emergency shack as a function of time.

Also shown on Figure III-B-A is a curve showing the predicted variations (Perkins and King correlation) of fission product gamma decay rate as a function of time after instantaneous fission. It is seen that the measured dose departs from the predicted variations in the time period from 30 - 150 minutes, during which time the readings are roughly constant. The draining of the tank took place about 105 minutes after the initial burst. The plateau at about 12 mr/hr from 24 - 84 minutes suggests continued operation at about 100 watts. However, the continuation of this plateau after 105 minutes suggests a different explanation such as contamination of the instrument on a nearby source such as discarded clothing.

FIGURE III-B-A

Variation of Measured Dose Rates at Emergency Shack with Time After the Initial Criticality



## B. Evidence of a Second Excursion - (Continued)

### 3. Continued Criticality at Low Power - (Continued)

The neutron exposure of the Superintendent would require his being exposed to a number of fissions given by the following:

$$Y = 1.72 \times 10^{13} \left(\frac{R}{\bar{r}}\right)^2 \quad (\text{III-B-1})$$

where R is the distance in inches of the Superintendent from the center of the tank. This calculation is based on the total uncollided neutron current density,  $J_S$ , estimated from the whole body sodium activity. If most of the exposure to neutrons is assumed to take place when the Superintendent is standing near the tank, the relation of  $J_S$  to the average thermal flux in the Superintendent's body,  $\phi_{th}$ , is given by:

$$J_S = 1.12 \phi_{th} \quad (\text{See Page 21, Equation III-D-3 for derivation}) \quad (\text{III-B-2})$$

$\phi_{th}$  is given in Table III-D-6, Page 30

$$\text{Then } J_S = 2.81 \times 10^9 \text{ n/cm}^2.$$

The current density to fission conversion factor in the final configuration is given in equation (III-C-8). If the hair sample and silver coins activity measurements are used, higher fission yields would be obtained.

The Superintendent was within one (1) foot of the tank surface for about 10 seconds. This corresponds to a fission rate of  $0.94 \times 10^{13}$  f/sec, which corresponds to 300 watts which power would produce higher radiation readings (30 mr/hr) at the emergency shack than were observed. This power would have produced 8500 R/hr. of gamma radiation at the tank surface. Several hundred R/hr. were observed.

The main evidence against continued criticality is the relative exposure of the two men. Continuous operation is inconsistent with the neutron flux to which the Supervisor was exposed since his nearest distance from the tank was 15 feet and his exposure was greater than that of the Superintendent (See Table III-D-6, Page 30)

### 4. Exposure by Delayed Neutrons

The Supervisor could have been exposed to delayed neutrons if the tank had been operating at constant power until it was drained or if an excursion had taken place just before it was drained. Calculations were made for neutron leakage from the one gallon jars with a delayed neutron source. Each delayed neutron in the gallon jar produced 0.17 fission neutrons and resulted in a leakage of 0.99 neutrons (Appendix B-1). The leakage is largely composed of delayed neutrons. Each delayed neutron in the 3" diameter column is expected to produce less fission neutrons. (The existence of fission neutrons is important because activation of the hair requires neutrons with energy 2.5 Mev, whereas the maximum energy of the delayed neutrons is 0.6 Mev.). The whole body neutron dose for the Supervisor, based on blood sodium is approximately 6 rad. from the data in Table III-D-12.

B. Evidence of a Second Excursion - (Continued)

4. Exposure by Delayed Neutrons - (Continued)

A crude calculation indicates that the gamma dose from fission products would exceed the neutron dose by at least a factor of 100 for all times greater than 30 seconds after an excursion. Consequently, the assumption of delayed neutrons producing the neutron dose requires that we ascribe a gamma dose of about 600 R to the Supervisor. Both clinical evidence and medical laboratory findings indicate a much lower dose. Therefore this alternative was discarded.

5. Exposure to a Second Burst

The most likely explanation for the neutron exposures of the Superintendent and the Supervisor is the following:

The initial burst expelled 10 or 11 liters of solution which was sufficient to make the container subcritical. This is substantiated by the criticality studies and chemical results presented in Sections B-1, A-3 and A-6 of the Appendix as follows:

- a. The multiplication factors, assuming the solution to be homogeneous, are given in Table B-1-1, Appendix B-1

42 liter case:  $k = 1.043$

41 liter case:  $k = 1.035$

- b. The distortion of the top surface decreases the reactivity by about 2.1%.
- c. The presence of the stainless steel stirrer causes a .0075 to .009 decrease in k.
- d. The presence of a concrete wall 15" away from the tank surface increases the reactivity approximately by .004.
- e. The temperature coefficient of reactivity is computed to be  $3.1 \times 10^{-4} / ^\circ\text{C}$ . A yield of  $10^{17}$  produces an elevation of temperature of  $20^\circ\text{C}$ . during the first excursion; this decreases k by about .006.
- f. Uranium content analysis (Appendix A-6) shows that there are some uncertainties in the total U involved in the accident. The results for the total uranium found in the solution drained from the tank are:

Idaho Falls, USAEC      1,934 g.

Oak Ridge National Lab. 1,978 g.

United Nuclear Corp.    2,087 g.

An average of 2,000 g. has been taken in the criticality calculations. The U-235 reactivity worth is estimated to be  $1.50 \times 10^{-4} / \text{g.}$  of U-235. The enrichment in U-235 is approximately 93.2%. Then the uncertainty in k from the error in uranium content determination is about 1%.

- g. The presence of precipitate particles result in a small but negative effect on reactivity due to self-protection in the particles;  $\sim -.006\%$  in k.

*evolution*

B. Evidence of a Second Excursion - (Continued)

5. Exposure to a Second Burst - (Continued)

In addition, the pouring and mixing experiments indicated that, following a period of rapid gas evaluation and pouring, precipitate particles were left attached to the tank walls above the final liquid level. Some of the uranium may therefore not have been in the final solution. The net result of these factors is that the criticality of the solution is estimated to have been in the range  $0.99 \leq k \leq 1.0$ .

The Superintendent and Supervisor went to the third floor. The Supervisor stayed at the door while the Superintendent went in, removed the bottle, and turned off the stirrer. The Superintendent passed the Supervisor in the doorway and had started down the stairs when the surface of the solution became flat enough to cause an increase of reactivity which resulted in a second excursion. The hypothesis of a second excursion is supported by the activation data. Estimates of the fission yield and doses using samples in and on the Superintendent and Supervisor's bodies presented below and in Section III-D can be understood only on the basis of a second burst.

6. Fissions in the Initial Burst

The number of fissions in the initial burst has been estimated at  $1.0 - 1.1 \times 10^{17}$  in two ways. The activation of material in and on the body of the Operator who left the room shortly after the initial criticality, provides one estimate. The ratio of fission products found outside the tank to material inside it provides another.

With respect to the first method, the calculation is sensitive to the distance assumed between the deceased and the tank. Table III-D-4 shows estimates of the neutron dose at different parts of the Operator's body. The distance of the Operator from the tank was selected to give the proper ratio of dose at the pubic hair area to dose at the head hair area. The location of the pubic hair area was estimated at 25.67 cm from the tank surface (48.53 cm from the center of the solution). Total neutron current density incident on different parts of the body is evaluated in Section III-D and presented in Table III-D-4. Neutron current density to fission conversion factor in the initial configuration is given by Equation III-C-7. Table III-B-1 following shows estimates of the number of fissions in the initial burst from several sources of data. A yield of  $1 \times 10^{17}$  fissions seems reasonable.

For the second method, we use the data in Table III-C-1 which shows that fission products from  $0.25 \times 10^{17}$  fissions were outside the tank. Take the amount of material ejected after the initial burst to be 11 liters. Let:

- $Y_1$  = yield of initial burst
- $Y_2$  = subsequent yield
- $Y = Y_1 + Y_2$ , total yield.

Using an extrapolation length of 2.5 cm and taking account of the axial flux distribution, the average flux in the top 11 liters is found to be 0.64 of the average flux in



TABLE III-B-1FISSIONS IN INITIAL BURST

(assuming pubic hair in tank  
center plane at 25.67 cm from  
the tank surface)

|             | Estimated Yields      | Remarks  |
|-------------|-----------------------|--|
| Pubic Hair  | $1.16 \times 10^{17}$ |  |
| Head Hair   | $1.16 \times 10^{17}$ | assuming 86 cm from pubic hair to head<br>when standing erect  |
| Indium Foil | $0.93 \times 10^{17}$ | assuming 41 cm distance between pubic<br>hair and foil   |
| Na in Blood | $1.02 \times 10^{17}$ | based on an average body distance of<br>55 cm from the tank center line. (32.5<br>cm from the surface of the tank) |

B. Evidence of a Second Excursion - (Continued)

6. Fissions in the Initial Burst - (Continued)

the total volume (52 liters). Therefore, fission products from

$$Y_1 \times 0.64 \times \frac{11}{52} = 0.136 Y_1$$

fissions are ejected from the tank.

An additional  $Y_2$  fissions in 41 liters, followed by a spill of 4 liters during draining, results in additional fission products from

$$(0.864 Y_1 + Y_2) \times \frac{4}{41} = 0.975 Y_2 + 0.0845 Y_1$$

fissions being outside the tank. Referring to Table III-C-1, we then have:

$$(0.0845 + 0.136) Y_1 + 0.0975 Y_2 = 0.25 \times 10^{17}.$$

Measurements give three values for the total yield. This equation was solved for those three values with the following results:

Distribution of Fissions

| <u><math>Y \times 10^{17}</math></u> | <u><math>Y_1 \times 10^{17}</math></u> | <u><math>Y_2 \times 10^{17}</math></u> |
|--------------------------------------|--|--|
| 1.05                                 | 1.18                                   | -0.13                                  |
| 1.26                                 | 1.03                                   | 0.23                                   |
| 1.55                                 | 0.80                                   | 0.75                                   |

We conclude that a total yield of  $1.26 \times 10^{17}$  fissions leads to about  $1 \times 10^{17}$  fissions in the initial burst. This is in good agreement with the value found above.

### C. Estimates of the Total Number of Fissions Which Occurred

Fission product analysis, sodium activation in the tank solution and activation of isolated samples (stainless steel clamps, screwdriver) provide the bases for the estimates of the total yield.

#### 1. Fission Product Analysis

Radiochemical analyses of the fission products are described in Appendix A-5. The resulting total yield,  $Y_T$  is estimated to be:

$$Y_T = (1.30 \pm .25) \times 10^{17} \text{ fissions}$$

This value is believed to be the most reliable estimate of the total yield and is consistent with the indirect estimates presented below. The value is an average of the measurements made at various laboratories; the data are presented in Tables A-5-2 and A-5-3, Appendix A-5, and summarized in the following table

TABLE III-C-1  
Total Yield  $\times 10^{17}$  Estimated from Fission Products

| Fission Products |                    | Total | Remarks (Note 1) |
|------------------|--------------------|-------|------------------|
| Found in Tank    | Found Outside      |       |                  |
| 0.81             | 0.24               | 1.05  | NSEC             |
| 1.01             | 0.28               | 1.29  | ORNL             |
| 1.30             | (0.25)<br>(Note 2) | 1.55  | AEC-ID           |

Note 1: Laboratories are identified as follows:

NSEC - Nuclear Science and Engineering Corporation  
AEC-ID - Health and Safety Division, Idaho Falls  
ORNL - Health Physics Division at Oak Ridge

Note 2: Assumed, not reported.

#### 2. Sodium Activation Analysis

Measurements of Sodium 24 activation and total sodium concentration in supernatant liquid samples taken over a precipitate in the jars filled with the solution found in the tank and spills are presented in Appendix A-4. The  $\text{Na}^{24}/\text{Na}^{23}$  atom ratio is assumed to be the same throughout liquids and solids of the tank materials because of the strong mixing action of the electric stirrer and the diffusion process.

C. Estimates of the Total Number of Fissions Which Occurred - (Continued)

2. Sodium Activation Analysis - (Continued)

Let  $\left[ \frac{N^*}{N} \right]_S$  be the  $\text{Na}^{24}/\text{Na}^{23}$  atom ratio in each sample.

Then the corresponding volume average time-integrated activation flux (essentially thermal) is given by

$$\bar{\Phi}_{th, s} = \frac{1}{\sigma_{th}} \times \left[ \frac{N^*}{N} \right]_S \quad (\text{III-C-2})$$

where  $\sigma_{th}$  is the maxwellian average activation cross section for Sodium 23, (.475 ± .009 barns).

A mean value for the volume average time-integrated thermal flux is then evaluated:

$$\bar{\Phi}_{th} = (.96 \pm .38) \times 10^{14} \text{ n/cm}^2 \quad (\text{III-C-3})$$

where we assumed 40% error in the flux determination caused mainly by the probable precision of ± 30% and the relative accuracy of ± 15% in the determination of Sodium 24. (Appendix A-4).

The total fission yield is then given by:

$$Y = N_{25} \sigma_f \times \bar{\Phi}_{th} \quad (\text{III-C-4})$$

where

- $N_{25}$  is the number of U-235 atoms present
- $\sigma_f$  is the microscopic thermal fission cross section of U-235

(The product  $N_{25} \sigma_f = 1.23 \text{ cm}^2$  for 1 gram of U-235)

The yield has been calculated for two values of  $N_{25}$  corresponding to:

- a. The amount of uranium (1900 gms.) necessary to reach prompt critical initially,
- b. The final configuration (42 liters, 2120 gms.).

The yields are  $2.24 \times 10^{17}$  and  $2.62 \times 10^{17}$ , respectively. It is believed that about 3/4 of the fissions occurred in the first burst and 1/4 in the final configurations. A reasonable estimate is

$$Y_T = (2.4 \pm 0.9) \times 10^{17} \text{ fissions}$$

This method assumes that the solution in the tank is uniformly mixed.

## C. Estimates of the Total Number of Fissions Which Occurred - (Continued)

### 3. Activation Analysis of Isolated Samples

Activation analysis of isolated samples provide another basis for determining total yield estimates. Methods of converting activation measurements into total\* neutron current density incident on the samples are discussed in Appendix B-5. It must be noted, however, that these methods make use of calculated leakage spectra from bare systems. The contribution of neutrons reflected from the walls and floor in the sample activation is difficult to assess, particularly where the neutron reaction is essentially thermal. Hence, total yields are best estimated using threshold activation reactions since it is reasonable to assume that a negligible amount of reflected fast neutrons may be incident on the samples.

From each of the threshold reactions, effective activation cross sections have been determined for the calculated leakage spectra (Appendix B-5), Section 2.2) above 3 Mev. From the measured activations one can then determine  $\bar{\phi}_1$ , the flux above 3 Mev. Since the calculations also give the leakage above 3 Mev per fission, the number of fissions is determined.

The total current density of neutrons incident on the sample is then given by

$$J_S = \frac{\bar{\omega}_1 \bar{\phi}_1}{i_{+,1}} \quad (\text{III-C-5})$$

where the subscript 1 denotes the highest energy group used in the calculations ( $E \geq 3$  Mev);

$\bar{\omega}_1$  is an approximately averaged value of the cosine of neutron incidence angles in the energy group 1. It is shown in Appendix B-5, 2.3 that  $\bar{\omega}_1 = 0.67$  on the tank outer surface and tends towards unity as the distance from the tank increases'

$i_{+,1}$  is the fraction of neutrons leaking from the core in group 1 (Appendix B-2).

$\bar{\phi}_1$  is the neutron flux in group 1.  $\bar{\phi}_1$  can be determined from the activation measurements using the corresponding effective cross sections,  $\bar{\sigma}_{E=3 \text{ Mev}}$

$$\bar{\phi}_1 = \frac{N^*/N_0}{\bar{\sigma}_{(E=3 \text{ Mev})}} \quad (\text{III-C-6})$$

where  $N^*/N_0$  is the measured activated-to-target atom ratio. (Appendix A-7).

---

\* The term total in this context means integrated over all energies.

C. Estimates of the Total Number of Fissions Which Occurred - (Continued)

3. Activation Analysis of Isolated Samples - (Continued)

Neutron leakage to fission conversion ratio are given in Appendix B-2. Assuming an inverse square distance attenuation, incident neutron current densities per fission are

$$J_{+} = 1.21 \times 10^{-4} \times \left(\frac{9}{R}\right)^2 \frac{n/cm^2}{\text{fission}} \quad (\text{III-C-7})$$

for the initial configuration (52 liters) and

$$J_{+} = 1.63 \times 10^{-4} \left(\frac{9}{R}\right)^2 \frac{n/cm^2}{\text{fission}} \quad (\text{III-C-8})$$

for the final configuration (42 liters). R is the distance in inches from the tank axis of symmetry to the sample.

Estimates of  $J_S$  and total yields assuming that all fissions occurred in the initial and final configuration respectively are presented in Table III-C-2 following. It can be seen in the table that two of the three measurements on the stainless steel clamp 174" away from the tank give much higher estimates of the fission yield than all the others. Discarding these two measurements as inconsistent, the estimates may be considered as independent estimates of the yield and the mean value and the probable error can be estimated.

Assuming that all fission occurred in the initial configuration,

$$Y_T = (1.76 \pm .20) \times 10^{17} \text{ fissions}$$

Assuming that all fissions occurred in the final configuration,

$$Y_T = (1.27 \pm .16) \times 10^{17} \text{ fissions}$$

In the initial configuration, it is assumed that all the fissions occurred when the total uranium solution (11 liters) is poured in the tank. The criticality studies (Appendix B-1) and the victim's testimony showed that the system reached the delayed supercritical state with the addition of approximately 8 - 10 liters of solution. The yield estimate in the initial configuration may therefore be too high. Further, the measurements accuracy is probably  $\pm 20\%$ . A reasonable estimate of the total yield from the activation measurements is, therefore,

$$Y_T = (1.3 \pm 0.4) \times 10^{17} \text{ fissions}$$

ESTIMATES OF TOTAL YIELD FROM THRESHOLD ACTIVATION MEASUREMENTS

| Item                      | Reaction                            | Laboratory | $(N^+/N) \times 10^{+24}$<br>(Note 1) | $\frac{\omega_1}{\sigma_{E=3}} \times \frac{1}{J_{+,1}}$<br>( $\times 10^{+24} \text{ cm}^2$ ) | Total uncollided<br>Current Incident<br>on Sample, $J_S$<br>( $n/\text{cm}^2$ ) | Total Yield,<br>Initial<br>Configuration | Total Yield,<br>Final<br>Configuration |
|---------------------------|-------------------------------------|------------|---------------------------------------|--|---|--|--|
| Screwdriver<br>Chem. sep. | $\text{Fe}^{54}(n,p)\text{Mn}^{54}$ | AEC-ID     | $1.56 \times 10^{12}$                 | 13.41  | $2.09 \times 10^{13}$   | $1.72 \times 10^{17}$                    | $1.28 \times 10^{17}$                  |
| Scanned                   | "                                   | "          | $1.25 \times 10^{12}$                 | 13.41  | $1.68 \times 10^{13}$   | $1.39 \times 10^{17}$                    | $1.03 \times 10^{17}$                  |
| "                         | "                                   | UNC-P      | $1.68 \times 10^{12}$                 | 13.41  | $2.25 \times 10^{13}$   | $1.86 \times 10^{17}$                    | $1.14 \times 10^{17}$                  |
| SS Hose Clamp<br>at 9"    | "                                   | AEC-ID     | $3.64 \times 10^{11}$                 | 13.41  | $4.88 \times 10^{12}$   | $1.62 \times 10^{17}$                    | $1.20 \times 10^{17}$                  |
|                           | $\text{Ni}^{58}(n,p)\text{Co}^{58}$ | "          | $5.31 \times 10^{11}$                 | 11.17  | $5.93 \times 10^{12}$   | $1.96 \times 10^{17}$                    | $1.45 \times 10^{17}$                  |
|                           | "                                   | NSEC       | $4.68 \times 10^{11}$                 | 11.17  | $5.23 \times 10^{12}$   | $1.73 \times 10^{17}$                    | $1.28 \times 10^{17}$                  |
| SS Hose Clamp<br>at 174"  | $\text{Fe}^{54}(n,p)\text{Mn}^{54}$ | AEC-ID     | $1.06 \times 10^{10}$                 | 13.47  | $1.42 \times 10^{11}$   | $4.86 \times 10^{17}$                    | $3.6 \times 10^{17}$                   |
|                           | $\text{Ni}^{58}(n,p)\text{Co}^{58}$ | "          | $1.80 \times 10^{10}$                 | 11.17  | $2.10 \times 10^{11}$   | $7.17 \times 10^{17}$                    | $5.3 \times 10^{17}$                   |
|                           | "                                   | UNC-P      | $0.53 \times 10^{10}$                 | 11.17  | $0.592 \times 10^{11}$  | $2.02 \times 10^{17}$                    | $1.50 \times 10^{17}$                  |

Note 1: Calculations of activated to target atoms,  $N^+/N_0$ , is presented in Appendix A-7

## D. Estimates of the Doses Received by Personnel

### 1. Estimates of Total Dose Received by the Deceased Operator

There are four sources of data from which to make estimates of the magnitude of the absorbed dose of ionizing radiation received by the deceased Operator. These are:

- a. Radioactive sodium in blood serum samples
- b. Phosphorus beta activity in pubic and head hair samples
- c. Indium foil gamma ray activity
- d. Film badge clip, spring and rivet neutron activation

Each of these sources of evidence was used to evaluate independent values for the exposure of the Operator to neutrons and gamma rays.

#### a. Blood Sodium Activation

Fast neutrons entering the body are moderated by the hydrogen, oxygen and carbon and reach the thermal energy range with a distribution throughout the body which is approximately independent of the neutron initial energies.<sup>+</sup> A small fraction of these neutrons is captured in the normal sodium to form the radioactive isotope  $\text{Na}^{24}$  which decays with a 14.8 hr half life by emitting a beta particle and two gamma rays of energy 2.75 Mev and 1.38 Mev. As blood is continually pumped throughout the body, the  $\text{Na}^{24}$  concentration assumes a constant value which is approximately independent of body orientation.

The use of  $\text{Na}^{24}$  in a body as a dosimetric system for monitoring nuclear incidents is discussed in detail by the originators of the method at Oak Ridge National Laboratory (ORNL), (References 1, 2, 3 and 4 - Appendix C). The general method of relating the  $\text{Na}^{24}$  activation measurements to the total uncollided incident neutron density,  $J_S$ , along with the assumptions used in the calculation, is given in Appendix B-5, Sections 1.2.3. It is found that

$$J_S = \frac{\bar{\mu}_a}{\bar{a}} \frac{V_{\text{man}}}{A_{\text{man}}} \bar{\phi}_{\text{oth}} \quad (\text{III-D-1})$$

where:

$\bar{\mu}_a$ , the Maxwell average body thermal absorption cross section, is calculated to be equal to  $.0206 \text{ cm}^{-1}$ ;  $\bar{a}$ , the spectral average probability that a neutron is captured in the body as a thermal neutron, is estimated to be equal to 0.435 at 9" from the surface of the tank. (Appendix B-5, Section 2.7).

$V_{\text{man}}$  and  $A_{\text{man}}$  are the body volume and area projected on a surface normal to the neutron beam. The method assumes the body can be replaced by a cylindrical phantom of radius,  $R_o = 15 \text{ cm}$ . Then  $\frac{V_{\text{man}}}{A_{\text{man}}} = 23.56 \text{ cm}$ .

---

<sup>+</sup> The human body is several mean free paths thick for fast neutrons.



a. Blood Sodium Activation - (Continued)

$\bar{\phi}_{\text{oth}}$  is the Maxwell average time integrated thermal flux in the body. It is related to the activated to target Na atom ratio by:

$$\bar{\phi}_{\text{oth}} = \frac{N^*/N}{\sigma_{\text{oth}}} \quad (\text{III-D-2})$$

with  $\sigma_{\text{th}} = .475$  barns.

Then, Equation (III-D-1) becomes:

$$J_S = 1.12 \bar{\phi}_{\text{oth}} = 2.32 \times 10^{24} \times \frac{N^*}{N} \quad (\text{III-D-3})$$

The neutron dose to incident current density conversion factors are calculated in Appendix B-3. It is shown that the spectral differences in fast leakage spectra for the configurations thought to be the actual ones is negligible. Then, the overall average first collision neutron dose per incident neutron current is:

$$D_o^{(1)} = 1.50 \times 10^{-9} \frac{\text{rad}}{(\text{n/cm}^2)} \quad (\text{III-D-4})$$

In addition, an overall "maximum" neutron dose per incident neutron current is computed as

$$D_o^{(\text{max})} = 2.45 \times 10^{-9} \frac{\text{rad}}{(\text{n/cm}^2)} \quad (\text{III-D-5})$$

The gamma-to-neutron dose ratio depends on the type of configuration. In the initial pouring excursion, it is shown in Appendix B-4 that

$$\frac{D_\gamma}{D_n^{(1)}} = 1.75 \quad (\text{III-D-6})$$

Experimental data on sodium activation are presented in Appendix A-8.

The sodium activity in blood serum corrected for decay is equal to  $2.64 \times 10^{-2}$   $\mu\text{c/cc}$  of blood serum. The sodium 23 concentration in blood serum is 3.21 g/l.

Then the number of  $\text{Na}^{24}$  atoms is given by

$$N^* = \frac{2.64 \times 10^{-8} \times 3.7 \times 10^{10}}{\lambda} \quad (\text{III-D-7})$$

where  $3.7 \times 10^{10}$  is the number of disintegration per sec. per curie and  $\lambda$  is the decay constant for  $\text{Na}^{24}$

$$N^* = 7.51 \times 10^7 \text{ atoms of } \text{Na}^{24}/\text{cc}$$

a. Blood Sodium Activation - (Continued)

The number of  $\text{Na}^{23}$  atoms is equal to

$$N = 3.21 \times 10^{-3} \times \frac{.6023 \times 10^{24}}{23} = (8.4 \times 10^{-5}) \times 10^{24}/\text{cc}$$

where  $.6023 \times 10^{24}$  is the Avogadro's number. Then,  $\frac{N^*}{N} = \boxed{.894 \times 10^{12}} \times 10^{-24}$ .

Introducing this ratio into Equations (III-D-2) and III-D-3) yields

$$\bar{\phi}_{\text{oth}} = 1.88 \times 10^{12} \text{ n/cm}^2$$

$$J_S = 2.07 \times 10^{12} \text{ n/cm}^2$$

Use of Equations (III-D-4), (III-D-5) and (III-D-6) gives the dose received by the Operator

$$D_n^{(1)} = 3,110 \text{ rads}$$

$$D_n^{(\text{max})} = 5,100 \text{ rads}$$

$$D_{\text{r}} = 3,430 \text{ rads}$$

An independent estimate of the dose received by the Operator using the blood sodium activation measurement can be made using experimental results and calculations performed at ORNL in connection with the Y-12 Plant accident. (See Reference 13, Appendix C). ORNL experimental data are given in Table 7 of (Reference 1, Appendix C) and yield the following conversion factor for the first collision dose:

$$f_E = 1.65 \times 10^5 \frac{\text{rad}}{\mu\text{c/ml of whole blood}}$$

or

$$f_E = .98 \times 10^5 \frac{\text{rad}}{\mu\text{c/ml of blood serum}}$$

where we assume that whole blood contains 83 MEQ/liter or 1.096 g. of sodium per liter of whole blood. Then the first collision neutron dose received by the Operator is given by

$$D_n^{(1)} = 2.64 \times 10^{-2} \times .98 \times 10^5 = 2,590 \text{ rads.}$$

The difference with the calculated value of 3110 rads can be explained as follows:

The Rhode Island and Y-12 Plant configurations are different. The neutron leakage spectrum from the Rhode Island system is expected to be harder than that of the Y-12 Plant. From the data given in Reference 13, Appendix C, the corresponding increase in dose is estimated at approximately 20%.

b. Hair Sulfur Activation

The high sulfur content of human hair has been utilized to estimate incident fast neutron dose by D. F. Peterson, et al, at Los Alamos Scientific Laboratory (See Reference 14, Appendix C). The procedure is based on the fact that phosphorus is almost completely absent in hair and hence, the  $S^{32}(n,p)P^{32}$  reaction is uncontaminated by thermal neutron activation of  $P^{31}$  in the  $P^{31}(n,\gamma)P^{32}$  reaction. The method of  $P^{32}$  beta activity measurements on heavily contaminated specimens is described in Reference 14, Appendix C.  $P^{32}$  decays with a 14.2 day half life; the fractional abundance of sulfur in hair is assumed to be .05 g./g. of hair. The reaction energy threshold is approximately 1.8 Mev. It should be emphasized that this method does not yield the average body exposure. However, the fixed anatomical location of hair offers the distinct advantage of providing a relative estimate of dose distribution.

The experimental data are presented in Appendix A-8. The number of disintegrations per minute per gram of hair,  $D(0)$ , is related to the activated phosphorus to target sulfur atom ratio,  $\frac{N^*}{N}$ , by the following relation

$$\frac{N^*}{N} = \frac{32}{.6023 \times 10^{24} \times .05} \times \frac{1}{\lambda} D(0) \quad (\text{III-D-8})$$

where  $\lambda$  is the decay constant in minute<sup>-1</sup>

$$\left( \lambda = \frac{0.693}{14.2 \times 24 \times 60} = 3.389 \times 10^{-5} \text{ minute}^{-1} \right)$$

then

$$\frac{N^*}{N} = (3.136 \times 10^7) \times 10^{-24} D(0) \quad (\text{III-D-9})$$

In Appendix A-8, 8,990 and 2,160 disintegrations per minute per gram of pubic and head hair respectively are reported. Then

$$\left\{ \begin{array}{l} \left[ \frac{N^*}{N} \right]_{P.P} = (2.82 \times 10^{11}) \times 10^{-24}, \text{ Pubic hair} \\ \left[ \frac{N^*}{N} \right]_{P.H.} = (.68 \times 10^{11}) \times 10^{-24}, \text{ Head hair} \end{array} \right. \quad (\text{III-D-10})$$

The method employed to relate  $\frac{N^*}{N}$  to total current incident on a sample located on the body surface is discussed in Appendix B-5. It is seen that the total uncollided neutron current density incident on the sample is given by

$$J_s = \frac{\varphi_1}{\left( \frac{1}{\omega_1} + 2\alpha_1 \right) j_{+,1}} \quad (\text{III-D-11})$$

where  $\alpha_1$  is the albedo for neutrons in group 1 ( $E \geq 3$  Mev) evaluated in Appendix B-5, Section 2-4:  $\alpha_1 = .036$ .

$\varphi_1$  is the neutron flux in energy group 1 ( $E \geq 3$  Mev) which is related to  $\frac{N^*}{N}$  through

b. Hair Sulfur Activation - (Continued)

the use of the appropriate effective sulfur activation cross section,  $\bar{\sigma}_{E=3 \text{ Mev}}$ .  $\bar{\sigma}$  is evaluated in Appendix B-5, Section 2.2 as  $\bar{\sigma}_{E=3} = .398$  barns.

Since the operator was near the tank surface,  $\bar{w}_1$  is taken as .70. Thus, Equation (III-D-10) can be written

$$J_S = 5.9\Phi_1 = 14.82 \times 10^{24} \times \frac{N^*}{N} \text{ (n/cm}^2\text{)} \quad \text{(III-D-12)}$$

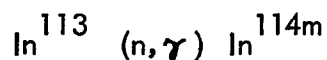
The calculated doses are then obtained by introducing Equation (III-D-10) into Equation (III-D-12) and using the conversion ratios given by Equations (III-D-4), (III-D-5) and (III-D-6). The results are summarized below

TABLE III-D-1

| Flux of neutrons above<br>3 Mev                | $\Phi_1 = \int_3^{\infty} \phi(E) dE$<br>(n/cm <sup>2</sup> ) | Pubic Hair            | Head Hair             |
|--|---|-----------------------|-----------------------|
|  |   | $7.09 \times 10^{11}$ | $1.71 \times 10^{11}$ |
| Total uncollided inci-<br>dent current density | $J_S$ (n/cm <sup>2</sup> )                                    | $4.18 \times 10^{12}$ | $1.01 \times 10^{12}$ |
| First collision neutron<br>dose                | $D_n^{(1)}$ (rad)   | 6,270                 | 1,515                 |
| Maximum neutron dose                           | $D_n^{(max)}$ (rad)   | 10,240                | 2,475                 |
| Gamma dose                                     | $D_\gamma$ (rad)  | 10,970                | 2,650                 |

c. Indium Foil Activation

Indium becomes activated with a 56 minute half life and a 50 day life. Measurements were performed only on the longer lived activity which is due to  $\text{In}^{114m}$  produced by the reaction.



The  $\text{In}^{114m}$  decays with a half life of 50 days, emitting a .190 Mev gamma ray with a branching ratio of 96.5% and a .722 Mev gamma ray with a branching ratio of .035. Measurements on either  $\gamma$ -ray may then be converted into the number of  $\text{In}^{114}$  atoms produced in the irradiation burst after use of the appropriate branching ratio, self absorption of the  $\gamma$ -ray in the foil, counter efficiency, and decay time between irradiation and counting.

c. Indium Foil Activation - (Continued)

Idaho Falls measurements and calculations of activated to target atom ratios,  $\frac{N^*}{N}$ , for the Operator's foil are presented in Appendix A-7. It is shown that, using .0423 as the abundance of  $\text{In}^{113}$  in natural Indium, these ratios are:

$$\frac{N^*}{N} = (5.44 \times 10^{13}) \times 10^{-24}$$

for a .212 g. foil sample and

$$\frac{N^*}{N} = (5.62 \times 10^{13}) \times 10^{-24}$$

for a .221 g. foil sample.

It is shown in Appendix B-5 that

$$\frac{N^*}{N} = \int_0^{\infty} \sigma(E) \varphi(E) dE \quad (\text{III-D-13})$$

where  $\varphi(E)$  is the time integrated flux in  $dE$  averaged over the sample volume and  $\sigma(E)$  is the reaction activation cross section. For an essentially thermal reaction, Equation III-D-13 can be written

$$\frac{N^*}{N} = \bar{\varphi}_{\text{oth}} \sigma_{\text{th}} \left[ f + f \frac{\int_{\text{non th}} \varphi(E) \sigma(E) dE}{\bar{\varphi}_{\text{th}} \sigma_{\text{th}}} \right] \quad (\text{III-D-14})$$

where  $\bar{\sigma}_{\text{th}}$  is the Maxwell average thermal activation cross section for  $\text{In}^{113}$ ,  $\sigma_{\text{th}} = 49.6$  barns;  $\bar{\varphi}_{\text{oth}}$  and  $\bar{\varphi}_{\text{th}}$  are the Maxwell average thermal fluxes at the foil location in the absence and the presence of the foil respectively, i.e.,  $\frac{\bar{\varphi}_{\text{th}}}{\bar{\varphi}_{\text{oth}}} = f$ , the thermal self shielding factor.

The thermal self shielding factor is determined by the total absorption cross section of the indium foil ( $\sigma_a = 196$  b at 2200 m/sec) and by the thickness. A thickness of about  $10^{-2}$  cm. then corresponds to .074 absorption mean free paths at 2200 m/sec, resulting in a self protection factor  $f$  which is a few to several percent below unity. Secondly, the ratio of  $\text{In}^{114\text{m}}$  activation by non-thermal neutrons to activation by thermal neutron is estimated to be in the neighborhood of 10%. Therefore, it is true to within several percent that

$$\frac{N^*}{N} = \bar{\varphi}_{\text{oth}} \sigma_{\text{th}} \quad (\text{III-D-15})$$

The relation between total uncollided current incident on a sample location on the body and the thermal flux has been derived in Appendix B-5.

$$J_S = \frac{\varphi_{\text{oth}}}{1/2 f_{\text{th}} (R) j_{+, \text{th}} \left( \frac{1}{\bar{w}_{\text{th}}} + 2 \alpha_{\text{th}} \right) + 2b j_{+, \text{non th}}} \quad (\text{III-D-16})$$

c. Indium Foil Activation - (Continued)

where:

$f_{th}(R)$  is the correction factor for scattered thermal neutrons. At foil position ( $R \approx 18''$ ) as discussed in Appendix B-5, Section 2-6, half the calculated 4.3 correction factor is used.

$j_{+, th}$  and  $j_{+, non\ th}$  are the thermal and non-thermal fractions of the normalized leakage spectrum. (Appendix B-2).

$\bar{w}_{th}$  is the average cosine of the thermal neutrons angular distribution. Assuming that the Operator was near the tank, it is seen in Appendix B-5, Section 2.3 that  $\bar{w}_{th} = 0.60$ .

$\alpha_{th}$  is the thermal neutron current albedo at the body surface,  $\alpha_{th} = 0.80$ .

$b$ , the non-thermal to thermal neutron current albedo, is estimated in Appendix B-5, Section 2.5 as  $b \approx 0.14$

Equation III-D-16 can therefore be written

$$J_S = \frac{\varphi_{oth}}{2.15 \times .075 \times \left[ \frac{1}{0.6} + 1.6 \right] + 0.925 \times 0.28}$$

or

$$J_S = 1.27 \times \varphi_{oth} \quad (\text{III-D-17})$$

Conversion ratios from total neutron density incident on the foil to doses are given in Equations (III-D-4), (III-D-5) and (III-D-6). The results are summarized below:

TABLE III-D-2

|  | OPERATOR FOIL         |                       |
|--|-----------------------|-----------------------|
|  | Sample No. 1          | Sample No. 2          |
| Thermal flux at foil location, $\varphi_{oth}$ ( $n/cm^2$ )        | $1.10 \times 10^{12}$ | $1.13 \times 10^{12}$ |
| Total uncollided neutron density incident on foil $J_S$ , $n/cm^2$ | $1.40 \times 10^{12}$ | $1.44 \times 10^{12}$ |
| First collision neutron dose, $D_n^{(1)}$ (rad)                    | 2,100                 | 2,160                 |
| Maximum neutron dose, $D_n^{(max)}$ (rad)                          | 3,430                 | 3,530                 |
| Gamma Dose, $D_\gamma$ (rad)                                       | 3,700                 | 3,780                 |

d. Film Badge Clip, Spring and Pin Neutron Activation

The threshold reaction  $\text{Fe}^{54} (n, p) \text{Mn}^{54}$  is used to determine the fast neutron flux at the film badge location and then the total neutron current density incident on the badge. It is shown in Section III-C and in Appendix B-5 that, the activated to target atom ratio,  $\frac{N^*}{N}$ , is related to the flux of neutrons above 3 Mev through an effective reaction cross section  $\bar{\sigma}_{E=3 \text{ Mev}}$  such that

$$\frac{N^*}{N} = \bar{\sigma}_{E=3 \text{ mev}} \times \phi_1 \quad (\text{III-D-18})$$

$\bar{\sigma}_{E=3 \text{ Mev}}$  has been evaluated in Appendix B-5, Section 2.2 for the  $\text{Fe}^{54} (n, p) \text{Mn}^{54}$  reaction,

$$\bar{\sigma}_{E=3 \text{ Mev}} = 0.442 \text{ barns} \quad (\text{III-D-19})$$

The total neutron current density incident on the badge is then given by Equation (III-D-11).

$$J_S = 5.9 \phi_1 = 13.35 \frac{N^*}{N} (\times 10^{24}) \quad (\text{III-D-20})$$

Measurements and values of  $\frac{N^*}{N}$  are given in Appendix A-7. The results are summarized below.

TABLE III-D-3

|  | Clip                  | Spring                | Pin                    |
|--|-----------------------|-----------------------|------------------------|
| Flux above 3 Mev $\phi_1$ ( $n/\text{cm}^2$ )      | $7.28 \times 10^{11}$ | $9.46 \times 10^{11}$ | $10.25 \times 10^{11}$ |
| Total incident neutron density ( $n/\text{cm}^2$ ) | $4.30 \times 10^{12}$ | $5.58 \times 10^{12}$ | $6.05 \times 10^{12}$  |
| First collision neutron dose, $D_n^{(1)}$ (rad)    | 6,450                 | 8,370                 | 9,075                  |
| Maximum neutron dose $D_n^{(\text{max})}$ (rad)    | 10,535                | 13,670                | 14,820                 |
| Gamma ray dose $D_\gamma$ (rad)                    | 11,290                | 14,650                | 15,880                 |

The results using the film badge clip, spring and pin activation measurements are not felt to be very reliable because (1) the internal consistency of the measurements is poor and (2) the cross section information for the  $\text{Fe}^{54} (n, p)$  reaction (Appendix B-5, Section 2.2) is incomplete and hence, calculated effective cross sections may be incorrect.

e. Summary of the Calculated Doses Received by the Operator

The calculated doses received by the Operator are summarized in Table III-D-4. Note that the values given in the table are rounded off computed values. An average value for the two indium activation measurements is given.

TABLE III-D-4

Dose Received by the Operator

|                                     | Total uncollided<br>incident current<br>$J_S, n/cm^2$ | "First Collision"<br>neutron dose<br>$D_n^{(1)}, rads$ | Maximum neu-<br>tron dose<br>$D_n^{(max)}, rads$ | Gamma<br>dose<br>$D_\gamma, rads$ | $D_n^{(1)} + D_\gamma$<br>rads | $D_n^{(max)} + D_\gamma$<br>rads |
|-------------------------------------|---|--|--|-----------------------------------|--------------------------------|----------------------------------|
| $Na^{24}$ in<br>blood               | $2.07 \times 10^{12}$                                 | 3,110  | 5,100  | 5,430                             | 8,540                          | 10,530                           |
| Pubic hair                          | $4.18 \times 10^{12}$                                 | 6,300  | 10,200   | 11,000                            | 17,300                         | 21,000                           |
| Head hair                           | $1.01 \times 10^{12}$                                 | 1,500  | 2,500  | 2,700                             | 4,200                          | 5,200                            |
| Indium foil<br>(on chest<br>pocket) | $1.42 \times 10^{12}$                                 | 2,150  | 3,500  | 3,750                             | 5,900                          | 7,250                            |
| Film Badge+<br>(on chest<br>pocket) |   |  |  |                                   |                                |                                  |
| Clip                                | $4.30 \times 10^{12}$                                 | 6,500  | 10,500   | 11,300                            | 17,800                         | 21,800                           |
| Spring                              | $5.58 \times 10^{12}$                                 | 8,400  | 13,700   | 14,700                            | 23,100                         | 28,400                           |
| Pin                                 | $6.05 \times 10^{12}$                                 | 9,100  | 14,800   | 15,900                            | 25,000                         | 39,800                           |

+Results based on the film badge Iron 54 activation are not consistent nor reliable.



## D. Estimates of the Doses Received by Personnel

### 2. Estimates of Doses Received by the Superintendent and Supervisor

The doses received by the Superintendent and the Supervisor are estimated using the following sources of information.

- a. Na24 activity in whole body
- b. Phosphorous activity in hair samples
- c. Indium foils neutron activation, although it is not sure that the indium foil attributed to the Superintendent was actually worn by him (Appendix A-7)
- d. Silver coins neutron activations for the Superintendent
- e. Cr51 activity in watch for the Supervisor

Methods used to determine the doses are discussed in Appendix B-5 and the experimental data are presented in Appendices A-7 and A-8.

The use of thermal activations at large distances from the tank leads to a large uncertainty in the dose estimates because it is difficult to relate the thermal flux to the fast neutron current which contributes most of the dose. The reflection of thermal neutrons by the walls is the cause of the uncertainty. It should be noted that the activation of hair yields doses in conflict with all other measurements of fast flux. The sodium activity in the body results mainly from non-thermal neutrons and is more reliable. Each of the five methods employed is discussed in turn.

#### a. Sodium Activation in Whole Body

Measurements made at the Massachusetts Institute of Technology on sodium activation in the whole body (Appendix A-8) are as follows:

$$\left\{ \begin{array}{l} (4.6 \pm 0.5) \times 10^{-9} \text{ curies for the Supervisor} \\ (2.2 \pm 0.3) \times 10^{-9} \text{ curies for the Superintendent} \end{array} \right.$$

as of 5:00 PM, EDT, 30 July 1964. The Supervisor's and Superintendent's weights are 83 and 90 kgs., respectively; body density is taken as 1 g./cc. Then the activities in  $\mu\text{c}/\text{cc}$  corrected for decay are given by:

$$\left\{ \begin{array}{l} (3.73 \pm 0.41) 10^{-5} \frac{\mu\text{c}}{\text{cc}} \text{ for the Supervisor} \\ (1.64 \pm 0.29) 10^{-5} \frac{\mu\text{c}}{\text{cc}} \text{ for the Superintendent} \end{array} \right.$$

Concentration of sodium 23 in whole body is 1.51 mg/liter (Appendix A-8) or  $(3.95 \times 10^{-5}) \times 10^{24}$  atoms of Na23 per cc. The ratio of Na24 to Na23 atoms are readily computed:

$$\left\{ \begin{array}{l} \frac{N^*}{N} = (2.69 \pm 0.29) \times 10^{-24} \text{ for the Supervisor} \\ \frac{N^*}{N} = (1.19 \pm 0.16) \times 10^{-24} \text{ for the Superintendent} \end{array} \right.$$

a. Sodium Activation in Whole Body

Use of Equations (III-D-1), (III-D-4) and (III-D-5) yields the total uncollided current density on the body,  $J_S$ , and the doses received by both men. The gamma to first collision neutron dose for the total configuration is:

$$\frac{D_\gamma}{D_n^{(1)}} = 1.34 \quad (\text{III-D-21})$$

The results are summarized in Table III-D-5. At this distance  $\bar{a}$  is 1.245 with large uncertainty.

TABLE III-D-5

| Na <sup>24</sup> Activation - Doses Received by the Supervisor and the Superintendent |                    |                    |
|---|--------------------|--------------------|
|   | Supervisor         | Superintendent     |
| Thermal flux $\varphi_{\text{oth}}$ (n/cm <sup>2</sup> )                              | $5.67 \times 10^9$ | $2.51 \times 10^9$ |
| Total incident current density $J_S$ (n/cm <sup>2</sup> )                             | $2.2 \times 10^9$  | $9.8 \times 10^8$  |
| "First collision" neutron dose $D_n^{(1)}$ , rads                                     | 3.3                | 1.5                |
| Maximum neutron dose $D_n^{(\text{max})}$ , rads                                      | 5.4                | 2.4                |
| Gamma dose $D_\gamma$ , rads  | 4.42               | 2.0                |
| Precision of the values   | 50%                | 50%                |

b. Phosphorous Activity in Hair

Measurements made at Los Alamos (Appendix A-8) on sulfur activation in hair samples provided the following disintegration rates per gram of hair corrected for decay (dpm/g. of hair):

|                |                            |
|----------------|----------------------------|
| Superintendent | Pubic Hair: 38             |
|                | Head Hair: 12              |
| Supervisor     | Pubic and Chest Hair: 51.8 |

The head hair sample was taken after a haircut and the sample may therefore be somewhat diluted. Use of Equation (III-D-9) gives the  $\frac{N^*}{N}$  ratio of  $P^{32}$  to  $S^{32}$  atoms for each sample.

Since both the Supervisor and the Superintendent were approximately 15 feet away from the critical assembly, the average cosine of the angular distribution of neutrons of energy higher than 3 Mev  $\bar{w}_1$ , is approximately 1. This value of  $\bar{w}_1$  is introduced in Equation (III-D-11) to compute the total neutron current density incident on the hair samples.

$$J_S = 8.26 \phi_1 = 20.75 \frac{N^*}{N} \quad (\text{III-D-22})$$

where  $\phi_1$  is the neutron flux above 3 Mev at the hair location. The calculated values of  $\phi_1$ ,  $J_S$ , and doses are summarized in Table III-D-6.

TABLE III-D-6

| Summary of Results Relating to the Hair Analysis   |                      |                       |                      |
|--|----------------------|-----------------------|----------------------|
|  | Supervisor           | Superintendent        |                      |
|  | Pubic and Chest Hair | Pubic Hair            | Head Hair            |
| $(N^*/N) \times 10^{24}$                           | $1.62 \times 10^9$   | $1.19 \times 10^9$    | $.38 \times 10^9$    |
| Neutron flux above 3 Mev $\phi_1$ ,<br>$n/cm^2$    | $4.07 \times 10^9$   | $2.99 \times 10^9$    | $.95 \times 10^9$    |
| Total incident current density<br>$J_S$ , $n/cm^2$ | $3.36 \times 10^9$   | $2.47 \times 10^{10}$ | $.79 \times 10^{10}$ |
| First collision neutron dose<br>$D_n^{(1)}$ , rads | 50.4                 | 37.1                  | 11.9                 |
| Maximum neutron dose,<br>$D_n^{(max)}$ , rads      | 82.3                 | 60.5                  | 19.4                 |
| Gamma dose $D_\gamma$ , rads                       | 67.5                 | 49.6                  | 15.9                 |

c. Indium Foil Activation

Methods of calculating thermal flux at the foil location and the corresponding total incident neutron current density have been described in Section III.D.I.C. Experimental results and calculated ratios of In 114m to In 113 atoms are presented in Appendix A-7 which also describes the assumption that a certain foil was worn by the Superintendent.

|                                | In <sup>114m</sup> to In <sup>113</sup> atom ratio, $\frac{N^*}{N} \times 10^{24}$ |
|--------------------------------|--|
| Superintendent's presumed foil | $6.14 \times 10^{10}$  |
| Supervisor's foil              | $10.0 \times 10^{10}$  |

The thermal Maxwell average thermal fluxes at the foil location are computed using Equation (III-D-14). The relation between total incident current density and thermal flux is given by Equation (III-D-15) in which 1 is taken as the average cosine of the thermal neutron angular distribution and 11.5 as the correction factor for scattered thermal neutrons (see Appendix B-5). Hence, we may write:

$$J_S = 0.40 \phi_{\text{oth}} = .00805 \frac{N^*}{N} \times 10^{+24} \quad (\text{III-D-23})$$

The calculated neutron current density incident on the foil and doses are presented in Table III-D-7 following.

TABLE III-D-7

| Summary of Results Relating to the Indium Foils            |                    |                    |
|--|--------------------|--------------------|
|  | Supervisor         | Superintendent     |
| Thermal flux $\phi_{\text{oth}}$ , n/cm <sup>2</sup>       | $2.02 \times 10^9$ | $1.24 \times 10^9$ |
| Total uncollided current density $J_S$ , n/cm <sup>2</sup> | $0.81 \times 10^9$ | $0.50 \times 10^9$ |
| "First Collision" neutron dose, $D_n^{(1)}$ , rads         | 1.2                | 0.75               |
| Maximum neutron dose, $D_n^{(\text{max})}$ , rads          | 2.0                | 1.22               |
| Gamma ray dose, $D_\gamma$ , rads                          | 1.6                | 1.0                |

d. Silver Coin Activations (Applies to Superintendent only)

Experimental results and calculations of Ag 110m to Ag 109 atom ratio presented in Appendix A-7 show that there are discrepancies between measurements made at United Nuclear Corporation Pawling Laboratories (UNC-P), the USAEC Idaho Falls Health Physics Division (AEC-ID), and at Oak Ridge National Laboratory (ORNL). The question of the accuracy of Ag 110m determinations is dealt in detail in Appendix A-7. The conclusion has been reached that the results obtained at UNC-P are reasonable and are in good agreement with results from ORNL. The values calculated from AEC-ID measurements should be reduced by about 31% to account for the contribution of the 0.935 Mev and higher energy gamma rays. Even so, the agreement is not satisfactory as can be seen in the following summary.

TABLE III-D-8

| Summary of Results Relating to the Superintendent's Silver Coins |                         |   |  |
|--|-------------------------|---|--|
| Item   | Laboratory              | Ratio of Ag <sup>110m</sup><br>Ag <sup>109</sup> atoms,<br>$N^*/N \times 10^{24}$ | Comments                                       |
| Dime #1 (right side pocket of trousers)                          | UNC-P<br>UNC-P          | $9.10 \times 10^9$<br>$10.04 \times 10^9$   | .66 Mev $\gamma$ -ray<br>.88 Mev $\gamma$ -ray |
| Dime #2 (left hip pocket)  | UNC-P<br>AEC-ID<br>ORNL | $8 \times 10^9$<br>$15 \times 10^9$<br>$7 \times 10^9$                            | Note 1<br>Note 2                               |
| Silver dollar (right side pocket)                                | UNC-P<br>AEC-ID<br>ORNL | $5.42 \times 10^9$<br>$7.78 \times 10^9$<br>$6.66 \times 10^9$                    | Note 1<br>Note 2                               |

NOTE 1 Measured values were reduced by 31% (Appendix A-7).

NOTE 2 Letter, J. Auxier to M. Shapiro, 11/11/64 in which Ag 110m activities are given as  $15.1 \pm 1.5$  and  $16.3 \pm 1.6$  picocuries/gm. for dollar and dime respectively.

The thermal flux at the coin locations is computed using Equation (III-D-14). Since the non-thermal contribution to the activation is negligible, Equation (III-D-14) can be written:

$$\frac{N^*}{N} = \varphi_{\text{oth}} \sigma_{\text{th}} f \quad \text{where } \sigma_{\text{th}} = 2.84 \text{ barns.} \quad (\text{III-D-24})$$

The self protection correction factors are estimated as follows:

Considering the coins as slab of thickness  $t$  in ( $\text{g}/\text{cm}^2$ ), the Maxwell average absorption cross section,  $\bar{\mu}_a$ , in  $\frac{\text{cm}^2}{\text{g}}$  for the coins is calculated

$$\bar{\mu}_a \approx 0.6023 \left[ .10 \times \frac{3.34}{63} + .90 \times \frac{77.1}{109} \right]$$

$$\bar{\mu}_a \approx 0.39 \frac{\text{cm}^2}{\text{g}}$$

where: 3.34 and 77.1 are the Maxwell average absorption cross sections of copper and silver respectively (in barns):

- .10 and .90 are the weight fraction of copper and silver respectively in the coins;
- 63 and 109 are their atomic masses.

The number of absorption mean free paths in the coins,  $\bar{\mu}_a t$ , can be evaluated if the weight and cross section area of the coins are measured.

$$\text{For the silver dollar: } \bar{\mu}_a t \text{ dollar} = .39 \times \frac{19.615}{11.40} = 0.671$$

$$\text{For the dimes: } \bar{\mu}_a t \text{ dime} = .39 \times \frac{2.47}{2.50} = 0.385$$

Self protection as a function of  $\frac{\bar{\mu}_a t}{2}$  in slab geometry<sup>+</sup> is tabulated and plotted in Reference 12, Appendix C.

We obtain

$$f_{\text{dollar}} = 0.49$$

$$f_{\text{dime}} = 0.61$$

Then the thermal fluxes are computed by introducing these values into Equation (III-D-24).

The relation between  $\varphi_{\text{oth}}$  and  $J_S$ , the total current density incident on the coins is given by:

$$J_S = .40 \varphi_{\text{oth}} \quad (\text{III-D-25})$$

Conversion factors for doses are given in Equations (III-D-4), (III-D-5) and (III-D-21). The results are summarized in Table III-D-9. It must be noted that after corrections, the results based on silver coin activation are consistent except for the dime in the left hip trouser pocket, which was measured at Idaho Falls.

+ Coins are assumed to be placed in a homogeneous region, which is not correct.

TABLE III-D-10

Doses Received by the Superintendent Based on Silver Coin Activation

| Item   | Laboratory          | Thermal Flux<br>$\phi_{th}, n/cm^2$ | Total Uncollided<br>Current Density Incident<br>$J_S, (n/cm^2)$ | First Collision<br>Neutron Dose,<br>$D_n^{(1)}, rads$ | Maximum Neutron<br>Dose rads<br>$D_n^{(max)}$ | Gamma Dose<br>$D_\gamma, rads$ |
|--|---------------------|-------------------------------------|---|---|---|--------------------------------|
| Dime in right<br>side trouser<br>pocket          | UNC-P               | $5.28 \times 10^9$                  | $.211 \times 10^{10}$   | 3.16  | 5.16  | 4.23                           |
|  | UNC-P               | $5.82 \times 10^9$                  | $.233 \times 10^{10}$   | 3.49  | 5.70  | 4.67                           |
| Dime in left<br>hip trouser<br>pocket            | UNC-P               | $4.64 \times 10^9$                  | $.185 \times 10^{10}$   | 2.78  | 4.45  | 3.72                           |
|  | AEC-ID <sup>+</sup> | $8.70 \times 10^9$                  | $.347 \times 10^{10}$   | 5.21  | 8.50  | 6.98                           |
|  | ORNL                | $4.10 \times 10^9$                  | $.164 \times 10^{10}$   | 2.46  | 3.93  | 3.29                           |
| Silver dollar<br>in right side<br>trouser pocket | UNC-P               | $3.90 \times 10^9$                  | $.156 \times 10^{10}$   | 2.34  | 3.82  | 3.14                           |
|  | AEC-ID <sup>+</sup> | $5.00 \times 10^9$                  | $.224 \times 10^{10}$   | 3.36  | 5.47  | 4.50                           |
|  | ORNL                | $4.71 \times 10^9$                  | $.189 \times 10^{10}$   | 2.83  | 4.62  | 3.80                           |

+ measured values were reduced by 31% (Appendix A-7)

e. Cr<sup>51</sup> Activity in Watch Case (Applies to Supervisor only)

The same approach as was used for the silver coins was followed to compute the thermal flux at the watch case. The composition of the watch case, given in Appendix A-9, is Cr - 12.62%; Ni - 12.51%; and Fe - 75%. A thermal absorption cross section for that composition is then evaluated and taking a thickness of .9 g/cm<sup>2</sup> for the watch case, it is found that  $\bar{\mu}_{at} \approx .03$ , which yields a self protection factor of .97. Then, from the Cr<sup>51</sup> activation measurements, presented in Appendix B-7, one gets:

$$\frac{N^*}{N} = 6.8 \times 10^{10} \quad (\text{III-D-27})$$

Introducing Equation (III-D-27) into Equation (III-D-24) yields:

$$C_{p \text{ oth}} = \frac{6.8 \times 10^{10}}{.97 \times 12.0} = 5.84 \times 10^9 \text{ n/cm}^2.$$

Total uncollided current density incident on the case is obtained using Equation (III-D-22).

$$J_S = .40 \times 5.84 \times 10^9 = 2.34 \times 10^9 \text{ n/cm}^2.$$

The first collision neutron dose is given by:

$$D_n^{(1)} = 3.5 \text{ rads.}$$

The maximum neutron dose is:

$$D_n^{(\text{max})} = 5.73 \text{ rads.}$$

The gamma dose is:

$$D_\gamma = 4.7 \text{ rads.}$$

f. Conclusions

The doses received by the Superintendent and the Supervisor, based on the sources of information considered in this section, are summarized in Tables III-D-10 and III-D-11 on the pages following.

In Appendix B-4, it is shown that the gamma dose from fission products received by a person standing at one foot from the extraction column during the draining of the tank could range from 40R to 114R. The higher dose results if draining started within 2 minutes after the second excursion and the lower, if draining started after 6 minutes. At 10 feet, the doses are lower by a factor of 23. The film badge worn by the Superintendent indicates a total gamma exposure of 50R. Of this, approximately 1-7R result from direct exposure to the second excursion based on blood Na activation, coin and indium foil activation. The remainder can be attributed to the dose received in the draining operation.



TABLE III-D-10

Doses Received by the Superintendent During Second Excursion

| Item   | Total Incident<br>Uncollided<br>Current Density<br>$J_S, (n/cm^2)$ | First Collision<br>Neutron Dose<br>$D_n^{(1)}$ rad | Maximum<br>Neutron Dose<br>$D_n^{(max)}$ , rad | Gamma Dose<br>$D_\gamma$ , rad | $D_n^{(1)} + D_\gamma$<br>rad | $D_n^{(max)} + D_\gamma$<br>rad |
|--|--|--|--|--------------------------------|-------------------------------|---------------------------------|
| Whole body Na <sup>24</sup><br>activation                    | $9.8 \times 10^8$  | 1.5  | 2.4  | 2                              | 3.5                           | 4.4                             |
| Indium foil (presumed)                                       | $.5 \times 10^8$   | .75  | 1.2  | 1.0                            | 1.75                          | 2.2                             |
| Silver coins, right hand<br>trouser pocket<br>dime (average) | $2.25 \times 10^9$   | 3.3  | 5.4  | 4.5                            | 7.8                           | 9.9                             |
| UNC silver dollar  | $1.56 \times 10^9$   | 2.3  | 3.8  | 3.1                            | 5.4                           | 6.9                             |
| AEC-ID " "   | $2.24 \times 10^9$   | 3.4  | 5.5  | 4.5                            | 7.9                           | 10.0                            |
| ORNL " "   | $1.90 \times 10^9$   | 2.8  | 4.6  | 3.8                            | 6.6                           | 8.4                             |
| Left hip trouser pocket<br>dime UNC-P                        | $1.85 \times 10^9$   | 2.8  | 4.5  | 3.7                            | 6.5                           | 8.2                             |
| " AEC-ID   | $3.47 \times 10^9$   | 5.2  | 8.5  | 7.                             | 12.2                          | 15.5                            |
| " ORNL   | $1.63 \times 10^9$   | 2.5  | 3.9  | 3.3                            | 5.8                           | 7.2                             |
| Hair- pubic  | $2.47 \times 10^{10}$  | 37   | 61   | 50                             | 87                            | 111                             |
| head   | $.79 \times 10^{10}$   | 12   | 19   | 16                             | 28                            | 35                              |

TABLE III-D-11

Doses Received by the Supervisor During Second Excursion

| Item                                    | Total Incident Current Density<br>$J_S$ (n/cm <sup>2</sup> ) | First Collision Neutron Dose<br>$D_n(1)$ , rad | Maximum Neutron Dose<br>$D_n(max)$ , rad | Gamma Dose<br>$D_\gamma$ , rad | $D_n(1) + D_\gamma$<br>rad | $D_n(max) + D_\gamma$<br>rad |
|---|--|--|--|--------------------------------|----------------------------|------------------------------|
| Whole body Na <sup>24</sup> activation  | $2.2 \times 10^9$  | 3.3  | 5.4                                      | 4.4                            | 7.7                        | 9.8                          |
| Indium foil                             | $8.1 \times 10^8$  | 1.2  | 2.0                                      | 1.6                            | 2.8                        | 3.6                          |
| Cr <sup>51</sup> activity in watch case | $2.34 \times 10^9$   | 3.5  | 5.7                                      | 4.7                            | 8.2                        | 10.4                         |
| Chest and pubic hair                    | $3.36 \times 10^{10}$  | 50.0   | 82.0                                     | 68.0                           | 118.0                      | 150.0                        |

f. Conclusions

There is no direct measurement of the gamma exposure of the Supervisor. From the blood sodium activation data, a gamma exposure of  $\sim 5R$  is estimated. The dose received during the draining operation should be of the same order of magnitude ( $\sim 50R$ ) as that received by the Superintendent. It may be somewhat higher due to the difference in the activities of the two men in the draining operation.

It must be noted that the dose values derived from the hair analysis and some silver coin activation measurements are inconsistent with the other calculated dose results.

Doses based on hair activation measurements are too high for the following reasons:

- (1) The neutron dose based on the Superintendent's pubic hair analysis is about 500 rem, using an RBE of 8.3 calculated from the spectrum to which personnel was exposed. The gamma exposure shown by the film badge is 50 rem. A total exposure of 550 rem is clearly inconsistent with the medical findings. The same conclusion is reached when the Supervisor's exposure is estimated from the hair analysis ( $\sim 740$  rem).

It must be noted that the Superintendent's head hair analysis leads to a much smaller dose which is probably due to the fact that the sample was taken after some haircuts. Indeed, the pubic and head hair should have been exposed to equal doses because the incident fast neutron flux should form a broad, approximately parallel beam over the entire body at a distance of 15 feet from the source.

- (2) There was no observable peak in the vicinity of 0.81 Mev when the  $Co^{58}$  activity in the Supervisor's watch case was measured. The experimental response from 770 kev to 845 kev has been summed up for the measurements with and without the watch case. The peak integral value given in Appendix A-7 is the difference between these sums. The calculated  $Co^{58}$  to  $Ni^{58}$  atom ratio is:

$$\frac{N^*}{N} = (1.35 \pm 1.06) \times 10^8$$

The effective cross section for the  $Ni^{58}$  (n, p) reaction used to compute the fast neutron flux above 3 Mev is 0.531 barns (Appendix B-5), Section 2.2. Then the flux above 3 Mev is:

$$\phi_1 = (2.54 \pm 1.99) 10^8 \text{ n/cm}^2$$

The ratio of this flux value to that computed from the hair analysis ( $4.07 \times 10^9 \text{ n/cm}^2$ ) is less than 1/16. If the flux above 3 Mev was equal to  $4 \times 10^9 \text{ n/cm}^2$ , the 0.81 Mev  $Co^{58}$  peak would have been clearly visible.

It is finally concluded that the activation of blood sodium provides the most reliable

f. Conclusions

estimate of the doses. The estimated doses are summarized as follows, based on Na<sup>24</sup> activation in the body:

|                       |                              |              |                        |
|-----------------------|------------------------------|--------------|------------------------|
| <u>Operator</u>       | First collision neutron dose | 3,100 rad    |                        |
|                       | Whole body* neutron dose     | 5,100        |                        |
|                       | Gamma ray dose               | <u>5,400</u> |                        |
|                       | Whole Body Dose              | 10,500 rad   |                        |
| <u>Superintendent</u> | First collision neutron dose | 0.8-3.0 rad  |                        |
|                       | Whole body neutron dose      | 1.2-5.0 rad  | 10-41 rem <sup>+</sup> |
|                       | First burst gamma dose       | 1-5          | 1-5                    |
|                       | Second burst gamma dose      | 49-45        | <u>49-45</u>           |
|                       | Total                        |              | 60-91 rem              |
| <u>Supervisor</u>     | First collision neutron dose | 1.2-3.5 rad  |                        |
|                       | Whole body neutron dose      | 2-6 rad      | 16.6-49.5 rem          |
|                       | First burst gamma dose       | 2-5 rad      | 2-5                    |
|                       | Second burst gamma dose      | 45-49        | <u>45-49</u>           |
|                       | Total                        |              | 64-104 rem             |

---

\*This is also known as the maximum neutron dose  $D_n^{(max)}$ .

<sup>+</sup> Neutron dose was corrected from rad to rem using an RBE of 8.3 calculated from the spectrum to which personnel were exposed. No conversion was attempted for the Operator because of the uncertainty in the value of the RBE for lethal doses.

#### IV CONCLUSIONS

The following conclusions were reached

- A. The first excursion occurred when a solution of concentrated uranyl nitrate (256 gms/l.) was poured from safe geometry into an 18" diameter vessel. Approximately 2600 grams of U235 were in the system when criticality first occurred.
- B. A second excursion probably occurred in the system, which still contained approximately 1870 grams U235, when the electric stirrer was turned off and the flattening of the liquid surface added approximately 0.02 in k.
- C. Total fissions which occurred are estimated as

|                  |                               |
|------------------|-------------------------------|
| First excursion  | $1.0 - 1.1 \times 10^{17}$    |
| Second excursion | $0.2 - 0.3 \times 10^{17}$    |
| Total            | $1.3 \pm 0.25 \times 10^{17}$ |

- D. Radiation doses received by personnel were estimated to be

|                |               |
|----------------|---------------|
| Operator       | 10,500 rads   |
| Superintendent | 60 - 91 rems  |
| Supervisor     | 64 - 104 rems |

APPENDIX

## INDEX

## APPENDIX - A

EXPERIMENTAL DATA

| <u>Number</u> | <u>Identification</u>   | <u>Page(s)</u> |
|---------------|---|----------------|
| A-1           | Physical Measurements of the Accident Environment                   | A-1.1 - 1.9    |
| A-2           | Radiation Readings in the Period Following the Incident             | A-2.1 - 2.3    |
| A-3           | Investigation of the Chemical Aspects Relating to the Incident      | A-3.1 - 3.6    |
| A-4           | Sodium Activation Analysis for Supernatant Liquid Samples           | A-4.1 - 4.3    |
| A-5           | Radiochemical Analysis of the Fission Products                      | A-5.1 - 5.6    |
| A-6           | Determination of Uranium and Sodium Contents in Tank                | A-6.1 - 6.4    |
| A-7           | Activation Analysis of Metallic Samples                             | A-7.1 - 7.10   |
| A-8           | Hair Sulfur and Blood and Whole Body Sodium Activation Measurements | A-8.1 & 8.2    |
| A-9           | Spectrographic Analysis of Metallic Samples                         | A-9.1          |
| A-10          | Miscellaneous Measurements  | A-10.1- 10.5   |

Activation measurements were made at several laboratories that will be referenced along with their data. It will be seen that activation determinations for some particular samples differ sometimes by large factors and these discrepancies remained unexplained after long discussions. Therefore, observed detector responses along with the various correction factors used to derive the activation will be presented in this data.

### THE ACCIDENT ENVIRONMENT

Criticality occurred in the carbonate make-up tank located in the third floor tower room. Figure A-1-A is a drawing of the plant layout. A door is 15 feet from the tank, reached by the stairwell and opens outward from the room into the landing. Between the stairwell and the tower room is a hollow concrete block wall. Figure A-1-B is a photograph of the room taken from the vicinity of the door. The wall switch operates the stirrer motor. The four-foot, 11 liter polyethylene container is shown on the floor in its final position following its removal from the tank by the Superintendent. The drain pipe can be seen leading from the bottom of the tank down past the valve, bending first to the wall and then to the left. The complete drainage path through the funnel on the second floor and into the pulse extractor column on the first floor is shown in Figure A-1-C. The second valve, tubing and funnel on the second floor are shown in the photograph, Figure A-1-D. A photograph of the extractor column (1-C-9) into which the tank was drained and out of which full jars were drawn off, is shown in Figure A-1-E. The yellow precipitate and clear supernatant liquid remaining in the columns may be seen. The photograph of Figure A-1-F shows some of the "gallon" jugs drained from the carbonate tank through column 1-C-9.

The carbonate tank is made of stainless steel. It consists of a cylinder  $1/8$ " wall thickness, 18" outside diameter, 23" high, flanged on top, and at the bottom welded to a rounded steel cap whose bottom point on the inside is  $3-5/8$ " below the cylindrical piece. (See Figure A-1-G) The liquid volume with the stirrer in place was measured as a function of liquid height. The results are:

| Volume of Liquid<br>(liters) | Height of Liquid Surface<br>Measured from bottom of<br>cylindrical portion (inches) |
|------------------------------|---|
| 30-1/2                       | 5   |
| 41                           | 7-9/16  |
| 51                           | 10-1/16   |

Again using the bottom of the cylindrical portion of the tank as reference point, the center of the stirrer blade which is close to the lower end of the stirrer rod, is  $2-3/4$ " in altitude and  $3-1/2$ " from the tank wall. The stirrer rod is at an angle to the vertical ( $32^\circ$ ). As the blade revolves, its tip approaches to within about  $1-1/2$ " of the tank wall and drops to a minimum altitude of about  $1-3/4$ ". The stirring action is quite strong at volumes in the 40-50 liter range. Air is sucked in, vortices are formed, and the surface departs from horizontal by several centimeters in altitude. The surface shape does not remain stationary, exhibiting slow changes under constant stirrer action. A photograph taken from moving pictures is given in Figure A-1-H. The stirrer blade is 201 g of stainless steel and the stirrer rod is 10 g/cm of stainless steel.

The drain pipe down to the second valve on the second floor (Figure A-1-D) has a total length of  $29-3/4$ " and flow area of  $0.304 \text{ in}^2$ , leading to a contained volume of 1.8 liters. The extractor column (1-C-9), shown in Figure A-1-E, has an inside diameter of 3 inches.



Factors Used at UNC-P in Calculation of Activations

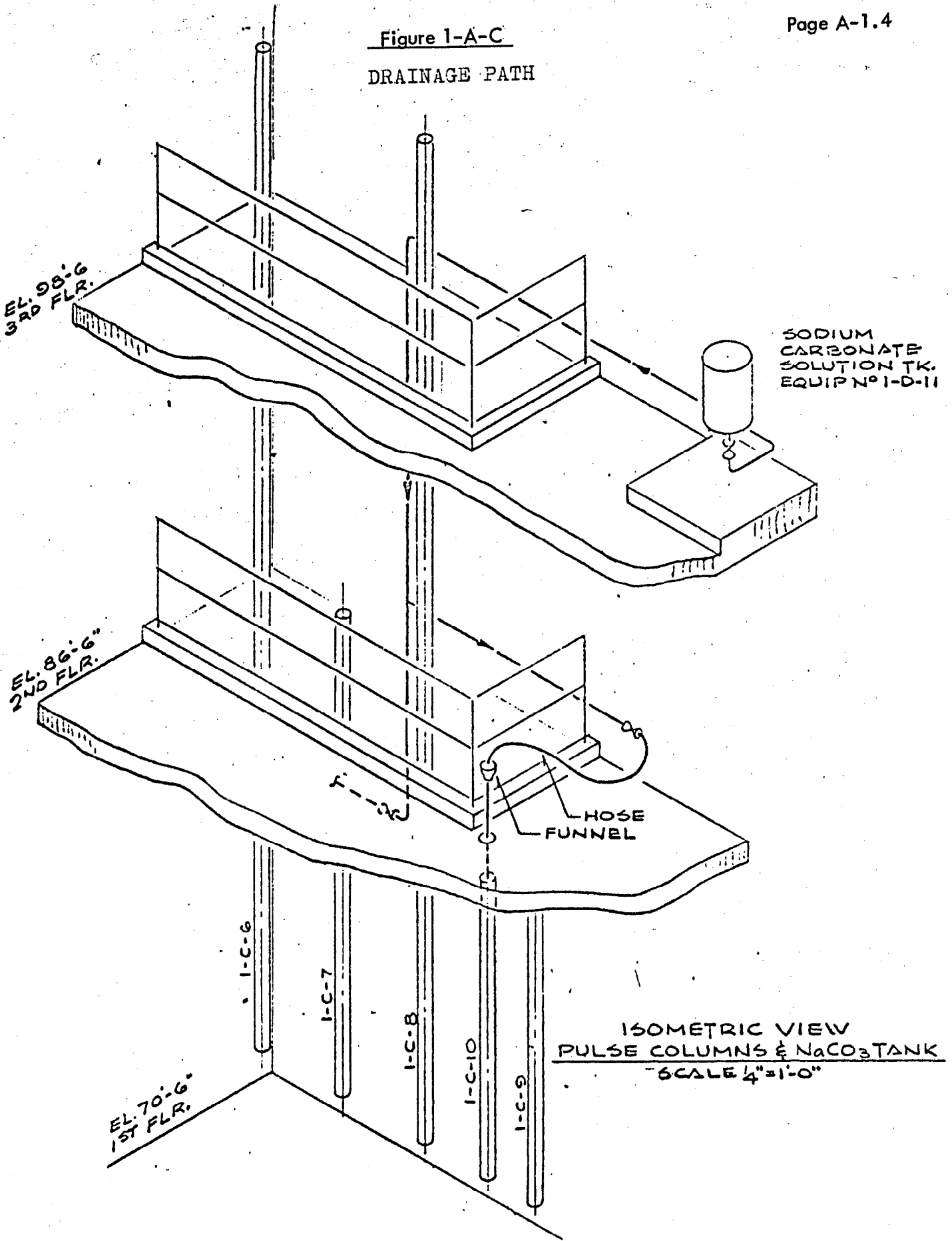
| Item                         | Gamma Energy (Mev.) | Isotope            | Detector (i) Efficiency | Branching Ratio | Gamma Attenuation Factor | $\lambda$ (sec. <sup>-1</sup> ) |
|------------------------------|---------------------|--------------------|-------------------------|-----------------|--------------------------|---------------------------------|
| Clamp #2<br>(away from tank) | .320                | Cr <sup>51</sup>   | .128                    | .098            | .805                     | $2.88 \times 10^{-7}$           |
|                              | .810                | Co <sup>58*</sup>  | .0397                   | 1               | .881                     | $1.11 \times 10^{-7}$           |
| Screwdriver                  | 1.29                | Fe <sup>59</sup>   | .00299                  | .44             | .81                      | $1.78 \times 10^{-7}$           |
|                              | .835                | Mn <sup>54</sup>   | .00454                  | 1               | .77                      | $2.65 \times 10^{-8}$           |
| Supervisor's<br>Watch Back   | .320                | Cr <sup>51</sup>   | .194                    | .098            | .944                     | $2.88 \times 10^{-7}$           |
|                              | .810                | Co <sup>58</sup>   | .0606                   | 1               | .963                     | $1.11 \times 10^{-7}$           |
| Indium Foils                 | .190                | In <sup>114m</sup> | .312                    | .1855           | .950                     | $1.60 \times 10^{-7}$           |
| Dime #1                      | .660                | Ag <sup>110m</sup> | .0575                   | 1.3             | .946                     | $3.17 \times 10^{-8}$           |
|                              | .880                | Ag <sup>110m</sup> | .0413                   | .95             | .954                     | $3.17 \times 10^{-8}$           |
| Dime #2                      | .660                | Ag <sup>110m</sup> | .0575                   | 1.3             | .946                     | $3.17 \times 10^{-8}$           |
| Silver Dollar                | .660                | Ag <sup>110m</sup> | .0492                   | 1.3             | .915                     | $3.17 \times 10^{-8}$           |
| Gold Ring                    | .411                | Au <sup>198</sup>  | .00865                  | 1.0             | .55                      | $2.97 \times 10^{-6}$           |

\* The assumption has been made that all of the activity is due to Co<sup>58</sup>. Since there is a small contribution from Mn<sup>54</sup> which cannot be resolved, the activation which is reported is an over-estimate.

(i) Detector efficiency includes the total detection efficiency, the peak-to-total ratio, a disk and coincidence loss corrections. To calculate the number of disintegrations per minute at time 0 the following expression is used:

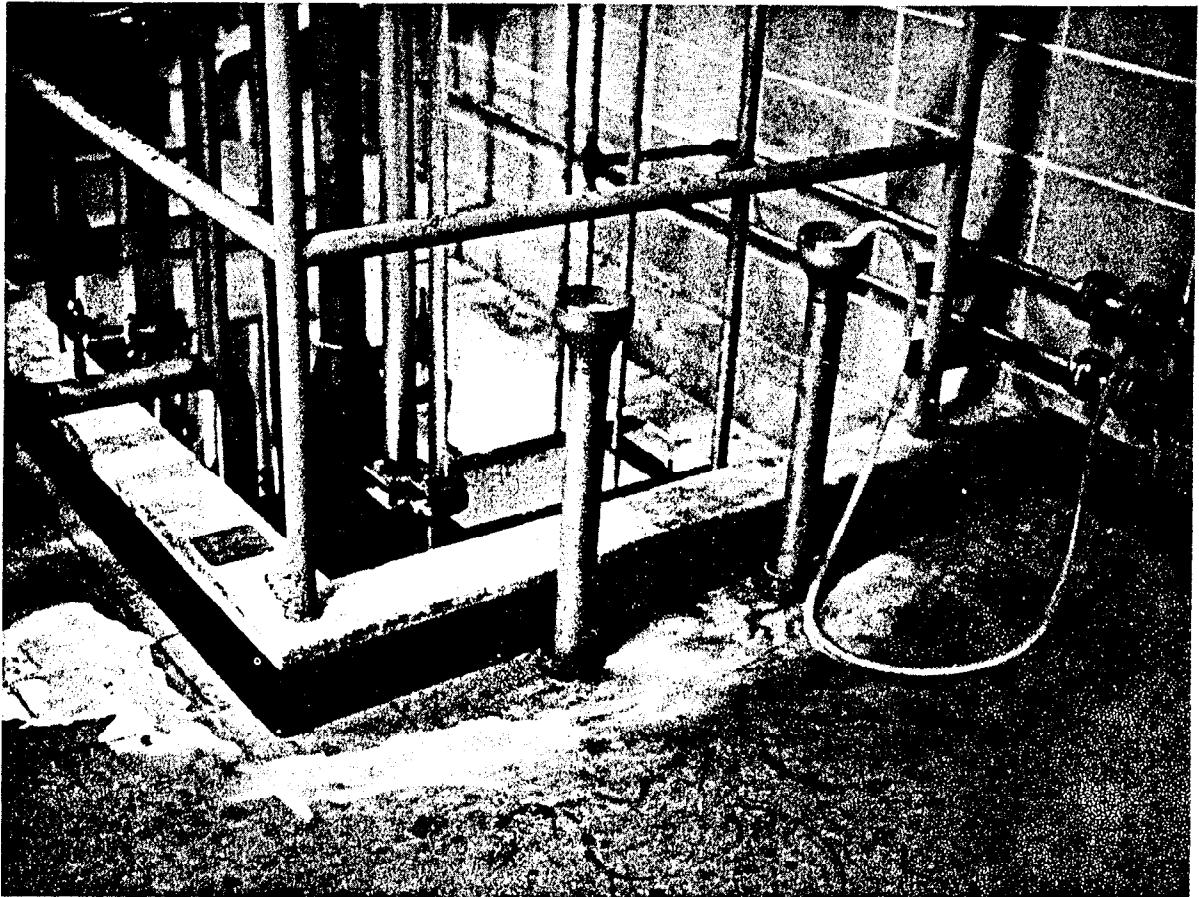
$$D(0) = \frac{\text{Peak Integral} \times \text{Decay Correction}}{\text{Detector efficiency} \times \text{Branching Ratio} \times \text{Gamma Attenuation Factor}}$$

Figure 1-A-C  
DRAINAGE PATH

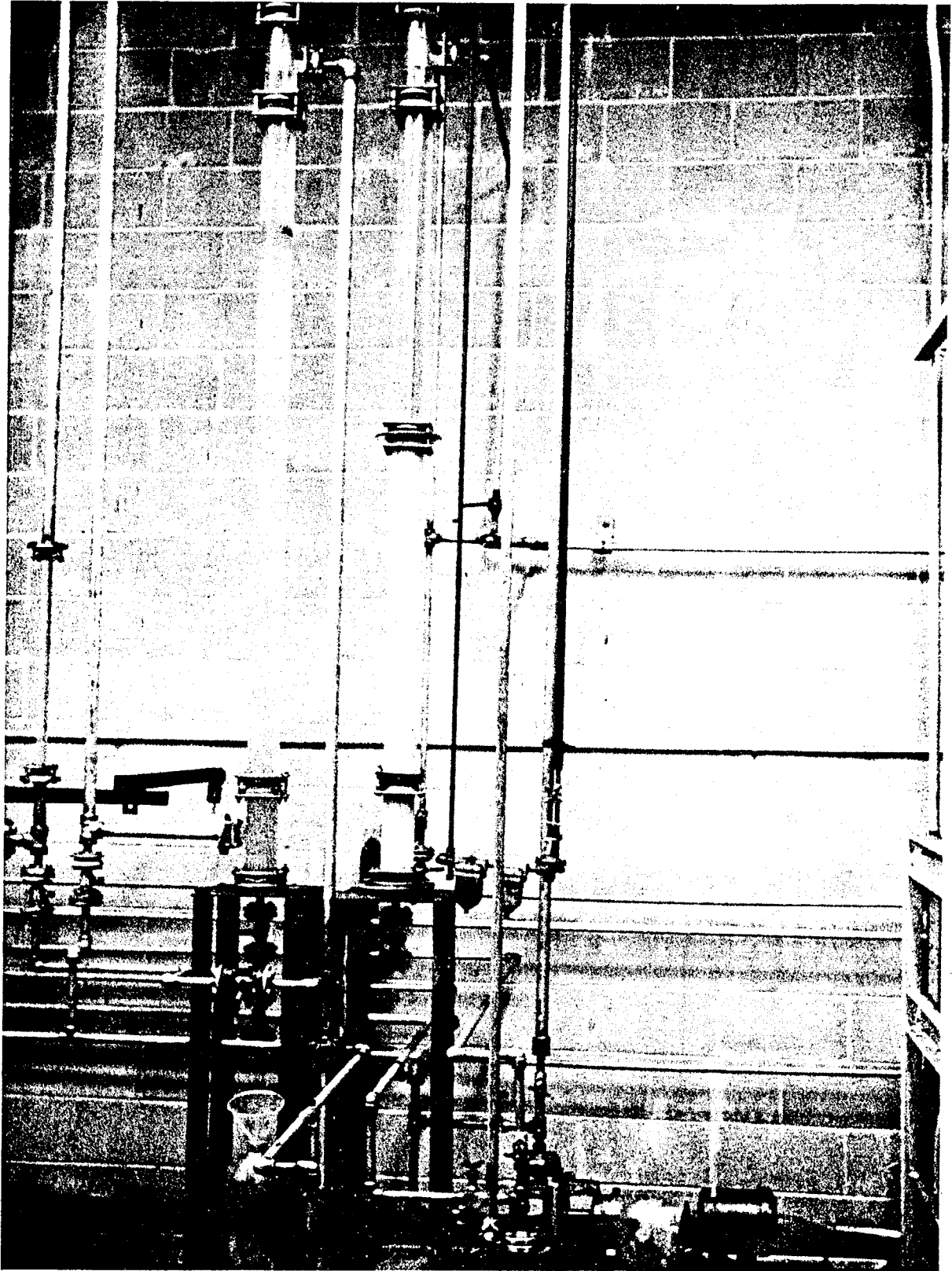


ISOMETRIC VIEW  
PULSE COLUMNS & NaCO<sub>3</sub> TANK  
SCALE 1/4" = 1'-0"

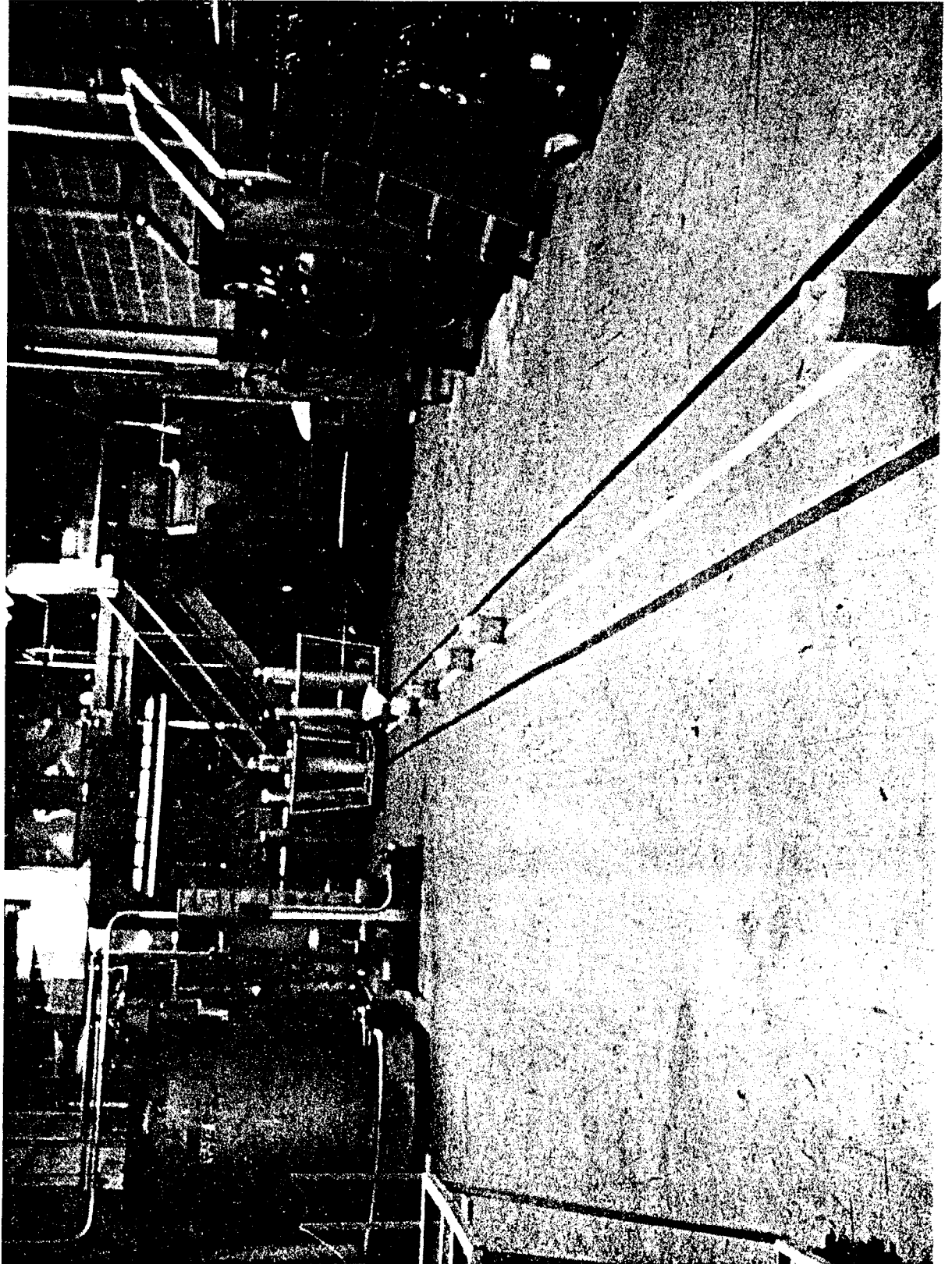
View of Second Floor Tower Room



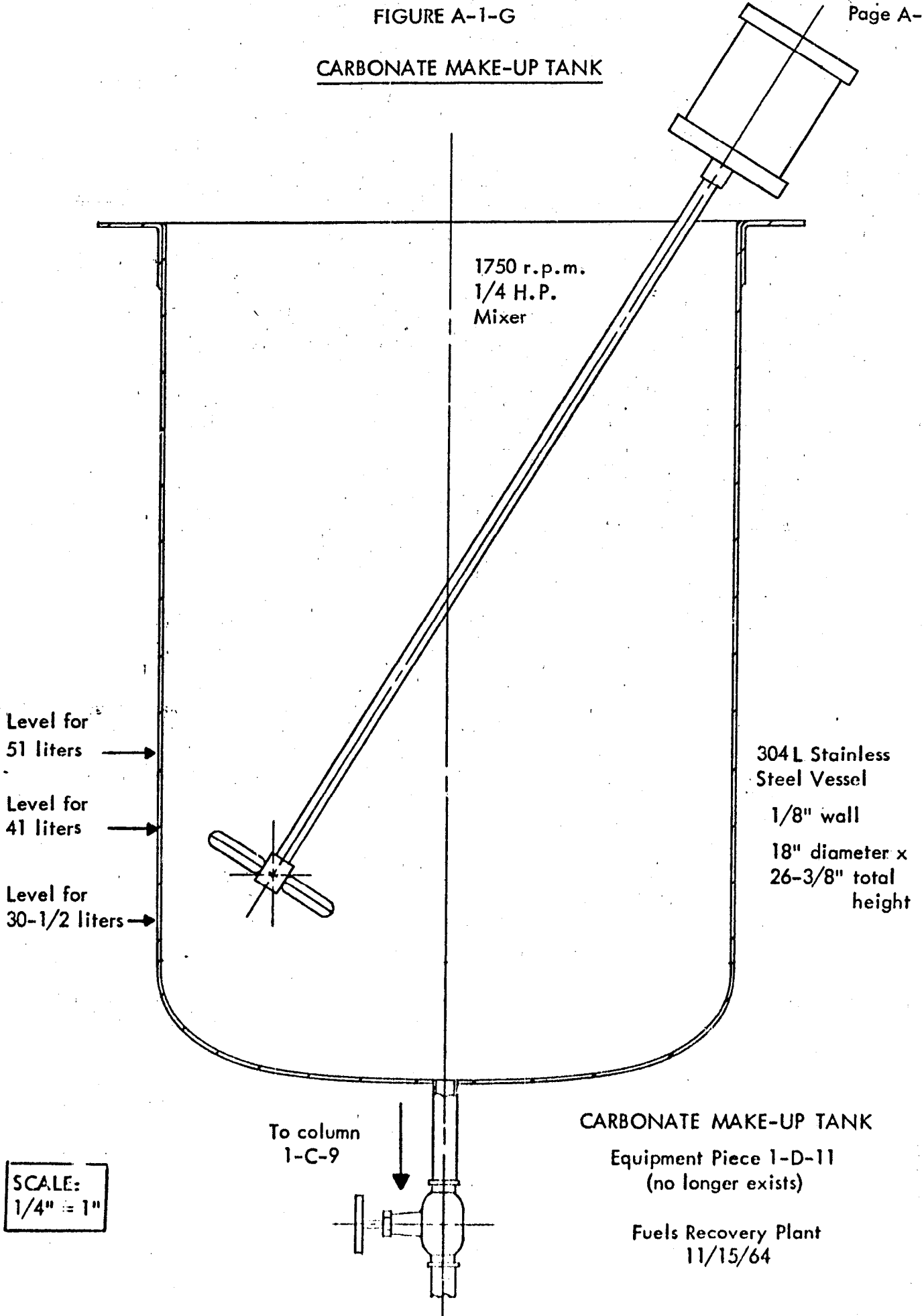
The Solvent Recovery Column (1-C-9) as seen after Make-Safe Operation. (Right Hand Column showing yellow precipitate and clear supernatant liquid).



Jars of Irradiated Material Drained from Tank after Incident (Looking east toward Evaporator (Precipitator) area).



CARBONATE MAKE-UP TANK



304 L Stainless Steel Vessel  
1/8" wall  
18" diameter x 26-3/8" total height

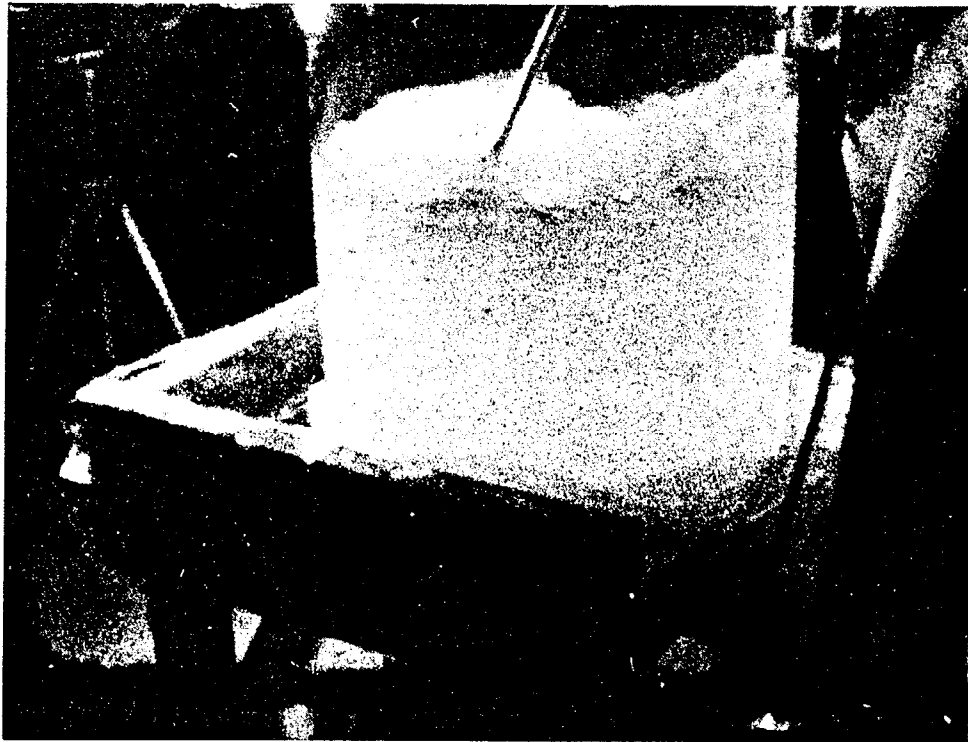
SCALE:  
1/4" = 1"

CARBONATE MAKE-UP TANK

Equipment Piece 1-D-11  
(no longer exists)

Fuels Recovery Plant  
11/15/64

Full Scale Experiment - View of the Surface Distortion  
Caused by the Electric Stirrer Action



### RADIATION READINGS IN THE PERIOD FOLLOWING THE INCIDENT

Beta/gamma instrument surveys of the plant area were conducted by the Superintendent and Supervisor with a low range counter and afterwards with two Victoreen CDV-720 Model 3A counters which can read dose rates above the 100 r/hr range.

The first two surveys with the low range meter were conducted to establish the 100 mr/hr boundary at 7:15 pm and 7:30 pm on July 24, 1964. No penetration of 100 mr/hr boundary was attempted. A complete discussion on these two surveys can be found in Reference 5 (See Appendix C) and the 100 mr/hr paths are shown in Figures A-2-A and A-2-B following.

At 7:45 pm, the Superintendent and Supervisor made the third re-entry with the objective to make the plant safe from further criticality. Using the high range meters on the 500 r/hr. scale, no significant reading was seen until the Superintendent held it over the edge of the tank at which time it read 200-300 r/hr. Within two seconds the Superintendent removed the instrument.

Because this reading is important in view of a complete description of the events following the initial criticality and the possible second critical excursion, a calibration survey of the two CDV-720 counters was made by the Radiological Office of the Rhode Island State Council of Defense (Reference 6, Appendix C) using 120 curies of Cesium 137.

The meters were found to be reading correctly to within 5% on all ranges. However, in reference to response time, in a radiation field of 550 r/hr, a reading of 300 r/hr was recorded in 2.3 seconds. Further, the specifications of CDV-720 state that after warm up of two minutes the meter responds to 95% of final reading of all dose rates measured on each scale in no more than 9 seconds. In conclusion, reading of 200-300 r/hr at the edge of tank may indicate an actual 500 r/hr dose rate if the reading time is two (2) seconds.

Other readings of interest for the subsequent calculations are the radiation intensity measurements at the emergency shack which is located approximately 450 feet from the incident. The data are summarized as follows:

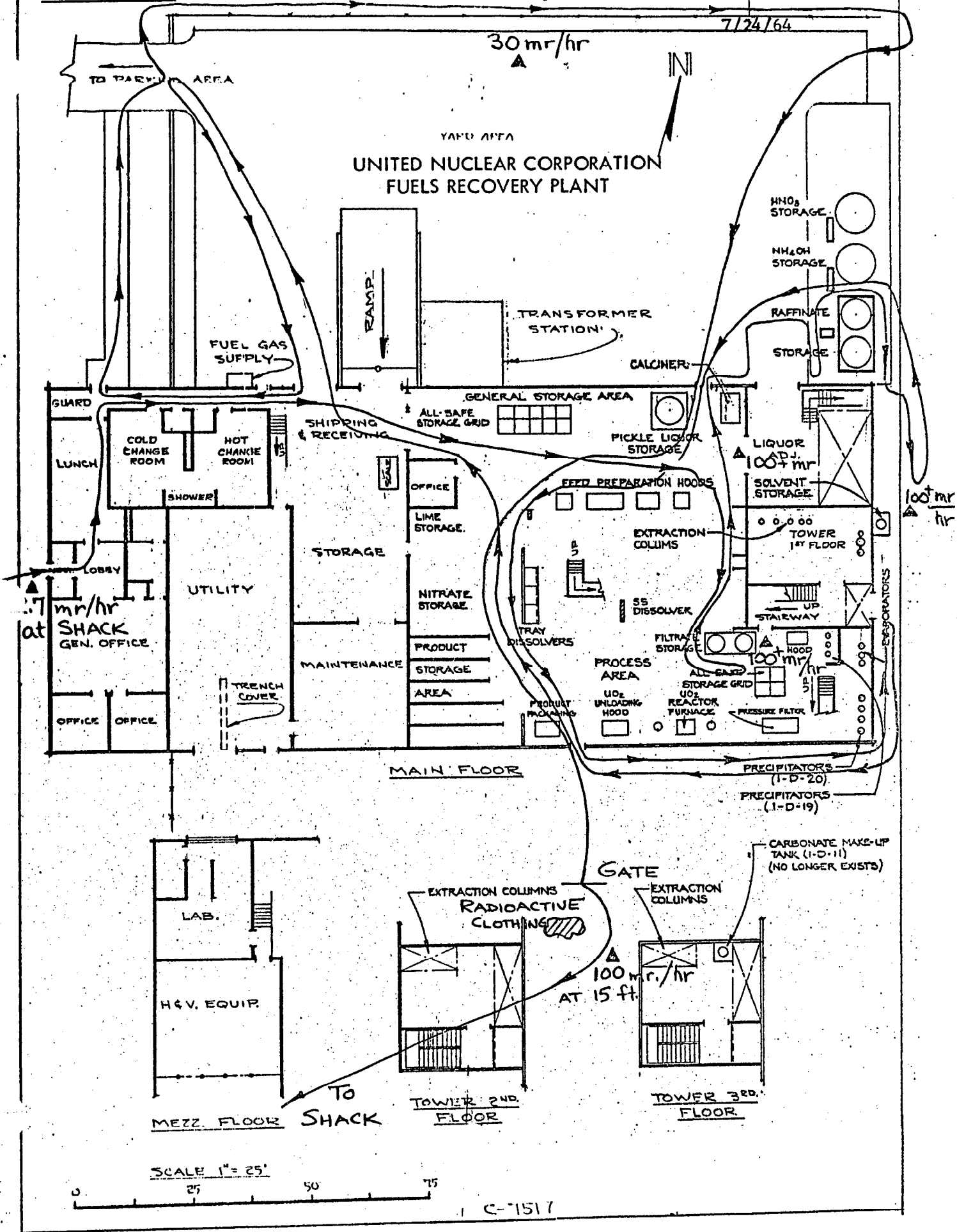
| Radiation Measurements at the Emergency Shack (using a low range counter) |                           |
|---|---------------------------|
| Time after initial criticality (minutes)                                  | Radiation Intensity mr/hr |
| 4   | 100                       |
| 9   | 60                        |
| 24  | 10-20                     |
| 84  | 12                        |
| 144   | 12                        |
| 184   | 12                        |
| 540   | 2-3                       |

The draining of the tank took place about 105 minutes after the initial burst. Hence, the plateau at about 12 mr/hr seems to continue after the entry of the personnel into the tower.

Gamma dosimetry of the film badge worn by the Superintendent showed an exposure of 50 r. The Supervisor did not wear a gamma-sensitive film badge.



FIGURE A-2-A ROUTE OF FIRST RE-ENTRY - Plant Superintendent 7:15 PM - 7:25 PM



C-7517

FIGURE A-2-B

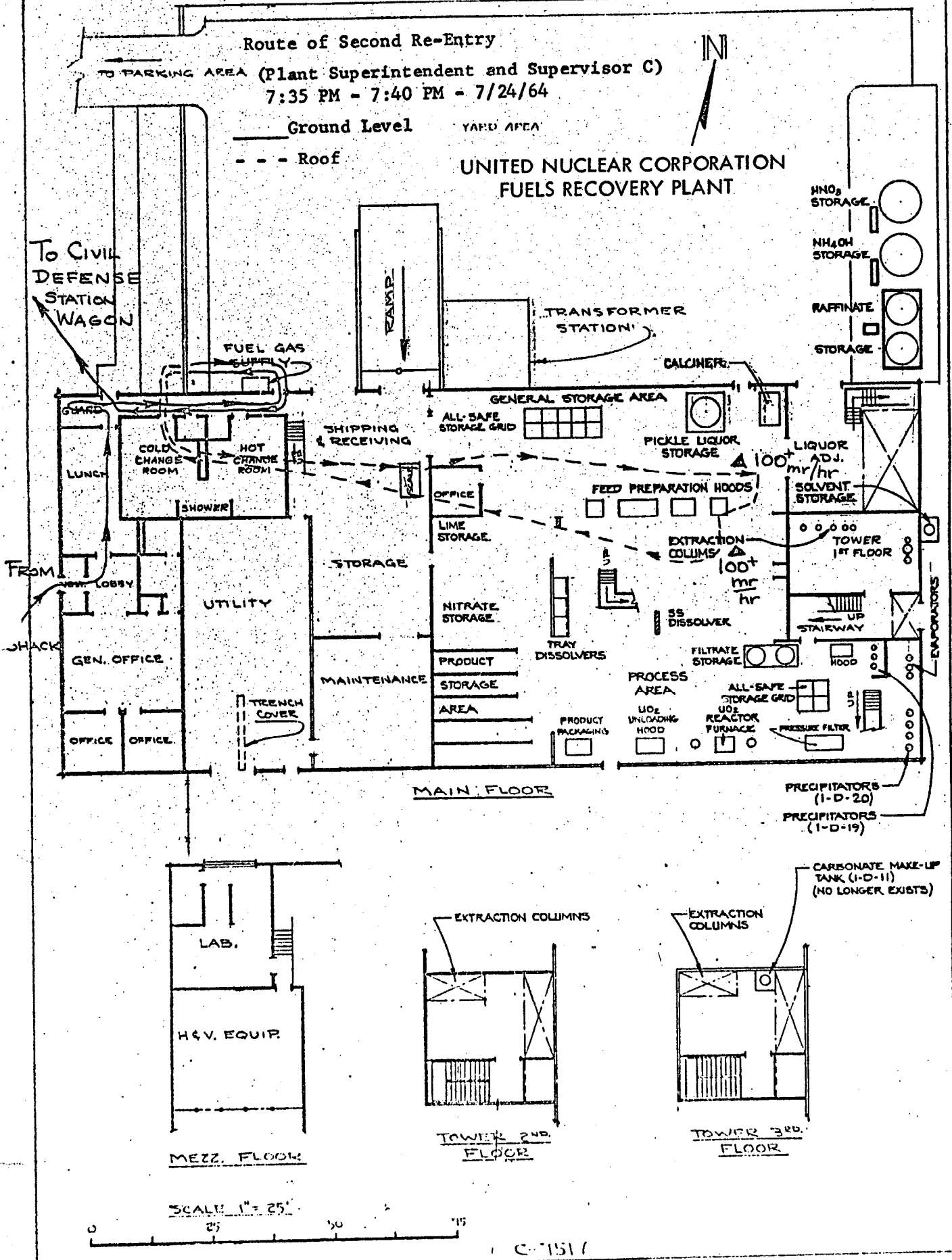


Figure A-2-B

INVESTIGATION of the CHEMICAL ASPECTS RELATING to the INCIDENT

An investigation of chemical aspects relating to the incident has also been conducted by United Nuclear Corporation. Tests and analyses were made on a laboratory scale at White Plains and on a large scale at Pawling using solution of sodium carbonate and natural uranyl nitrate in an attempt to duplicate experimentally the conditions of the accident. The following discussion summarizes the observed behavior of uranyl nitrate and sodium carbonate solutions.

Conditions under which precipitation is induced when a uranyl nitrate solution is mixed with a sodium carbonate solution at room temperature are quite limited. The principal factors which determine whether precipitation will occur are:

1. pH of the solutions after mixing.
2. Concentration of sodium carbonate solution.
3. The relative volumes of the uranyl nitrate and sodium carbonate solutions.
4. The concentration of free acid in the uranyl nitrate solution.

Of these, pH is the most significant factor. Precipitation occurs only if the resultant pH after mixing is  $<6.0$ . At higher pH, uranium remains in solution as the soluble tri-carbonate complex. The factors enumerated above are interrelated since the combination of factors must be such that final pH is  $<6.0$ .

When the uranyl nitrate is added at a fast rate to a stirred sodium carbonate solution, the mixed solution is initially yellow-green in color. As the pH approaches 6.0, the color of the solution changes to orange. This color change is followed by evolution of carbon dioxide gas and precipitation then occurs. The elapsed time between the addition of the uranyl nitrate and the occurrence of precipitation is variable and appears to depend upon the pH of the mixed solutions and speed of stirring. At a final pH of 5.5, the time between mixing and precipitation is approximately 10 seconds. The time interval is increased if the final pH is higher, amounting to more than 1 minute at a pH of 6.0. For the conditions postulated at Rhode Island (11 liters of uranyl nitrate solution containing 256 g. uranium per liter added to 41 liters of 0.54 molar sodium carbonate), the pH of the mixed solution was observed to be 5.5 and elapsed time 10 seconds between mixing and precipitation.

Although the precipitate forms at a pH of 6 or less, the precipitate does not redissolve when the pH of the suspension is increased after precipitation occurs. The pH can be increased to 7.0 - 7.5 by boiling the suspension. Heating at lower temperatures, however, does not increase pH significantly.

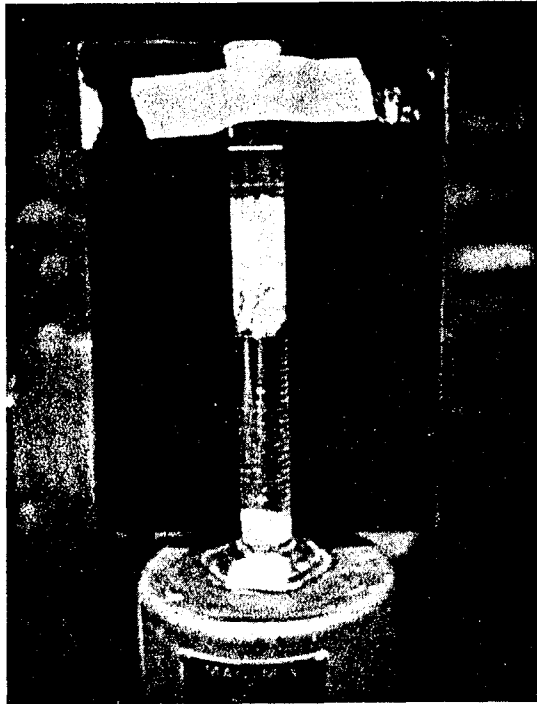
The composition of the precipitate corresponds to the compound, sodium uranyl tricarbonate ( $\text{Na}_4\text{UO}_2(\text{CO}_3)_3$ ). A yellow crystalline precipitate that had been separated from the tank solution was analyzed at Idaho Falls AEC. The conclusion is that the compound is moderately soluble sodium uranyl carbonate with a suggested formula to be  $\text{Na}_4\text{UO}_2(\text{CO}_3)_3 \cdot 2 \text{H}_2\text{O}$ .

The photographs in Figures A-3-A, A-3-B and A-3-C show the results of a laboratory test which closely approximated the initial concentrations and volumes: 41 ml. of 0.54 molar sodium carbonate was mixed with 11 ml. of natural uranyl nitrate solution containing 255 g. uranium per liter. Mixing was made by a magnetic stirrer. The photographs were taken 15 seconds, 2 hours and 3 hours after mixing, respectively. The photograph in Figure A-3-D indicates the size of individual particles and agglomeration of particles. The precipitate appears to be highly agglomerated with individual particles of 1 micron or less. The average size of agglomerates is estimated to be 20 microns.

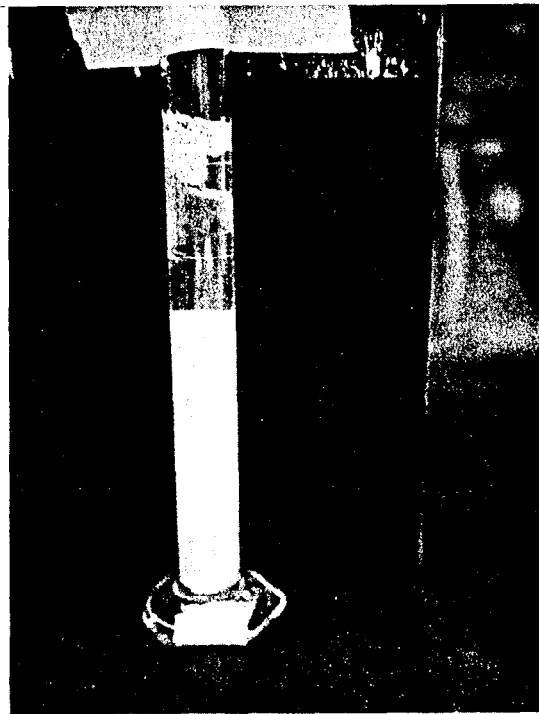
Full scale experiments indicate further:

1. The electric stirrer quickly dispersed the poured uranium solution throughout the volume. A reasonable pouring time is anywhere from 10 to 30 seconds.
2. Considerable bubble formation (presumably  $\text{CO}_2$ ) took place 20 seconds after all the solution had been poured. A maximum increase of 25% in volume occurred.
3. With 40 liters of solution in the tank, the motion of the stirrer caused severe distortion of the surface. Moving pictures that were taken show that a variation of  $\pm 3$  cm. occurred.
4. The formation of the precipitate probably occurred during the gas formation. On this basis, it may be expected that the initial criticality occurred before the precipitate formed and while the solution was homogeneous.

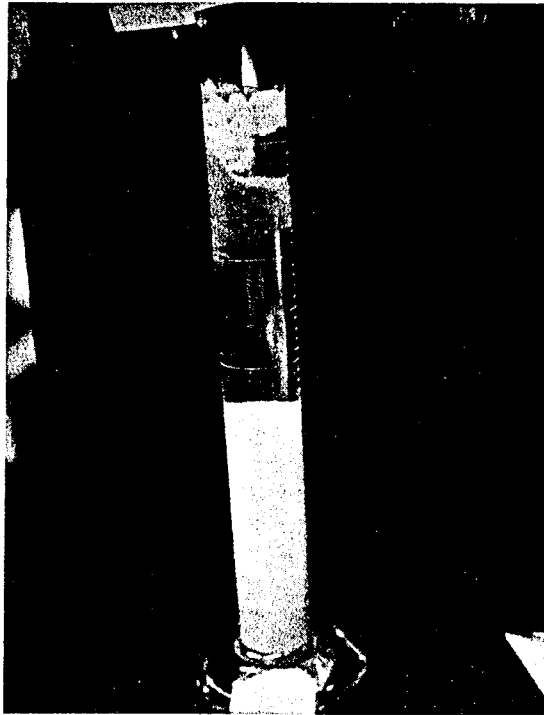
Photograph taken 15 Seconds after Mixing  
(see text for chemical composition)



Photograph taken 2 Hours after Mixing  
(see text for chemical composition)

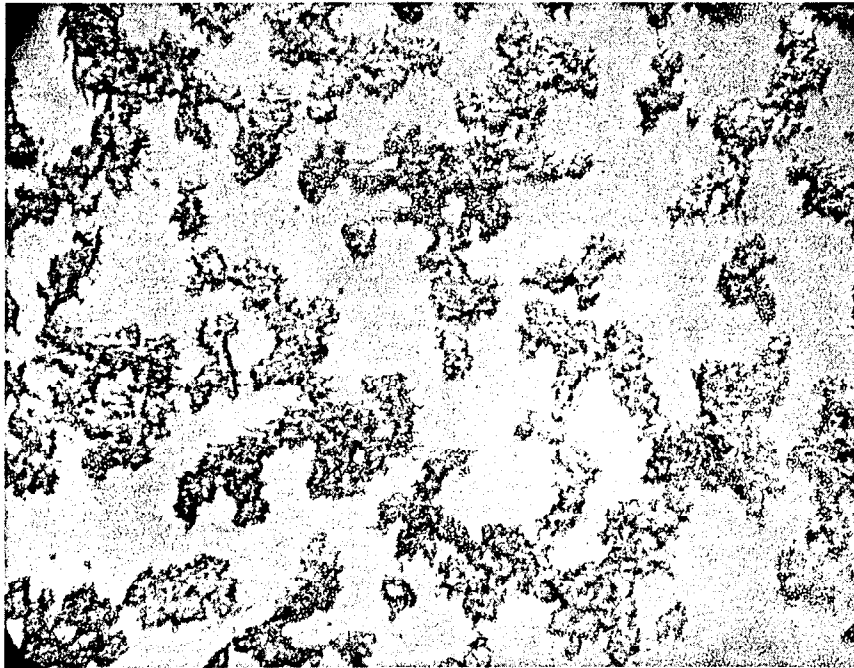


Photograph taken 3 Hours after Mixing  
(see text for chemical composition)



Photomicrograph of Precipitate Particles

500 X





### SODIUM ACTIVATION ANALYSIS of SUPERNATANT LIQUID SAMPLES

A simple method, in principle, of estimating the numbers of fissions which occurred in solution is to determine the ratio of Sodium 24 to total sodium.

Samples of liquid taken from over the precipitate in the 22 jugs filled during the plant clean-up were sent for analysis to Nuclear Science and Engineering Corporation (NSEC) and to Oak Ridge National Laboratory (ORNL).

Because of the short half life of Na<sup>24</sup> (15.0 hours), there was no time to dissolve the precipitate and only samples from the supernatant liquid were sent. It is assumed that the ratio of Sodium 24 to total sodium atoms is constant in both supernatant and precipitate.

A description of samples taken is given in Table A-4-1 following. NSEC received the samples on July 29, 1964 and gamma spectrometry was performed at 8PM on nine (9) samples. The other samples were assayed at a later date but too late to obtain significant results. No results were reported by ORNL.

Table A-4-2 summarizes the results of activation measurements along with the total sodium concentrations measured at ORNL.

The absolute accuracy of the Na<sup>24</sup> determination is probably no better than  $\pm 15\%$ . (See Reference 7, Appendix C).

Sample 2 was also measured at United Nuclear Corporation, Pawling Laboratories (UNC-P). Comparison after decay correction with the NSEC yields a ratio:

$$\frac{N_o^* \text{ (UNC-P)}}{N_o^* \text{ (NSEC)}} = \frac{3.115 \times 10^{10}}{2.42 \times 10^{10}} = 1.29$$

which falls within the absolute accuracy.

Description of Samples Taken for Sodium Activation Analysis

| <u>Sample Number</u> | <u>Description</u>   |
|----------------------|--|
| 1                    | 1 gallon on floor - hot.   |
| 2                    | 1 gallon on floor - hot.   |
| 3                    | 1 gallon on floor - hot.   |
| 4                    | 1 gallon on floor - hot.   |
| 5                    | 1 gallon with funnel on floor - not hot.   |
| 6                    | 11 liters on floor - not in all-safe cart.   |
| 7                    | 11 liters on floor - in all-safe cart - label marked "concentrated liquid from precipitator that has been filtered". |
| 8                    | 11 liters on floor - not in all-safe cart - about 10% full - label marked "ADU filtrate".                            |
| 9                    | 11 liters on floor - in all-safe cart - label marked "1-13-16 wash from evaporator - TCE wash from evaporator".      |
| 10                   | 11 liters on floor - in all-safe cart - almost empty - label marked "O.K. liquor that has been filtered".            |
| 11                   | Floor spill behind bottles at the rear of the room.  |
| 12                   | 11 liters on floor - in all-safe cart - leaking - not sampled.   |
| 13                   | Floor spill from leaking bottle of sample No. 12.  |
| 14-21                | 1 gallon - first floor tower.  |
| 22                   | Spill from first floor tower.  |
| 23                   | Second floor spill was dry, no sample.   |
| 24                   | Spill from third floor tower.  |

Results of Na<sup>24</sup> Activation Measurements

| Sample Number | Measured Na <sup>24</sup> Disintegration <sup>(1)</sup> Rate on 7/29/64 at 8 pm (dpm/cc) | Na <sup>24</sup> Concentration At Time 0, N <sub>0</sub> <sup>*</sup> in atom/cc | Total Na Concentration <sup>(2)</sup> In Sample p23 (mg/cc) |
|---------------|--|--|---|
| 1             | $8.1 \times 10^4$  | $2.97 \times 10^{10}$  | 21.2  |
| 2             | $6.6 \times 10^4$  | $2.42 \times 10^{10}$  | 20.1  |
| 3             | $5.6 \times 10^4$  | $2.05 \times 10^{10}$  | 17.8  |
| 4             | $5.0 \times 10^4$  | $1.83 \times 10^{10}$  | 17.0  |
| 15            | $7.0 \times 10^4$  | $2.56 \times 10^{10}$  | 22.1  |
| 18            | $4.5 \times 10^4$  | $1.65 \times 10^{10}$  | 22.2  |
| 20            | $5.3 \times 10^4$  | $1.94 \times 10^{10}$  | 20.6  |
| 21            | $6.1 \times 10^4$  | $2.23 \times 10^{10}$  | 20.5  |
| 24            | $2.0 \times 10^5$  | $7.32 \times 10^{10}$  | 77  |

(1) See Reference 8, Appendix C, Bibliography

(2) See Reference 9, Appendix C, Bibliography

## RADIOCHEMICAL ANALYSIS OF THE FISSION PRODUCTS

### 1. Brief Description of the Samples Taken

On August 6 and 7, 1964, the uranium solutions and precipitates involved in the nuclear accident were processed to dissolve the precipitates and obtain homogeneous samples for analysis. The solutions and precipitates were contained in 17 one-gallon polyethylene bottles. The amounts of solution and precipitates varied from bottle to bottle. The volume of each bottle which was more than 50% full was adjusted by transferring under pressure one half of the contents into an empty bottle. Thus each bottle described in Appendix A-4 which showed some activity at contact was divided into two (2) portions that are identified by HA and HB in Table A-5-3. Approximately 5N. nitric acid was added in small portions to dissolve the precipitate. A 50 ml. sample was then withdrawn by pipette and subdivided for distribution. The acidified bottles were finally weighed and stored.

The same procedure was followed to obtain samples from the material remaining in the solvent recovery column 1-C-9. Twenty-five (25) samples containing 10 ml. of the homogenized and acidic solutions which presented some activity at contact were sent for analysis to NSEC, ORNL and AEC Idaho Falls. In addition, two (2) weighed composite samples of materials from clean-up water were obtained and sent on August 31, 1964 with identification Numbers 1 and 2.

### 2. Radiochemical Methods of Determining the Number of Fissions

From a known volume of the solution containing the non-volatile fission products, a single fission product is isolated and its concentration (in atoms/cc.) determined. The number of atoms is obtained from the absolute disintegration rate of the sample (corrected for losses during isolation and purification), a knowledge of its decay scheme and of its radioactive decay constant. From the known fission yield of the isolated fission product, the corresponding number of fissions per cc. is then evaluated. Hence, the following equation is used:

$$\text{Number of fissions per aliquot counted} = \frac{D}{e^{-\lambda t} \lambda Y} \quad (\text{Table A-5-1})$$

where D = disintegration rate of the fission product

$e^{-\lambda t}$  = correction factor for decay of the fission product

t = elapsed time from incident

$\lambda$  = decay constant of the fission product

Y = fission yield of the isolated fission product

Further if the specific gravity,  $\rho_s$ , of each sample is measured and the total weight in the entire solution from which the sample was withdrawn,  $W_s$ , is known, then the total number of fissions events can be computed.

### 3. Results

The isolated fission products used in the analysis of the Rhode Island Incident are Molybdenum-99, Barium-140 along with its daughter Lanthanum-140, and Cerium-141. The analytical procedures used in the analysis are described in Reference 10 in Appendix C. Constants used in calculations are given in Table A-5-1. Results and summation of total number of fissions are presented in Tables A-5-2 and A-5-3.

Conclusions on the total number of fissions that occurred in the solution are summarized as follows:

|                 |                                |
|-----------------|--------------------------------|
| NSEC:           | $1.05 \times 10^{17}$ fissions |
| ORNL:           | $1.30 \times 10^{17}$ fissions |
| AEC-Idaho Falls | $1.55 \times 10^{17}$ fissions |

The measurements made at Idaho Falls on three (3) different fission products are in very good agreement. Comparison with results from other laboratories is, however, rather poor. NSEC gives a probable accuracy of 20% on their results. The same error is certainly applicable to the ORNL results.

Fission product analysis in supernatant liquid samples described in Appendix A-4 were performed. The results were used to determine which of the bottles contained solutions from the incident. They are presented in Table A-5-4.

TABLE A-5-1

Constants Used in Fission Product Analysis

| Nuclide | Half Life | Fission Yield | $\gamma$ -ray Energy | Branching Ratio |
|---------|-----------|---------------|----------------------|-----------------|
| Ba 140  | 12.8 d.   | 6.35%         | 1.6 Mev              | 0.88            |
| Ce 141  | 32.5 d.   | 6.00%         | 140 kev              | 0.48            |
| Mo 99   | 66 hr.    | 6.06%         | 750 kev              | 0.163           |

TABLE A-5-2

## AEC-IDAHO FALLS Measurements and Results (Note 1)

| Bottle Number  | Bottle Volume (ml.) | Ba 140                |                                  | Ce 141                                       |                                  | Mo 99          |                |                         |                                  |
|----------------|---------------------|-----------------------|----------------------------------|--|----------------------------------|----------------|----------------|-------------------------|----------------------------------|
|                |                     | $\Sigma$ 1.73<br>1.54 | Fissions<br>( $\times 10^{15}$ ) | $\Sigma$ 0.170<br>0.110<br>( $\times 10^5$ ) | Fissions<br>( $\times 10^{15}$ ) | Decay<br>Corr. | Chem.<br>Yield | $\Sigma$ 0.820<br>0.700 | Fissions<br>( $\times 10^{15}$ ) |
| HA1            | 1,874               | 33,486                | 10.4                             | 1.67   | 7.8                              | 420            | 0.783          | 602                     | 8.6                              |
| HA2            | 1,211               | 42,057                | 8.39                             | 1.97   | 6.1                              | 540            | .580           | 577                     | 9.2                              |
| HA3            | 865                 | 53,474                | 7.23                             | 2.25   | 4.9                              | 195            | .307           | 1,050                   | 8.2                              |
| HA4            | 932                 | 36,771                | 5.67                             | 1.50   | 3.7                              | 545            | .527           | 438                     | 6.0                              |
| HA15           | 1,718               | 38,405                | 10.9                             | 1.25   | 5.8                              | 420            | .543           | 218                     | 4.1                              |
| HA17           | 1,162               | 34,678                | 6.63                             | 2.55   | 7.4                              | 195            | .650           | 980                     | 4.8                              |
| HA18           | 1,507               | 41,050                | 10.2                             | 2.31   | 8.9                              | 195            | .650           | 1,205                   | 8.1                              |
| HA20           | 1,256               | 40,041                | 8.29                             | 1.93   | 6.2                              | 420            | .947           | 773                     | 6.1                              |
| HA21           | 1,854               | 35,482                | 10.9                             | 1.61   | 7.6                              | 420            | .650           | 595                     | 10.0                             |
| 1-1C9          | 1,886               | 45,767                | 13.4                             | 1.81   | 8.7                              | 196            | .527           | 1,480                   | 15.0                             |
| HA2-1C9        | 1,102               | 9,427                 | 2.57                             | .91  | 2.7                              | 545            | .783           | 137                     | 1.5                              |
| HA3-1C9        | 1,403               | 6,736                 | 1.56                             | .74  | 2.2                              | 420            | .413           | 200                     | 4.1                              |
| HA4-1C9        | 740                 | 6,501                 | .75                              | .78  | 1.5                              | 195            | .610           | 245                     | 8.2                              |
| HB1            | 1,649               | 8,346                 | 2.27                             | 1.31   | 5.4                              | 420            | .650           | 190                     | 2.9                              |
| HB2            | 1,731               | 5,299                 | 1.51                             | 1.04   | 4.5                              | 195            | .543           | 125                     | 1.1                              |
| HB3            | 1,977               | 5,804                 | 1.79                             | 1.17   | 6.0                              | 196            | .703           | 192                     | 1.5                              |
| HB4            | 1,087               | 3,425                 | .58                              | .85  | 2.3                              | 194            | .853           | 85.4                    | .30                              |
| HB15           | 1,955               | 6,010                 | 1.95                             | 1.14   | 5.7                              | 540            | .820           | 81.5                    | 1.5                              |
| HB17           | 2,181               | 1,356                 | .46                              | .102   | .57                              | 194            | .670           | 450                     | 4.5                              |
| HB18           | 2,537               | 3,932                 | 1.66                             | .78  | 4.8                              | 420            | .547           | 77.9                    | 2.2                              |
| HB20           | 1,516               | 12,286                | 3.06                             | 1.30   | 5.0                              | 420            | .650           | 383                     | 5.3                              |
| HB21           | 2,275               | 7,322                 | 2.75                             | .89  | 5.5                              | 545            | .717           | 89.6                    | 2.2                              |
| HB1-1C9        | 1,911               | 34,106                | 10.8                             | 1.66   | 8.6                              | 545            | .850           | 611.5                   | 11.0                             |
| HB2-1C9        | 2,196               | 3,220                 | 1.16                             | .94  | 5.3                              | 194            | .747           | 63.5                    | .51                              |
| HB3-1C9        | 1,746               | 2,678                 | .78                              | .66  | 3.1                              | 545            | .683           | 30.2                    | .61                              |
| Total (Note 2) |                     |                       | $1.26 \times 10^{17}$            |  | $1.30 \times 10^{17}$            |                |                |                         | $1.28 \times 10^{17}$            |

$\Sigma$  - Events per minute in the index photopeak

TABLE A-5-2 (Continued)

**Note 1** See Reference 11 in Appendix C.

**Note 2** Fission events in spills and clean-up water were not counted.

## ORNL and NSEC Fission Products Measurements-Ba 140

| Sample Number | Bottle Weight (g) | ORNL MEASUREMENTS |   |  | NSEC MEASUREMENTS |   |  |
|---------------|-------------------|-------------------|---|--|-------------------|---|--|
|               |                   | Density (g/cc)    | No. Fissions per gr. ( $\times 10^{12}$ ) | Total Fission Events per Bottle ( $\times 10^{15}$ ) | Density (g/cc) *  | No. Fissions per cc. ( $\times 10^{12}$ ) | Total Fission Even per Bottle ( $\times 10^{15}$ ) |
| HA1           | 2216              | 1.167             | 3.78                                      | 8.376  | 1.1575            | 3.5                                       | 6.701  |
| HA2           | 1469              | 1.151             | 4.60                                      | 6.757  | 1.1697            | 4.3                                       | 5.40   |
| HA3           | 1077              | 1.173             | 5.52                                      | 5.945  | 1.1834            | 5.3                                       | 4.82   |
| HA4           | 1133              | 1.151             | 4.06                                      | 4.600  | 1.1535            | 3.8                                       | 3.73   |
| HA15          | 2051              | 1.163             | 3.80                                      | 7.794  | 1.1629            | 3.9                                       | 6.88   |
| HA17          | 1372              | 1.130             | 3.71                                      | 5.090  | 1.1468            | 3.6                                       | 4.31   |
| HA18          | 1829              | 1.148             | 4.76                                      | 8.706  | 1.1604            | 4.3                                       | 6.78   |
| HA20          | 1512              | 1.153             | 4.53                                      | 6.849  | 1.3216            | 4.2                                       | 4.80   |
| HA21          | 2195              | 1.139             | 4.00                                      | 8.780  | 1.1670            | 3.6                                       | 6.77   |
| HA1-1C9       | 2256              | 1.162             | 4.78                                      | 10.784   | 1.1795            | 4.6                                       | 8.80   |
| HA2-1C9       | 1250              | 1.091             | 1.17                                      | 1.463  | 1.0881            | .97                                       | 1.11   |
| HA3-1C9       | 1562              | 1.075             | .841                                      | 1.314  | 1.0906            | .70                                       | 1.00   |
| HA4-1C9       | 852               | 1.081             | .701                                      | 0.597  | 1.0850            | .63                                       | .495   |
| HB1           | 1796              | 1.092             | 1.02                                      | 1.831  | 1.1044            | .97                                       | 1.58   |
| HB2           | 1937              | 1.092             | .537                                      | 1.040  | 1.0943            | .54                                       | .956   |
| HB3           | 2189              | 1.079             | .694                                      | 1.519  | 1.0978            | .52                                       | 1.037  |
| HB4           | 1228              | 1.075             | .331                                      | 0.406  | 1.1226            | .31                                       | .339   |
| HB15          | 2178              | 1.089             | .707                                      | 1.540  | 1.0794            | .54                                       | 1.089  |
| HB17          | 2438              | 1.086             | .189                                      | 0.461  | 1.0966            | .13                                       | .289   |
| HB18          | 2827              | 1.092             | .514                                      | 1.453  | 1.0914            | .39                                       | 1.010  |
| HB20          | 2730              | 1.111             | 1.53                                      | 4.177  | 1.1152            | 1.30                                      | 3.182  |
| HB21          | 2533              | 1.084             | .861                                      | 2.181  | 1.1040            | .70                                       | 1.606  |
| HB1-1C9       | 2222              | 1.144             | 3.71                                      | 8.243  | 1.1045            | 3.5                                       | 7.041  |
| HB2-1C9       | 2384              | 1.063             | .326                                      | .777   | 1.0612            | .27                                       | .606   |
| HB3-1C9       | 1910              | 1.058             | .336                                      | .642   | 1.0750            | .24                                       | .426   |
| Subtotal      |                   |                   |   | $1.01 \times 10^{17}$                                |                   |   | $.81 \times 10^{17}$                               |
| No. 1         | 56,240            | 1.129             | $.521 \times 10^{12}$                     | $0.26 \times 10^{17}$                                | 1.129             | $.43 \times 10^{12}$                      | $.22 \times 10^{17}$                               |
| No. 2         | 111,132           | 1.069             | $.0210 \times 10^{12}$                    | $0.02 \times 10^{17}$                                | 1.069             | $.019 \times 10^{12}$                     | $.02 \times 10^{17}$                               |
| TOTAL         |                   |                   |   | $1.29 \times 10^{17}$                                |                   |   | $1.05 \times 10^{17}$                              |

\*Density Measurements were made at UNC, Rhode Island



Ba-140 Disintegration Rate Measurements for Supernatant Liquid Samples

| Sample No. * | Fissions/ml †        |
|--------------|----------------------|
| 1            | $3.5 \times 10^{11}$ |
| 2            | $3.9 \times 10^{11}$ |
| 3            | $3.8 \times 10^{11}$ |
| 4            | $3.3 \times 10^{11}$ |
| 5            | ---                  |
| 6            | ---                  |
| 7            | ---                  |
| 8            | ---                  |
| 9            | $1.3 \times 10^8$    |
| 10           | ---                  |
| 11           | $1.5 \times 10^8$    |
| 13           | ---                  |
| 14           | $5.0 \times 10^8$    |
| 15           | $2.7 \times 10^{11}$ |
| 16           | $1.8 \times 10^{10}$ |
| 17           | ---                  |
| 18           | $1.1 \times 10^{11}$ |
| 19           | $1.2 \times 10^8$    |
| 20           | $2.9 \times 10^{11}$ |
| 21           | $4.2 \times 10^{11}$ |
| 22           | ---                  |
| 24           | $2.3 \times 10^{12}$ |

\* - Identification of the sample is given in Appendix A-4.

† - NSEC Measurements.

DETERMINATION OF URANIUM AND SODIUM CONTENTS IN TANK

The samples taken for fission product analysis (Appendix A-5) were also used to determine the uranium and sodium concentration in the vessel where criticality occurred. Uranium in samples taken from the drained tank solution was determined spectrophotometrically at UNC-Rhode Island, Oak Ridge National Laboratory (ORNL) and Idaho Falls-AEC. Uranium in spills and clean-up water and sodium in all samples were measured at ORNL. Results are presented in Tables A-6-1 and A-6-2.

The enrichment of uranium in U-235 was taken as 93.2%. However, Idaho Falls measurements on a surface ionization mass spectrometer gives the following isotopic composition of uranium.

|       |        |
|-------|--------|
| U-235 | 92.75% |
| U-234 | 1.00%  |
| U-236 | .26%   |
| U-238 | 5.62%  |

The sodium to uranium ratio was computed for each original bottle described in Appendix A-4. This was done by combining the results for HA-1 and HB-1 to obtain the result for sample 1, etc. The results are presented in Table A-6-3.

It can be seen that two jars (17 and 18) have an unusually high ratio indicating they contained a mixture of solution from the tank and plain sodium carbonate solution which was contained in the pipe and column below the tank prior to the incident.

Hence, to determine the correct amount of sodium found in jars, the amounts of sodium and uranium in samples 17 and 18 were subtracted from the total sodium and uranium to evaluate a corrected sodium to uranium ratio.

$$\text{Total Na} - \text{Na in samples 17 and 18} = 601.92 \text{ g.}$$

$$\text{Total U} - \text{U in samples 17 and 18} = 1883.45.$$

Corrected  $\frac{\text{Na}}{\text{U}} = .358$  which leads to a total Na content of  $(.358)(2820) = 1010 \text{ g.}$  which corresponds to a sodium carbonate molarity of 0.54 when dissolved into 41 liters. In spills and clean-up water, the sodium to uranium ratio is equal to .56, which indicates presence of sodium in the detergent used to clean up the plant.

In conclusion, the chemical data that will be used in calculations are:

Uranium found in the jars:..... 2000 g.

Uranium found on floors, walls: ..... 820 g.

Sodium found in the jars (corrected for the amount of sodium in the pipe and column below the tank): ..  $.358(2000) = 715 \text{ g.}$

Molarity of the sodium carbonate solution: ..... 0.54

## Total Uranium and Sodium Measurements ORNL and UNC-Rhode Island Results

| Sample Number | Bottle Weight | ORNL - Results           |                           |                        |                  |                        |                             | UNC Results                    |                       |
|---------------|---------------|--------------------------|---------------------------|------------------------|------------------|------------------------|-----------------------------|--------------------------------|-----------------------|
|               |               | Specific Gravity (gr/cc) | Total U mg/gr of Solution | Total U in Bottle (gr) | Total Na (mg/cc) | Total Na in Bottle (g) | Weight Ratio $\frac{Na}{U}$ | Total U in g per g of Solution | Total U in Bottle (g) |
| HA-1          | 2216          | 1.167                    | 69.6                      | 154.234                | 18.9             | 35.89                  | .23                         | .06281                         | 139.187               |
| HA-2          | 1469          | 1.151                    | 62.0                      | 91.078                 | 18.2             | 23.23                  | .26                         | .07376                         | 108.353               |
| HA-3          | 1077          | 1.173                    | 80.2                      | 86.375                 | 19.0             | 17.44                  | .20                         | .08447                         | 90.974                |
| HA-4          | 1133          | 1.151                    | 62.0                      | 70.246                 | 17.3             | 17.03                  | .24                         | .06411                         | 72.637                |
| HA-15         | 2051          | 1.163                    | 65.2                      | 133.725                | 18.6             | 32.80                  | .25                         | .06623                         | 135.838               |
| HA-17         | 1372          | 1.130                    | 45.3                      | 62.152                 | 21.9             | 26.59                  | .43                         | .04794                         | 65.774                |
| HA-18         | 1829          | 1.148                    | 57.7                      | 105.533                | 19.4             | 30.91                  | .29                         | .05952                         | 108.862               |
| HA-20         | 1512          | 1.153                    | 70.6                      | 106.747                | 20.2             | 26.49                  | .25                         | .06483                         | 98.023                |
| HA-21         | 2195          | 1.139                    | 59.8                      | 131.261                | 19.4             | 37.39                  | .28                         | .06424                         | 141.007               |
| HA-1-1C9      | 2256          | 1.162                    | 68.2                      | 153.859                | 16.0             | 31.06                  | .20                         | .07335                         | 165.478               |
| HA-2-1C9      | 1250          | 1.091                    | 27.4                      | 34.250                 | 14.2             | 16.27                  | .48                         | .03080                         | 38.500                |
| HA-3-1C9      | 1562          | 1.075                    | 23.2                      | 36.238                 | 13.1             | 19.03                  | .53                         | .02537                         | 39.628                |
| HA-4-1C9      | 852           | 1.081                    | 21.6                      | 18.403                 | 12.7             | 10.01                  | .54                         | .02369                         | 20.184                |
| HB-1          | 1796          | 1.092                    | 32.5                      | 58.370                 | 18.4             | 30.26                  | .52                         | .03446                         | 61.890                |
| HB-2          | 1937          | 1.092                    | 25.2                      | 48.812                 | 18.4             | 32.64                  | .67                         | .02773                         | 53.713                |
| HB-3          | 2189          | 1.079                    | 26.4                      | 57.790                 | 16.7             | 33.88                  | .58                         | .02840                         | 62.168                |
| HB-4          | 1228          | 1.075                    | 21.4                      | 26.279                 | 15.8             | 18.05                  | .69                         | .02366                         | 29.054                |
| HB-15         | 2178          | 1.089                    | 27.7                      | 60.331                 | 18.2             | 36.40                  | .60                         | .02989                         | 65.100                |
| HB-17         | 2438          | 1.086                    | 25.0                      | 60.950                 | 21.0             | 47.14                  | .77                         | .02702                         | 65.875                |
| HB-18         | 2827          | 1.096                    | 31.1                      | 87.920                 | 19.8             | 51.26                  | .58                         | .03310                         | 93.574                |
| HB-20         | 2730          | 1.111                    | 38.0                      | 103.740                | 19.8             | 49.50                  | .48                         | .04028                         | 109.964               |
| HB-21         | 2533          | 1.084                    | 29.7                      | 75.230                 | 18.6             | 43.46                  | .58                         | .03126                         | 79.182                |
| HB-1-1C9      | 2222          | 1.144                    | 59.2                      | 131.542                | 16.8             | 32.63                  | .25                         | .06626                         | 147.230               |
| HB-2-1C9      | 2384          | 1.063                    | 20.0                      | 47.680                 | 14.8             | 33.19                  | .70                         | .02066                         | 49.253                |
| HB-3-1C9      | 1910          | 1.058                    | 18.8                      | 35.916                 | 14.0             | 25.27                  | .70                         | .02369                         | 45.248                |
| Sub Total     |               |                          |                           | 1,978.661              |                  | 757.82                 |                             |                                | 2,086.669             |
| #1            | 56240         | 1.129                    | 13.48                     | 671.250                | 6.88             | 342.502                |                             |                                |                       |
| #2            | 111132        | 1.069                    | 1.39                      | 144.472                | 1.08             | 112.243                |                             |                                |                       |
| TOTAL         |               |                          |                           | 2,794.483              |                  | 1212.565               |                             |                                |                       |

Total Uranium Evaluation - AEC - Idaho Falls Measurements

| Bottle Number | Bottle Volume ml | Uranium (gms) |
|---------------|------------------|---------------|
| HA-1          | 1874             | 136           |
| HA-2          | 1211             | 98.3          |
| HA-3          | 865              | 82.1          |
| HA-4          | 932              | 71.0          |
| HA-15         | 1718             | 132           |
| HA-17         | 1162             | 59.4          |
| HA-18         | 1507             | 101           |
| HA-20         | 1256             | 101           |
| HA-21         | 1854             | 132           |
| HA-1-1C9      | 1886             | 150           |
| HA-2-1C9      | 1102             | 32.6          |
| HA-3-1C9      | 1403             | 35.5          |
| HA-4-1C9      | 740              | 17.4          |
| HB-1          | 1649             | 92.2          |
| HB-2          | 1731             | 47.8          |
| HB-3          | 1977             | 55.9          |
| HB-4          | 1087             | 25.5          |
| HB-15         | 1955             | 66.3          |
| HB-17         | 2181             | 59.5          |
| HB-18         | 2537             | 87.3          |
| HB-20         | 1516             | 64.4          |
| HB-21         | 2275             | 76.4          |
| HB-1-1C9      | 1911             | 123           |
| HB-2-1C9      | 2196             | 47.9          |
| HB-3-1C9      | 1746             | 37.2          |
| Solids        | (20.694 g)       | 2.40          |
| <b>TOTAL</b>  |                  | 1,934 gms     |

Sodium to Uranium Weight Ratios in Original Bottles

| Sample | Na/U |
|--------|------|
| 1      | .311 |
| 2      | .399 |
| 3      | .356 |
| 4      | .363 |
| 15     | .357 |
| 17     | .599 |
| 18     | .425 |
| 20     | .361 |
| 21     | .392 |
| 1C9-1  | .223 |
| 1C9-2  | .604 |
| 1C9-3  | .620 |
| 1C9-4  | .54  |

average Na/U ratio in column 1C9 is .366

ACTIVATION ANALYSIS OF METALLIC SAMPLES

The samples collected for data included:

1. Isolated samples taken from the incident room: screwdriver, hose clamps at 9" and 174" from the tank surface.
2. Samples located on the deceased Operator: indium film badges, clip, spring and pin attached to the film badge, gold ring.
3. Samples located on the Superintendent: dimes, silver dollar, indium foil.
4. Samples located on the Supervisor: watch case, indium foil.

Analyses were performed at United Nuclear Corporation-Pawling Laboratory (UNC-P), (Reference 15, Appendix C) and at Idaho Falls-Health and Safety Division, USAEC (AEC-ID) (Reference 16, Appendix C). In addition, the stainless steel clamp located 9" away from the tank was analyzed at Nuclear Science and Engineering Corporation (NSEC) (Reference 17, Appendix C).

Mild steel objects were analyzed for:

- a. Fe-59 from the thermal Fe-58 (n,  $\gamma$ ) Fe-59 reaction
- b. Cr 51 (if any) from the thermal Cr-50 (n,  $\gamma$ ) Cr-51 reaction
- c. Mn-54 from the fast Fe-54 (n, p) Mn-54 reaction
- d. Co-58 (if any) from the fast Ni-58 (n, p) Co-58 reaction

Indium foils and silver coins were analyzed for In-114m and Ag-110m from the thermal In-113 (n,  $\gamma$ ) In-114m and Ag-109 (n,  $\gamma$ ) Ag-110m reactions respectively.

The results of the activation measurements are presented in Tables A-7-1 through A-7-4.

## Summary of Experimental Results for Isolated Samples

|                      | Reaction  | Laboratory | Item                            | Number of Activated Atoms | Ratio of Activated to target atoms<br>$\frac{N}{N_0} = \frac{B}{A} \int_0^{\infty} \sigma(E) \phi(E) dE$<br>$\left[ \frac{n}{\text{cm}^2} \times \text{barn} \right]$ |
|----------------------|---|------------|---------------------------------|---------------------------|---|
| 1. Fast Reactions    | $\text{Fe}^{54}(n,p)\text{Mn}^{54}$<br>scanned          | AEC-ID     | Screwdriver                     | $1.75 \times 10^{10}$     | $1.56 \times 10^{12}$   |
|                      | chemically separated                                    | AEC-ID     | "                               | $1.40 \times 10^{10}$     | $1.25 \times 10^{12}$   |
|                      | scanned   | UNC-P      | "                               | $1.88 \times 10^{10}$     | $1.68 \times 10^{12}$   |
|                      | $\text{Fe}^{54}(n,p)\text{Mn}^{54}$<br>(chem. sep.)     | AEC-ID     | SS hose clamp at 9" from tank   | $4.14 \times 10^9$        | $3.64 \times 10^{11}$   |
|                      | $\text{Ni}^{58}(n,p)\text{Co}^{58}$<br>(chem. sep.)     | AEC-ID     | "                               | $5.51 \times 10^9$        | $5.31 \times 10^{11}$   |
|                      | scanned   | NSEC       | "                               | $4.86 \times 10^9$        | $4.68 \times 10^{11}$   |
|                      | $\text{Fe}^{54}(n,p)\text{Mn}^{54}$<br>scanned          | AEC-ID     | SS hose clamp at 174" from tank | $1.18 \times 10^8$        | $1.06 \times 10^{10}$   |
|                      | $\text{Ni}^{58}(n,p)\text{Co}^{58}$<br>scanned          | AEC-ID     | "                               | $1.95 \times 10^8$        | $1.88 \times 10^{10}$   |
|                      | $\text{Ni}^{58}(n,p)\text{Co}^{58}$<br>scanned          | UNC-P      | "                               | $5.49 \times 10^7$        | $.53 \times 10^{10}$  |
| 2. Thermal Reactions | $\text{Fe}^{58}(n,\gamma)\text{Fe}^{59}$<br>(chem. sep) | AEC-ID     | Screwdriver                     | $4.97 \times 10^{10}$     | $4.79 \times 10^{12}$   |
|                      | scanned   | AEC-ID     | "                               | $4.92 \times 10^{10}$     | $4.74 \times 10^{12}$   |
|                      | scanned   | UNC-P      | "                               | $7.10 \times 10^{10}$     | $6.84 \times 10^{12}$   |
|                      | $\text{Fe}^{58}(n,\gamma)\text{Fe}^{59}$<br>(chem. sep) | AEC-ID     | SS hose clamp at 9" from tank   | $3.39 \times 10^{10}$     | $3.26 \times 10^{12}$   |
|                      | $\text{Cr}^{50}(n,\gamma)\text{Cr}^{51}$<br>(chem. sep) | AEC-ID     | "                               | $3.52 \times 10^{11}$     | $2.92 \times 10^{13}$   |
|                      | scanned   | NSEC       | "                               | $2.30 \times 10^{11}$     | $1.91 \times 10^{13}$   |
|                      | $\text{Fe}^{58}(n,\gamma)\text{Fe}^{59}$<br>scanned     | AEC-ID     | SS hose clamp at 174" from tank | $2.54 \times 10^9$        | $2.44 \times 10^{11}$   |
|                      | $\text{Cr}^{50}(n,\gamma)\text{Cr}^{41}$<br>scanned     | AEC-ID     | "                               | $1.93 \times 10^{10}$     | $1.61 \times 10^{12}$   |
|                      | $\text{Cr}^{50}(n,\gamma)\text{Cr}^{41}$<br>scanned     | UNC-P      | "                               | $1.24 \times 10^{10}$     | $1.03 \times 10^{12}$   |

Summary of Experimental Results for Samples Taken on Operator

|                                  | Item               | Laboratory | Ratio of Activated to Target Atoms<br>$N_B/N_A = \int_0^{\infty} \frac{\sigma(E)\phi(E)dE}{(n/cm^2)x}$ barns | Reaction                      |
|----------------------------------|--------------------|------------|--|-------------------------------|
| 1. Fast Reaction                 | Film Badge Clip    | AEC-ID     | $3.22 \times 10^{11}$  | $Fe^{54}(n,p)Mn^{54}$         |
|                                  | Spring             | "          | $4.18 \times 10^{11}$  | "                             |
|                                  | Pin                | "          | $4.53 \times 10^{11}$  | "                             |
| 2. Essentially Thermal Reactions | Film Badge Clip    | AEC-ID     | $2.13 \times 10^{12}$  | $Fe^{58}(n,\gamma)Fe^{59}$    |
|                                  | Spring             | "          | $2.90 \times 10^{12}$  | "                             |
|                                  | Pin                | "          | $3.17 \times 10^{12}$  | "                             |
|                                  | Indium Badge No. 1 | AEC-ID     | $5.44 \times 10^{13}$  | $In^{113}(n,\gamma)In^{114m}$ |
|                                  | No. 2              | "          | $5.62 \times 10^{13}$  | "                             |
|                                  | Gold Ring          | UNC-P      | $5.23 \times 10^{13}$  | $Au^{197}(n,\gamma)Au^{198}$  |



## Summary of Experimental Results for Samples Taken on the Superintendent

(All Reactions are Essential Thermal)

| Item   | Laboratory      | Ratio of Activated to Target Atoms<br>$N_B/N_A = \int_0^{\infty} \sigma(E)\phi(E)dE$ (n/cm <sup>2</sup> ) x barn | Reaction                  |
|--|-----------------|--|---------------------------|
| Dime No. 1<br>.66 Mev- $\gamma$<br>.88 Mev- $\gamma$ | UNC-P<br>"      | 9.10 x 10 <sup>9</sup><br>10.04 x 10 <sup>9</sup>  | Ag109(n, $\gamma$ )Ag110m |
| Dime No. 2   | UNC-P<br>AEC-ID | 8.06 x 10 <sup>9</sup><br>19.0 x 10 <sup>9*</sup>  | Ag109(n, $\gamma$ )Ag110m |
| Silver Dollar  | UNC-P<br>AEC-ID | 5.42 x 10 <sup>9</sup><br>9.84 x 10 <sup>9*</sup>  | Ag109(n, $\gamma$ )Ag110m |
| Indium Foil (presumed)                               | UNC-P           | 6.14 x 10 <sup>10</sup>  | In113(n, $\gamma$ )In114m |

\* If the values are reduced by 31% to account for contribution of .937 Mev- $\gamma$  and high-energy gammas, one gets 15 x 10<sup>9</sup> and 7.78 x 10<sup>9</sup> for the dime and dollar respectively.

Summary of Experimental Results for Samples Taken on the Supervisor

|                                  | Item        | Laboratory | Ratio of Activated to Target Atoms<br>$N_B/N_A = \int_0^{\infty} \sigma(E)\phi(E)dE$ (n/cm <sup>2</sup> ) x barn | Reaction                                    |
|----------------------------------|-------------|------------|--|---|
| 1. Essentially Thermal Reactions | Watch Case  | UNC-P      | $6.8 \times 10^{10}$   | $\text{Cr}^{50}(n,\gamma)\text{Cr}^{51}$    |
|                                  | Indium Foil | UNC-P      | $10.0 \times 10^{10}$  | $\text{In}^{113}(n,\gamma)\text{In}^{114m}$ |
| 2. Fast Reaction                 | Watch Case  | UNC-P      | $(1.35 \pm 1.06) \times 10^8$  | $\text{Ni}^{58}(n,p)\text{Co}^{58}$         |

Gamma ray spectrometry was used to determine absolute disintegration rates. AEC-ID employs a standard 3" x 3" NaI (TI) crystal coupled with a 400 channel pulse height analyzer. UNC-P uses a 2" x 2" in NaI crystal coupled with the same type of analyzer. NSEC uses the 3" x 3" in NaI crystal coupled with a 512 channel analyzer.

Comparison of the activation results obtained at these laboratories show they are not always consistent. It is, therefore, useful to present the correction factors (which enter the determination of the activation from the observed detector response) that were used at AEC-ID and UNC-P. Tables A-7-5 and A-7-6 present the constants used in the calculations of activities by AEC-ID and UNC-P respectively.

**TABLE A-7-5**

Constants Used at AEC-ID in Calculation of Activation

| Nuclide | Gamma Ray (Mev) Energy | Half Life | Branching Ratio | Counting Position (cm) | 1 TPA (Note 1) |
|---------|------------------------|-----------|-----------------|------------------------|----------------|
| Fe 59   | 1.3                    | 45 d      | 0.44            | 3                      | 38.7           |
| Mn 54   | 0.84                   | 314 d     | 1.0             | 3                      | 25.7           |
| Cr 51   | 0.31                   | 27.8 d    | 0.09            | 3                      | 10.4           |
| In 114m | 0.72                   | 50 d      | 0.035           | 3                      | 22.1           |
| Ag 110  | 0.88                   | 249 d     | 0.72            | 3                      | 27.0           |
| Co 58   | 0.81                   | 71 d      | 1.0             |                        | 24.6           |

Note 1 A composite factor for the gamma-ray measured containing the absolute detection efficiency, peak-to-total ratio, and correction for a 760 mg cm<sup>-2</sup> polystyrene beta absorber. Values were taken from a table of gamma-ray conversion factors (Note 2). To calculate disintegrations per minute at time 0, the following expression can be used:

$$\frac{(\text{Peak integral}) (1/\text{TPA}) (\text{Decay Correction})}{(\text{Branching Ratio})}$$

Note 2 G. Olson USAEC Report IDO 14613, January 1964.

Factors Used at UNC-P in Calculation of Activations

| Item                         | Gamma Energy (Mev.) | Isotope            | Detector (i) Efficiency | Branching Ratio | Gamma Attenuation Factor | $\lambda$ (sec. <sup>-1</sup> ) |
|------------------------------|---------------------|--------------------|-------------------------|-----------------|--------------------------|---------------------------------|
| Clamp #2<br>(away from tank) | .320                | Cr <sup>51</sup>   | .128                    | .098            | .805                     | $2.88 \times 10^{-7}$           |
|                              | .810                | Co <sup>58*</sup>  | .0397                   | 1               | .881                     | $1.11 \times 10^{-7}$           |
| Screwdriver                  | 1.29                | Fe <sup>59</sup>   | .00299                  | .44             | .81                      | $1.78 \times 10^{-7}$           |
|                              | .835                | Mn <sup>54</sup>   | .00454                  | 1               | .77                      | $2.65 \times 10^{-8}$           |
| Supervisor's<br>Watch Back   | .320                | Cr <sup>51</sup>   | .194                    | .098            | .944                     | $2.88 \times 10^{-7}$           |
|                              | .810                | Co <sup>58</sup>   | .0606                   | 1               | .963                     | $1.11 \times 10^{-7}$           |
| Indium Foils                 | .190                | In <sup>114m</sup> | .312                    | .1855           | .950                     | $1.60 \times 10^{-7}$           |
| Dime #1                      | .660                | Ag <sup>110m</sup> | .0575                   | 1.3             | .946                     | $3.17 \times 10^{-8}$           |
|                              | .880                | Ag <sup>110m</sup> | .0413                   | .95             | .954                     | $3.17 \times 10^{-8}$           |
| Dime #2                      | .660                | Ag <sup>110m</sup> | .0575                   | 1.3             | .946                     | $3.17 \times 10^{-8}$           |
| Silver Dollar                | .660                | Ag <sup>110m</sup> | .0492                   | 1.3             | .915                     | $3.17 \times 10^{-8}$           |
| Gold Ring                    | .411                | Au <sup>198</sup>  | .00865                  | 1.0             | .55                      | $2.97 \times 10^{-6}$           |

\* The assumption has been made that all of the activity is due to Co<sup>58</sup>. Since there is a small contribution from Mn<sup>54</sup> which cannot be resolved, the activation which is reported is an over-estimate.

(i) Detector efficiency includes the total detection efficiency, the peak-to-total ratio, a disk and coincidence loss corrections. To calculate the number of disintegrations per minute at time 0 the following expression is used:

$$D(0) = \frac{\text{Peak Integral} \times \text{Decay Correction}}{\text{Detector efficiency} \times \text{Branching Ratio} \times \text{Gamma Attenuation Factor}}$$

Because of the inconsistency of the results on the silver coins, the factors in Table A-7-6 were experimentally verified. Silver foils, bare and indium covered, were irradiated in a known thermal flux. The thermal flux was determined by Pratt and Whitney personnel at CANEL from the activation of manganese foils adjacent to the silver foils.

The expected counting rates from sub-cadmium activations using data in Table A-7-6 and the measured thermal flux were compared with the measured counting rates for two gamma ray energy ranges. For the range 0.600 to 0.735 Mev, the ratio of expected to measured count rate was 1.07. For the range 0.82 to 1.00 Mev, the ratio was 0.96. The use of data in Table A-7-6 yields results which agree within  $\pm 6\%$  with experiments.

Tables A-7-7 and A-7-8 contain the activation results obtained in two laboratories. The activation of the  $\text{Ag}^{110\text{m}}$  in the dime and the silver dollar as reported by Dr. Olson of the AEC was based on net integrated counts between .82 and 1.0 Mev of 187 for the dime and 818 for the dollar. These values should be reduced by 25% to account for the contribution of the .935 Mev gamma ray and by an additional 6% to account for the contribution of the higher energy gamma.

It must be noted that dime No. 1 and the silver dollar were taken from the right hand pocket of the Superintendent's trouser while dime No. 2 was in the left hip pocket.

The Superintendent's indium film badge was not positively identified. Two badges found in the guard's desk at the Rhode Island plant showed radioactivity. The more active badge was assumed to be the Superintendent's.

## Activation of Samples: AEC-ID Results

| Nuclide  | Sample Wt., g. | Decay Correction | $I_d/I_o^*$ | Peak Integral (events per minute) |
|--|----------------|------------------|-------------|-----------------------------------|
| Fe 59  | 4.245          | 1.24             | 0.86        | 54.5                              |
| Mn 54  | 4.245          | 1.03             |             | 200.7                             |
| Screwdriver Scanned as a 1" Disc                 |                |                  |             |                                   |
| Fe 59  | 9.53           | 1.22             | 0.75        | 1072                              |
| Mn 54  | 9.53           | 1.03             | 0.68        | 3823                              |
| Film Badge Clip                                  |                |                  |             |                                   |
| Fe 59  | 1.6            | 1.17             |             | 9.96                              |
| Mn 54  | 1.6            | 1.02             |             | 19.43                             |
| Film Badge Spring                                |                |                  |             |                                   |
| Fe 59  | .594           | 1.52             |             | 3.87                              |
| Mn 54  | .594           | 1.05             |             | 9.1                               |
| Film Badge Pins                                  |                |                  |             |                                   |
| Fe 59  | .596           | 1.52             |             | 4.4                               |
| Mn 54  | .596           | 1.05             |             | 9.9                               |
| Hose Clamp 9" from Vessel (chemically separated) |                |                  |             |                                   |
| Fe 59  | .697           | 1.30             |             | 6.88                              |
| Mn 54  | .697           | 1.02             |             | 9.83                              |
| Cr 51  | .178           | 1.53             |             | 285                               |
| Co 58  | .110           | 1.16             |             | 82.3                              |
| Hose Clamp 174" from Vessel (scanned)            |                |                  |             |                                   |
| Fe 59  | .708           | 1.34             |             | 0.5                               |
| Mn 54  | .708           | 1.04             |             | 0.28                              |
| Cr 51  | .178           | 1.60             |             | 14.7                              |
| Co 58  | .110           | 1.19             |             | 2.54                              |
| Indium Foils (scanned)                           |                |                  |             |                                   |
| No. 1  | .212           | 1.15             |             | 34.4                              |
| No. 2  | .221           | 1.15             |             | 37.2                              |
| Silver Coins                                     |                |                  |             |                                   |
| Dime #2  | 2.23           | 1.10             | .93*        | 4.68                              |
| Dollar   | 17.7           | 1.10             | .88*        | 20.4                              |

$\frac{I_d}{I_o}$  - absorption of gamma rays in the source

## Activation of Samples - UNC-P Results

| Item  | Gamma Energy (Mev.) | Peak Integral                  | Mass (g) Of Isotope | Decay Correction |
|---|---------------------|--------------------------------|---------------------|------------------|
| Clamp No. 2<br>away from tank                                 | .320                | 72,700 counts in 1,416 minutes | .1207               | 5.09             |
|   | .810                | 8,000 counts in 1,416 minutes  | .847                | 1.92             |
| Screwdriver   | 1.29                | 4,938 counts in 100 mins.      | .062                | 1.26             |
|   | .835                | 13,015 counts in 100 mins.     | 1.282               | 1.035            |
| Supervisor's<br>Watch Back                                    | .320                | 2,400 counts in 1,556 mins.    | .0246               | 4.03             |
|   | .810                | 200±150 counts in 1,556 mins.  | .390                | 1.71             |
| Indium Foils<br>Supervisor<br>Superintendent*                 | .190                | 6,775 counts in 941 mins.      | .043                | 1.67             |
|   | .190                | 2.2 counts per minute          | .0197               | 1.64             |
| Dime No. 1  | .660                | 6,000 counts in 900 mins.      | 1.08                | 1.06             |
|   | .880                | 3,600 counts in 900 mins.      | 1.08                | 1.06             |
| Dime No. 2  | .660                | 6 counts per minute            | 1.08                | 1.075            |
| Silver Dollar   | .660                | 8,000 counts in 300 mins.      | 8.58                | 1.06             |
| Gold Ring   | .411                | 156,500 counts in 10 mins.     | 1.5**               | 1.3              |
| * It is assumed that the foil was worn by the superintendent. |                     |                                |                     |                  |
| ** Approximate weight of gold in the ring.                    |                     |                                |                     |                  |

NSEC results for the hose clamp at 9" are given directly in disintegrations per minute measured on July 31, 1964:

$$\text{Co}^{58}: 1.2 \times 10^3 \quad \text{and} \quad \text{Cr}^{51}: 1.7 \times 10^4.$$

The weight of the sample was 0.6 g. Data on the factors used are not mentioned.

The experimental results were used to compute the number of activated atoms,  $N_B$ , per g. of the target A and the ratio of activated atoms to target atoms,  $\frac{N_B}{N_A}$ . This ratio is useful for subsequent calculations of fluxes since it can be shown that

$$\frac{N_B}{N_A} = \int_0^{\infty} \sigma(E) \phi(E) dE$$

where  $\sigma(E)$  is the activation cross section.

A summary of the activation calculations is presented in Tables A-7-1, A-7-2, A-7-3 and A-7-4.

HAIR SULFUR and BLOOD and WHOLE BODY SODIUM ACTIVATION MEASUREMENTS

Hair samples from the UNC accident were submitted to analysis and results of the Los Alamos measurements (Reference 18, Appendix C) corrected for decay are as follows:

| Sample           |                         | Disintegration Rate<br>(dpm/g. of hair <sup>(i)</sup> ) |
|------------------|-------------------------|---|
| Operator -       | Pubic hair              | 8990  |
|                  | Head hair               | 2160  |
| Superintendent - | Pubic hair              | 38  |
|                  | Head hair               | 12 <sup>(ii)</sup>                                      |
| Supervisor -     | Pubic and<br>Chest hair | 51.8 <sup>(iii)</sup>                                   |

- (i) Abundance of sulfur in all samples: 0.05 g./g. of hair
- (ii) Haircut before sample was submitted
- (iii) Decay had gone to ~4.5 half lives before analysis

A precision of  $\pm 5\%$  and an accuracy of  $\pm 30\%$  are claimed for the data.

When fast neutrons are moderated to thermal energy in the body, a small fraction of them are captured by a  $(n, \gamma)$  process in the Na 23 in the body giving rise to Na 24 which, by virtue of its emission of high energy gamma rays is easily detected. (Half life of 14.8 hrs.)

It has been shown (Reference 19, Appendix C) that

1. The probability of neutron capture in Na 23 in the body is not a strong function of the energy of the fast neutrons.
2. The probability of thermal capture for neutrons initially in the fast region is higher than the probability of capture in the thermal region.
3. Na 23 is uniformly distributed in the body and in the blood system.

The results of Na 24 activation measurements are summarized in the medical report from the Massachusetts General Hospital to the division of Compliance, USAEC. (Reference 20, Appendix C).

Sample of blood serum were obtained from the Operator at 7 hours and 16.5 hours after the accident and sent for analysis.

Gamma spectra from these samples were essentially identical and were consistent only with the presence of Na-24. Both samples were extrapolated to zero time and indicated a sodium activity at that time of  $2.64 \times 10^{-2}$  micro-curies per ml. of blood serum.



Body burden measurements on the Superintendent and Supervisor were made by the Department of Physics, Massachusetts Institute of Technology, on July 30 and 31, 1964.  $\text{Na}^{24}$  activity was found in both of them and appeared to be generally distributed on and/or in their bodies. The measurements on their hands and chest showed no significant disproportionate excess activity in these regions. Assuming the  $\text{Na}^{24}$  to be distributed uniformly the whole body activity is calculated to be:

$$(4.6 \pm 0.5) \times 10^{-9} \text{ curies for the Supervisor}$$

$$(2.2 \pm 0.3) \times 10^{-9} \text{ curies for Superintendent}$$

both as of 17:00, July 30, 1964.

Correcting these measurements for decay assuming that both men were exposed to neutrons on July 24, 1964 at 20:00, the activities at time zero were:

$$3.102 \times 10^{-6} \text{ curies for the Supervisor}$$

$$1.484 \times 10^{-6} \text{ curies for the Superintendent}$$

The respective weights of the Supervisor and the Superintendent are 83 and 90 kilograms. Assuming a density of 1 g/cc for the body, the disintegration rates per cc. can then be calculated. The total sodium concentration in blood serum was measured (Reference 20, Appendix C) as 3.21 g/liter. Total sodium concentration in the whole body is derived from the fact that 105 g. of Na are found in a "Standard Man" weighing 69.5 kgs. using the body atomic comparison (Reference 21, Appendix C). Thus, one obtains a concentration of 1.51 g. of Na per liter of man.

The data on Na activation are summarized as follows:

|                | Laboratory                                 | $\text{Na}^{23}$ Concentration<br>(gm/liter) | $A^{24} = \text{Na}^{24}$<br>Activity<br>( $\mu\text{c}/\text{cc}$ ) | D(O) Disintegration<br>rate (dpm/cc) |
|----------------|--|--|--|--------------------------------------|
| Operator       | Blood serum<br>(Mass. General<br>Hospital) | 3.21   | $2.64 \times 10^{-2}$  | $5.86 \times 10^4$                   |
| Supervisor     | Whole body<br>MIT                          | 1.51   | $3.73 \times 10^{-5}$  | 83                                   |
| Superintendent | Whole body<br>MIT                          | 1.51   | $1.64 \times 10^{-5}$  | 36.6                                 |

SPECTROGRAPHIC ANALYSIS OF METALLIC SAMPLES

Mild steel objects, including the screwdriver, film badge clip, spring and rivets, were analyzed for Fe-59 and Mn-54 produced from the Fe-58 (n,  $\gamma$ ) Fe-59 and Fe-54 (n, p) Mn-54 neutron reactions. When no other activation products deriving from alloy steel were present, the conventional composition of 99% iron was assumed along with the natural isotopic abundances of 5.84% and .31% of Fe-54 and Fe-58 respectively.

This composition was verified by X-ray analysis at Idaho Falls on the film badge clip and the screwdriver.

When Cr-51 and Co-58 products were detected, the samples were submitted for analysis. The analytical results reported by Lucius Pitkin, Inc. and Idaho Falls are as follows:

| Sample                        | Composition      |                   | Laboratory          |
|-------------------------------|------------------|-------------------|---------------------|
| SS hose clamps at 9" and 174" | Fe-71%<br>Ni-11% | Cr-17%<br>Mn 1-2% | USAEC-Idaho Falls   |
| SS hose clamp at 9"           | Cr-19.2%         | Ni 9.42%          | Lucius Pitkin, Inc. |
| SS hose clamp at 174"         | Cr-18.79%        | Ni-8.42%          | Lucius Pitkin, Inc. |
| Supervisor's watch case       | Cr-12.62%        | Ni-12.51%         | Lucius Pitkin, Inc. |

It can be seen that the watch case has an unusual Cr to Ni ratio. It is thought that the case is chromium plated. The silver coins were assumed to have the composition given by the Federal Reserve Bank: 90% Ag - 10% Cu.

MISCELLANEOUS MEASUREMENTS

## Level of Activation in Tank and Stirrer Materials

Both the tank and the shaft of the stirrer were examined to determine the level of activation of the materials in them. In both materials the activity was observed with a NaI scintillation counter feeding a multichannel pulse height analyzer so that a representation of the energy deposited in the NaI crystal by the gamma-rays emitted in the material was obtained. From these distributions it is possible to determine the energy of the gamma ray emitted and in general to correlate this energy with the expected activity in the constituents of stainless steel.

There are three activities which are expected:

1. the  $\text{Cr}^{51}$  produced by low energy neutron absorption in  $\text{Cr}^{50}$
2.  $\text{Co}^{58}$  produced by a fast neutron n,p reaction in  $\text{Ni}^{58}$
3.  $\text{Mn}^{54}$  produced by a fast neutron n,p reaction in  $\text{Fe}^{54}$

In an 18-8 stainless steel the  $\text{Co}^{58}$  activity is expected to dominate the gamma ray production in the vicinity of 800 Kev. In a low nickel steel, however, the  $\text{Mn}^{54}$  activity may be important.

The exact composition of neither the tank nor the stirrer rod was known. In both cases, a prominent peak at 320 Kev corresponding to the gamma ray emitted by  $\text{Cr}^{51}$  was observed and a well defined peak in the vicinity of 810 Kev, the energy of the gamma ray emitted by  $\text{Co}^{58}$ , was observed. To expedite the interpretation of the data, the manner of determining the relative intensities of the observed activity is to evaluate the amplitude of the peak of the appropriate gamma ray line in each measurement and to compare these peak amplitudes. No attempt to subtract background, to account for shifts in resolution, or possible shift in the relative contributions of  $\text{Co}^{58}$  and  $\text{Mn}^{54}$  to the 800 Kev peak has been made.

The results for the stirrer rod are shown in Figure A-10-A. These results were obtained with the detector collimated so that a 1" (approximately) length of the stirrer rod was viewed at a time. The indicated points are therefore the average activation over a 1" interval. The stirrer blade which was removed from the shaft to make these measurements was located approximately 1" from the end of the shaft, that is, at the position labeled "1 in.". The decrease in the observed activity at this end of the rod may in part be the result of the presence of the stirrer blade itself during the irradiation.

The results for the stainless steel tank wall are shown in Figures A-10-B and A-10-C. Here the four sets of measurements represent traverses made along the tank wall parallel to the axis of the tank, viewing an area of the tank approximately 1" high and 4" wide. The four traverses were made  $90^\circ$  apart around the wall of the tank with the  $0^\circ$  position representing the weld seam which was located facing the wall of the plant building. In this coordinate system, the stirrer blade was located at approximately  $235^\circ$ . The data

in this set of curves is reported in exactly the same way as the data for the stirrer rod is shown, the peak amplitude for the 320 Kev line representing the intensity of the activity for the  $\text{Cr}^{51}$  and the peak of the 310 Kev line representing the fast activation. Substantially less structure is evident in these curves than is apparent in the thermal neutron distribution represented by the  $\text{Cr}^{51}$  activity in the stirrer rod. The fast neutron activation of the tank wall shows some variation with azimuth, the variation being larger near the top of the tank than it is near the bottom of the tank. The azimuthal variation in the thermal neutron distribution is most prominent at the weld, which suggests that there may be a difference in composition, a difference in the chromium content, in the vicinity of the weld.

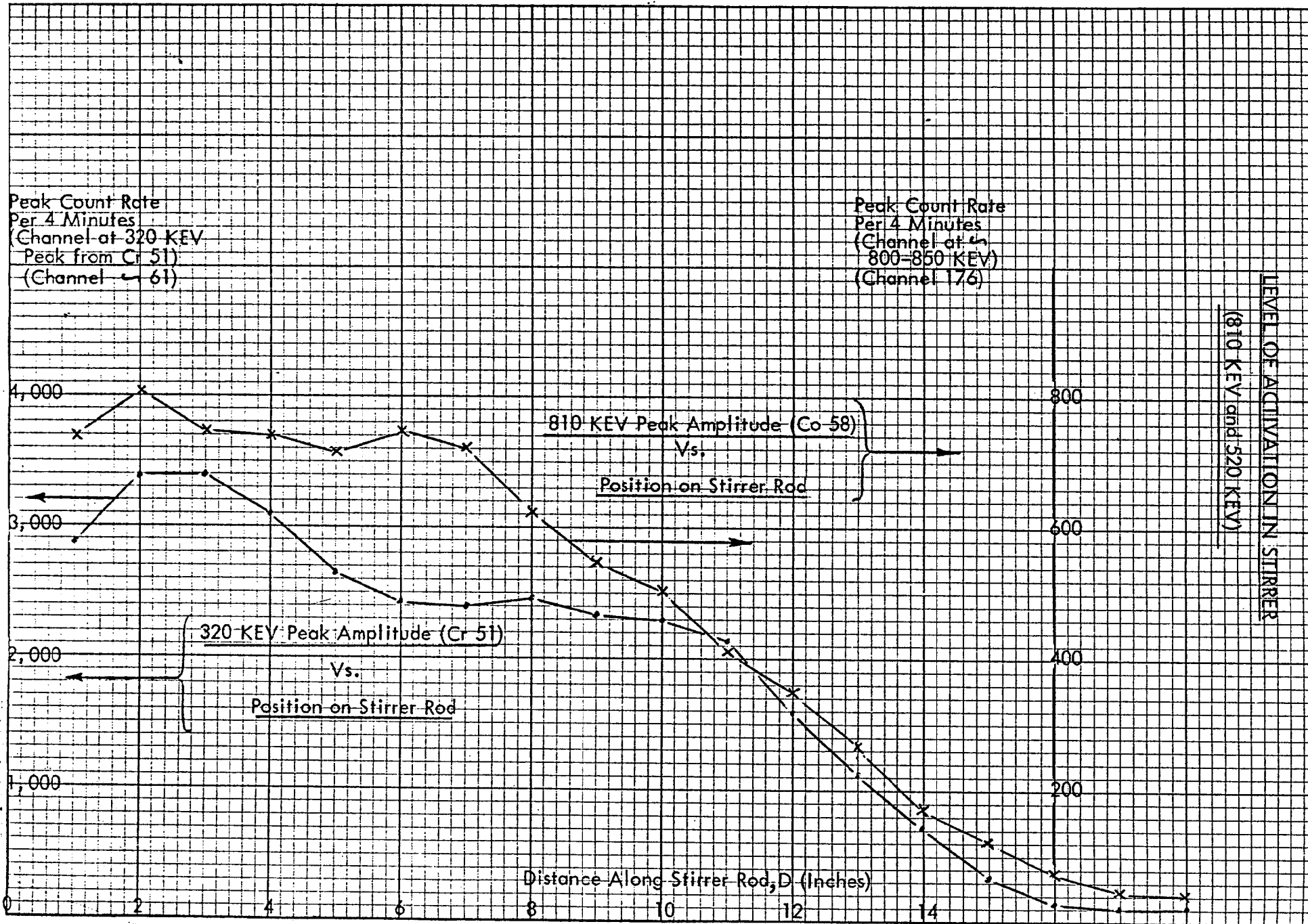


FIGURE A-10-A

FIGURE A-10-B

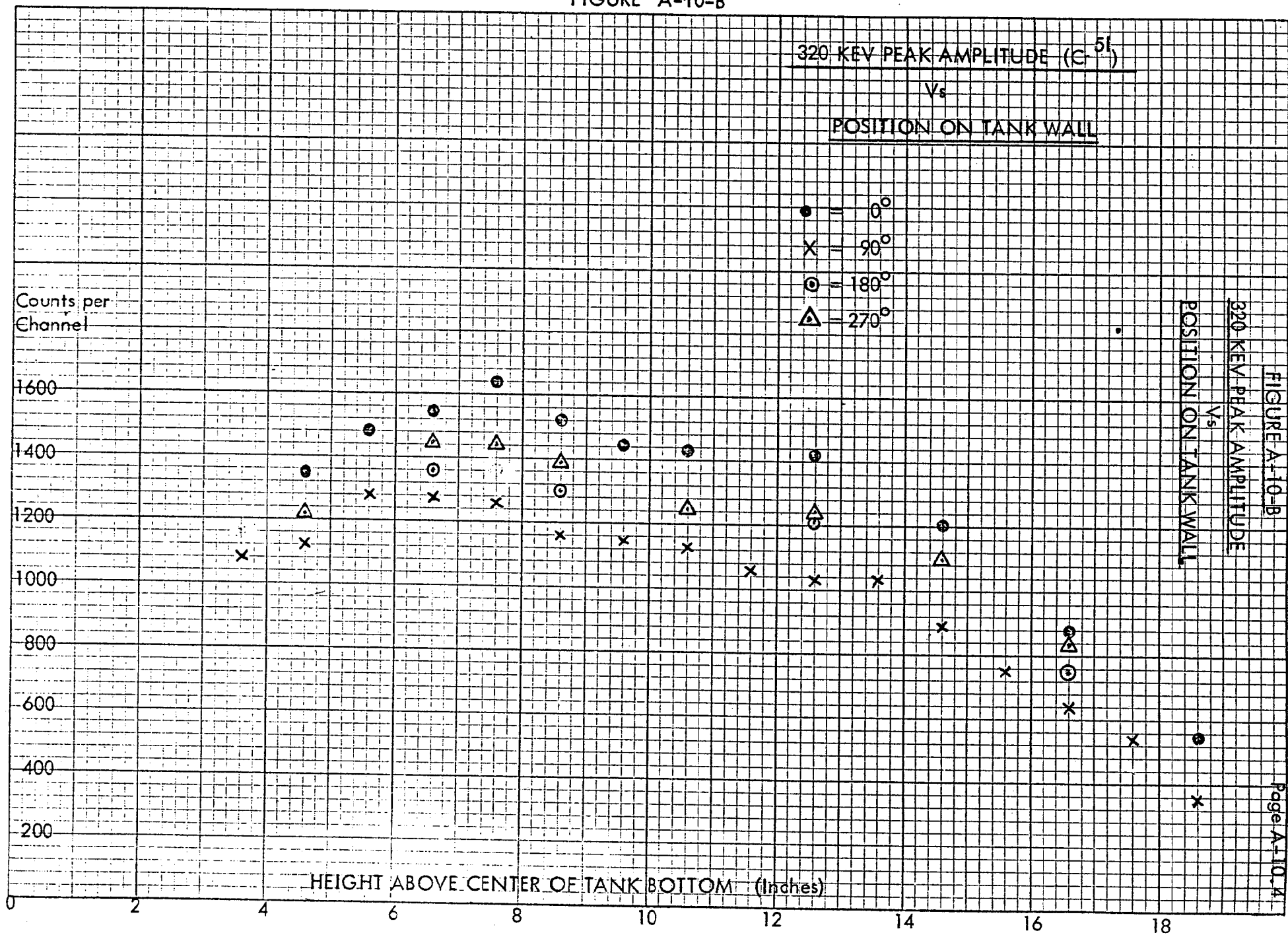


FIGURE A-10-C

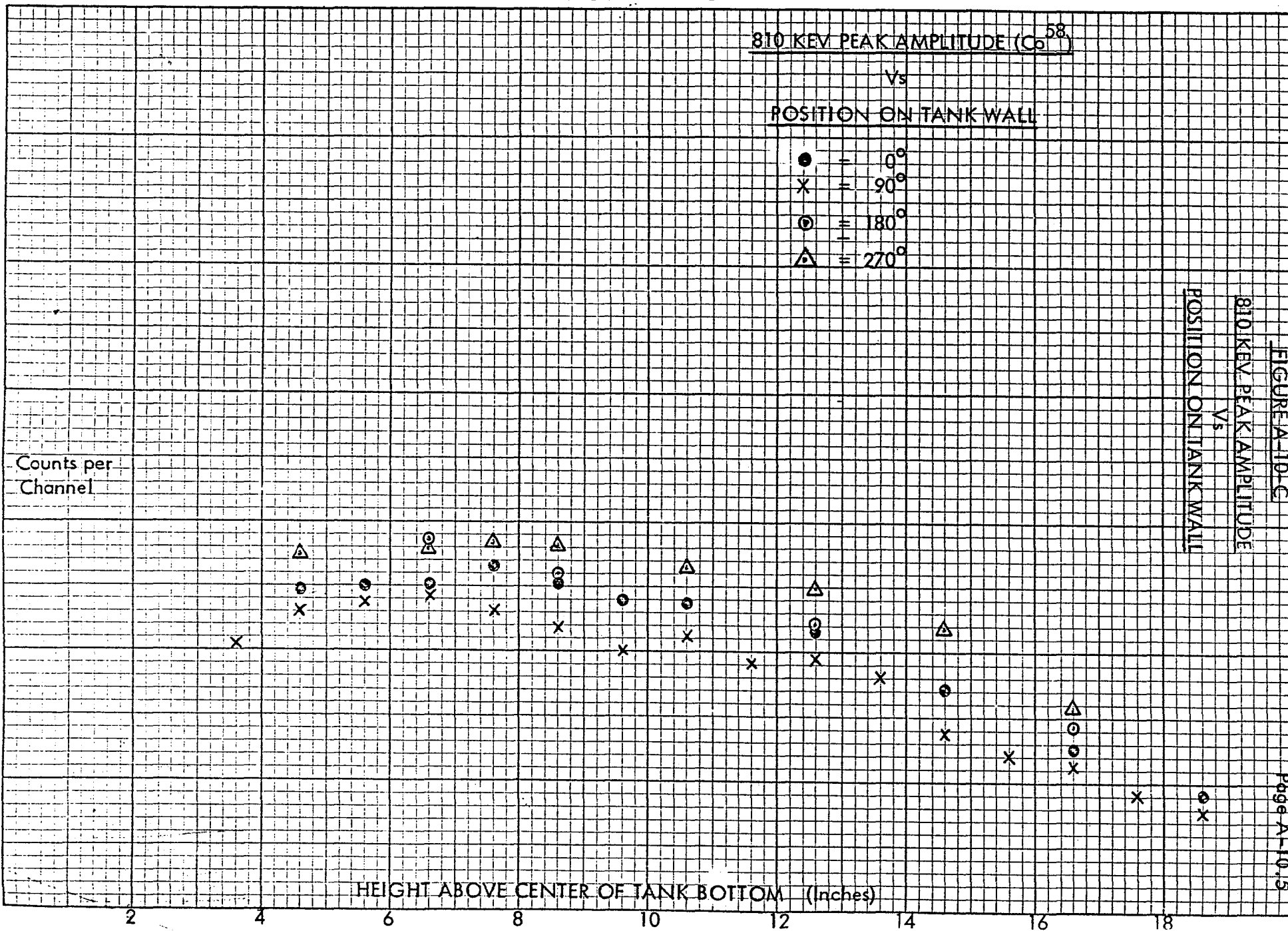


FIGURE A-10-C

Page A-10.15

CRITICALITY STUDIES ON THE RHODE ISLAND INCIDENT1. Introduction

The radiochemical analysis of samples taken from the deceased Operator, the Superintendent and the Supervisor and chemical results on uranium contents in the solution showed the possibility of at least two critical excursions. The following study gives the results and a brief description of the methods of solution to two basic criticality problems associated with what is thought to be the initial and final conditions of the Rhode Island assembly. In addition, a number of peripheral problems are also treated in order to get a complete picture of the critical events.

The first problem considers the initial pouring of the uranium solution by the deceased Operator. Eleven (11) liters of uranyl nitrate aqueous solution, having a total-uranium concentration of 255 g. per liter (enriched to 93.2% in U-235), were gradually<sup>+</sup> poured into a 1/8" wall stainless steel cylindrical vessel of inner diameter 17-3/4" and height 26-1/8" <sup>++</sup>. Forty-one (41) liters of .54 molar strength of sodium carbonate solution were already in the vessel before the pouring process. The critical conditions (volume, height and mass U-235) of the cylindrical solution are to be determined here. An estimate of the final multiplication factor,  $k$ , when all eleven (11) liters are poured is also to be made. This is referred to hereafter as the Continuous Pouring Problem.

The second problem analyzes the assembly in the final conditions. Consider the solution of the first problem after pouring the eleven (11) liters of uranium solution. Assume that a given amount of the homogeneous solution is spilled out. The problem consists of evaluating the multiplication factor,  $k$ , for the resulting configuration. Chemical analysis shows that approximately ten (10) liters of the solution were ejected. Thus, an estimate of  $k$  for this configuration is desired. This is referred to hereafter as the Final Configuration Problem.

The peripheral problems concern the Final Configuration Problem and are to estimate the effect on reactivity of:

1. Temperature rise over a reasonable range.
2. Height increase of the uranium solution.
3. Presence of a 336 g. stainless steel stirrer.
4. Presence of a wave at the top surface of the liquid ( $\pm 3$  cms. above and below the unperturbed surface) due to the action of the stirrer.
5. Effect of the presence of a concrete wall fifteen (15) inches from the tank.
6. Effect of self shielding in precipitate molecules.
7. Neutron leakage from the 3" drain pipe and gallon jug with delayed neutrons as a source.
8. Prompt neutron lifetime of the system.
9. Shutdown mechanisms.

---

+ Static cases are only treated; rate of pouring is not pertinent.

++ The actual stainless steel vessel had a slight curved bottom. This is not taken into account.



## 2. General Methods of Solution and Confidence in Results

The methods of solving these problems are briefly:

- a. All one-dimensional reactivity calculations employed the UNC DTF Code ( $S_N$  method) together with the Hansen-Roach (LASL) 16 group cross section set. Anisotropic scattering cross sections were used for hydrogen.
- b. An equivalent-sphere model was used in all "k" calculations. This is based on equating geometric bucklings of a sphere to that of the actual finite cylinder under study employing experimental extrapolation distances for  $UO_2F_2$  solutions contained in 1/16" Al vessels. The core compositions of cylinder and sphere are taken to be identical and the "k" of the equivalent sphere is then taken to be the "k" of the finite cylinder.

To attain some confidence in the above calculational approach, the above methods were used to analyze previously measured  $UO_2F_2 - H_2O$  critical systems. In addition, the results of the two major problems were compared to experimental curves of  $UO_2F_2 - H_2O$  solutions in stainless steel containers. In each case agreement with experiment was excellent.

To estimate the effect of distortion of the top surface of the tank solution caused by the action of the electric stirrer, a set of two dimensional problems were solved using UNC 2DF code ( $S_N$  method). To avoid excessive machine time, the Hansen-Roach 16 group cross sections were collapsed to four (4) groups using UNC FAINT-group collapsing code. Although the four group structure used was not as accurate in calculating the multiplication factor, the assumption is that the reactivity change predicted from two such calculations is correct.

## 3. Results for Specific Problems

### a. Continuous Pouring Problems

The results are displayed in Figure B-1A. The effective multiplication factor is plotted as a function of various variables; number of liters of uranium solution formed in the tank, amount of U-235 in the tank, total volume of mixture in tank, height of solution in tank and hydrogen-to-U-235 atom ratio.

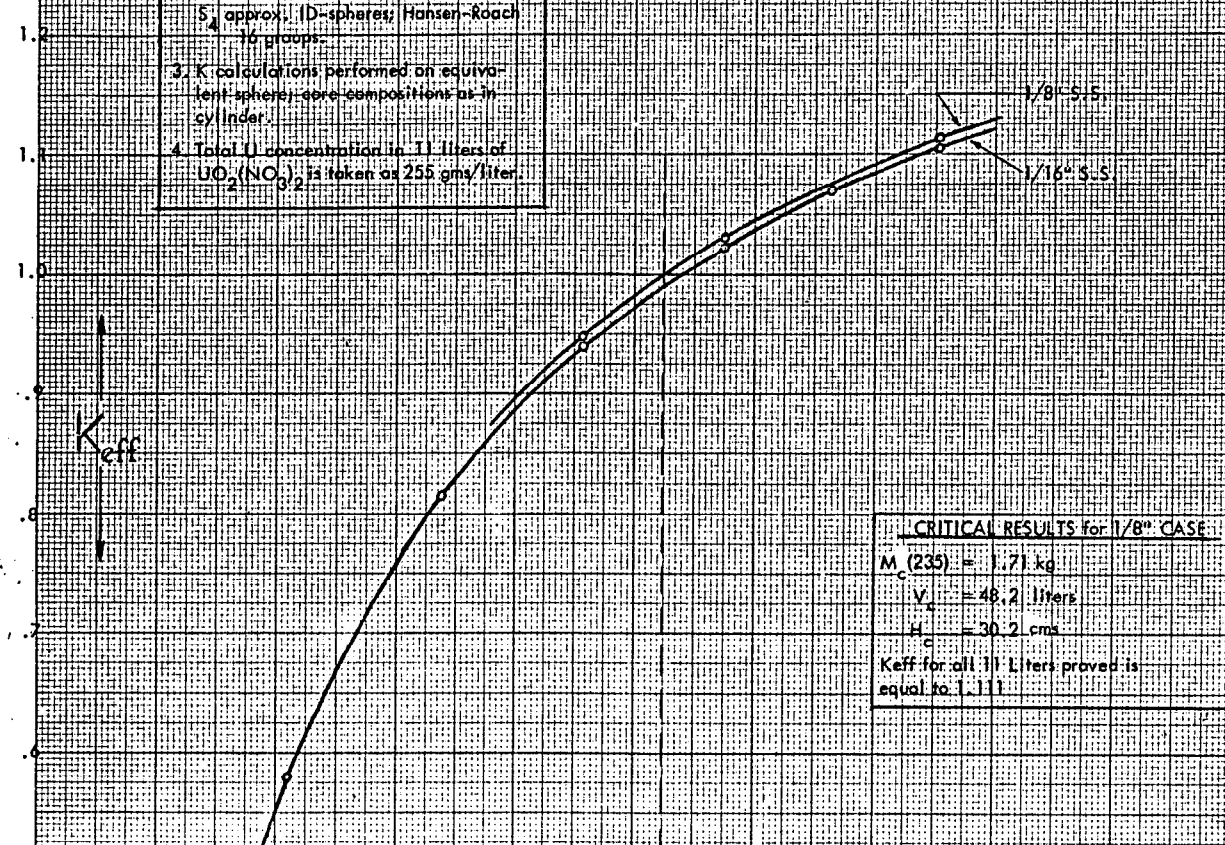
It can be seen that the multiplication factor in the absence of the electric stainless steel stirrer, distortion of solution top surface, temperature and self shielding in precipitate particle is equal to 1.111 when all eleven (11) liters are poured. In the same condition, criticality of the system is obtained when 7.2 liters of uranium solution have been poured.

FIGURE B-1-A  
CONTINUOUS POURING PROBLEM

$K_{eff}$  versus liters of enriched  $UO_2(NO_3)_2$  aqueous solution poured into 7-3/4" I.D., 1/8" thick Stainless Steel Vessel containing .54 Molar Solution (41 Liters)  $Na_2CO_3$ .

**BASIS OF CALCULATION**

1. Enrichment taken as 93.2% in U-235
2.  $K$  calculations based on DTF results,  $S_4$  approx., D-spheres, Hansen-Koach 14 groups.
3.  $K$  calculations performed on equivalent sphere core compositions as in cylinder.
4. Total U concentration in 11 liters of  $UO_2(NO_3)_2$  taken as 255 gms/liter.



**CRITICAL RESULTS for 1/8" CASE**

$M_c(235) = 1.71 \text{ kg}$

$V_c = 48.2 \text{ liters}$

$H_c = 30.2 \text{ cms}$

$K_{eff}$  for all 11 Liters proved is equal to 1.11

|   |  |       |       |       |      |       |       |       |          |          |
|---|--|-------|-------|-------|------|-------|-------|-------|----------|----------|
| A | Liters of $UO_2(NO_3)_2 + H_2O$ poured into 41 liters of $(Na_2CO_3 + H_2O)$ | 2     | 4     | 6     | 7.2  | 8     | 9.5   | 11    | (Liters) |          |
| B | Kg U235 in cylinder after pouring  | .475  | .95   | 1.43  | 1.71 | 1.90  | 2.26  | 2.61  | 3        | (Kg 235) |
| C | Total Volume of mixture in cylinder after pouring (Liters)                   | 43    | 45    | 47    | 48.2 | 49    | 50.5  | 42    | (Liters) |          |
| D | Height of cylinder after pouring (cms)                                       | 26.94 | 28.19 | 29.45 | 30.2 | 30.70 | 31.64 | 32.58 | (cms)    |          |
| E | H/U235 of mixture after pouring  | 2346  | 1223  | 850   | 730  | 662   | 662   | 509   |          |          |

The base case reactivity needed to produce criticality is 1.028, computed from Table B-1-4 as follows:

|                        |              |
|------------------------|--------------|
| Base Case Reactivity   | 1.028        |
| Stainless Steel Effect | -.008        |
| Surface Distortion     | -.021        |
| Wall Reflection        | +.004        |
| No Top SS Reflection   | <u>-.003</u> |
|                        | 1.000        |

From Figure B-1A, the critical parameters are:

|                       |            |
|-----------------------|------------|
| Critical Volume       | 49 liters  |
| Critical Mass (U-235) | 1.90 kgs.  |
| Height                | 30.70 cms. |

b. Final Configuration Problem

The results are presented in Figure B-1-B. The effective multiplication factor is plotted as a function of solution volume and height. It is thought that 10 to 11 liters of solution had been expelled during the initial excursion. Thus, the final configuration has a volume of 41 to 42 liters. Figure B-1-B shows that the corresponding multiplication factors are 1.035 and 1.043 without perturbations.

The critical conditions are summarized using data from Table B-1-4.

|  | 41 liters | 42 liters |
|--|-----------|-----------|
| Base case reactivity                     | 1.035     | 1.043     |
| Stainless steel stirrer                  |           | -.008     |
| Surface distortion                       |           | -.021     |
| Wall reflection                          |           | +.004     |
| No top SS reflection                     |           | -.003     |
| Temperature increase (20°C)              |           | -.006     |
| Self Protection and precipitate settling |           | -.002     |
| Corrected reactivity                     | 0.999     | 1.007     |
| Critical mass, U-235                     | 2065g.    | 2116g.    |

c. Verification of the Equivalent Sphere Method

The method is used to analyze two  $\text{UO}_2\text{F}_2 - \text{H}_2\text{O}$  (93.4% U enrichment) criticals contained in 1/16" stainless steel vessels reported in ANL 5800 (2nd Edition, p. 183). Data and results of calculating these via the equivalent sphere procedure are given below in tabular form:

| Case    | Vol. (liters) | Dia. cms. | Height cms. | L/D | H/U | Crit.mass U-235 kg. | Radius Eq. Sph. | k calculated |
|---------|---------------|-----------|-------------|-----|-----|---------------------|-----------------|--------------|
| Crit. A | 30.8          | 38.1      | 27.0        | .71 | 499 | 1.61                | 18.58           | .995         |
| Crit. B | 41.6          | 50.8      | 20.5        | .40 | 499 | 2.17                | 18.43           | -.t-         |

+ the slightly smaller equivalent radius would yield a slightly smaller value of k.

Comparison of two calculated results to experimental values of similar configurations are presented in Figure B-1-C, B-1-D and B-1-E.

d. Peripheral Problems

In the following problems, the volume is 42 liters. The composition is fixed at 54.05 g-235/liter, 45.2 g  $\text{Na}_2\text{CO}_3$ /liter, H:U-235 is 509.

(1) Effect of Temperature Rise

Changes in solution density caused by increasing the temperature are assumed to be similar to that of water. One dimensional problems were run to estimate reactivity changes due to given uniform temperature increases. It is found that

$$\Delta k = -2.3 \times 10^{-4} \text{ per degree centigrade}$$

An estimate of the change in thermal base gives  $-0.8 \times 10^{-4}/^\circ\text{C}$ . Combining this with the density effect gives the total temperature coefficient as:  $-3.1 \times 10^{-4}/^\circ\text{C}$ .

(2) Effect of Increasing the Solution Height

This effect can be obtained directly from Figure B-1-B. To go from critical to prompt critical, one can read that the solution height must be increased by 0.43 cm.

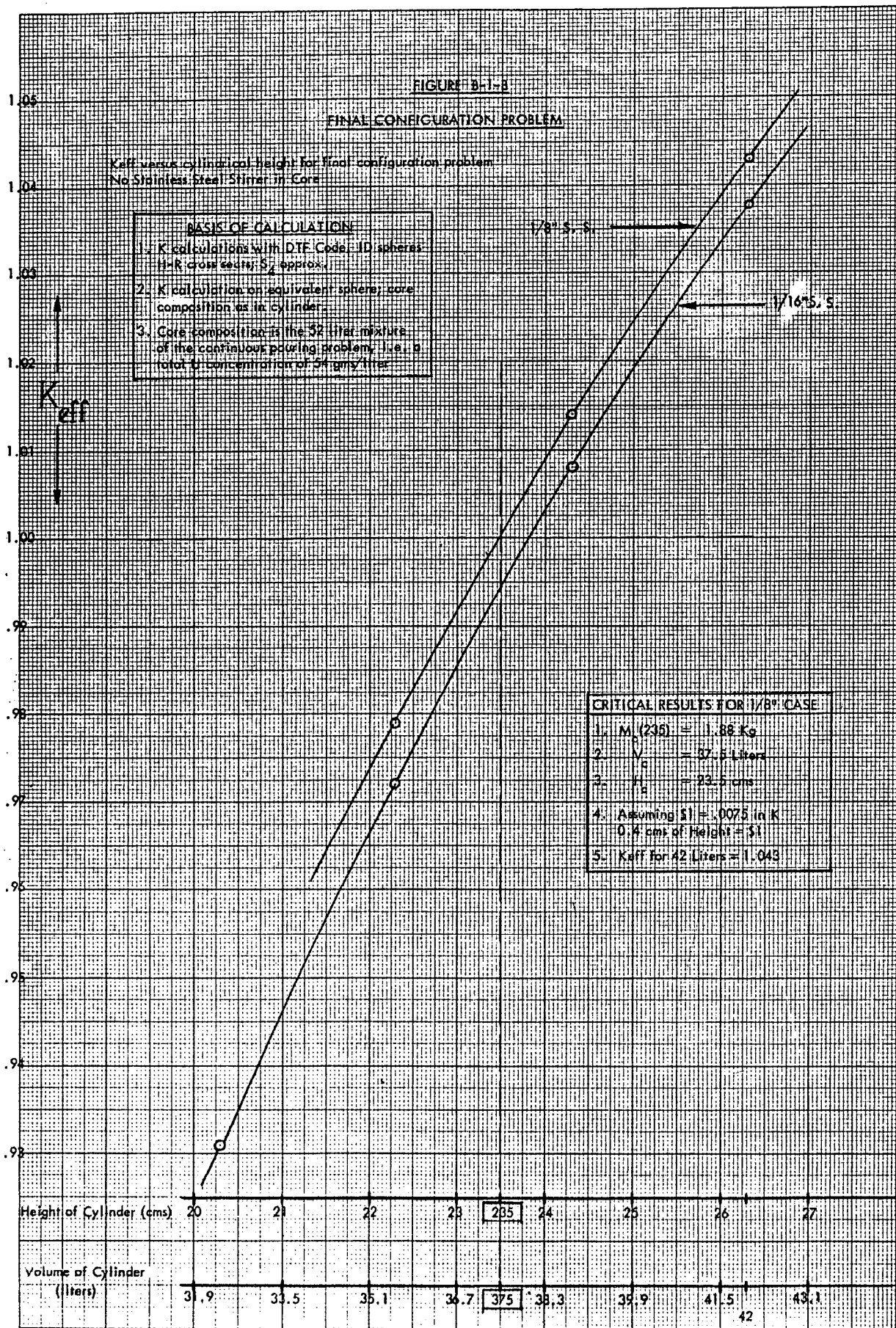
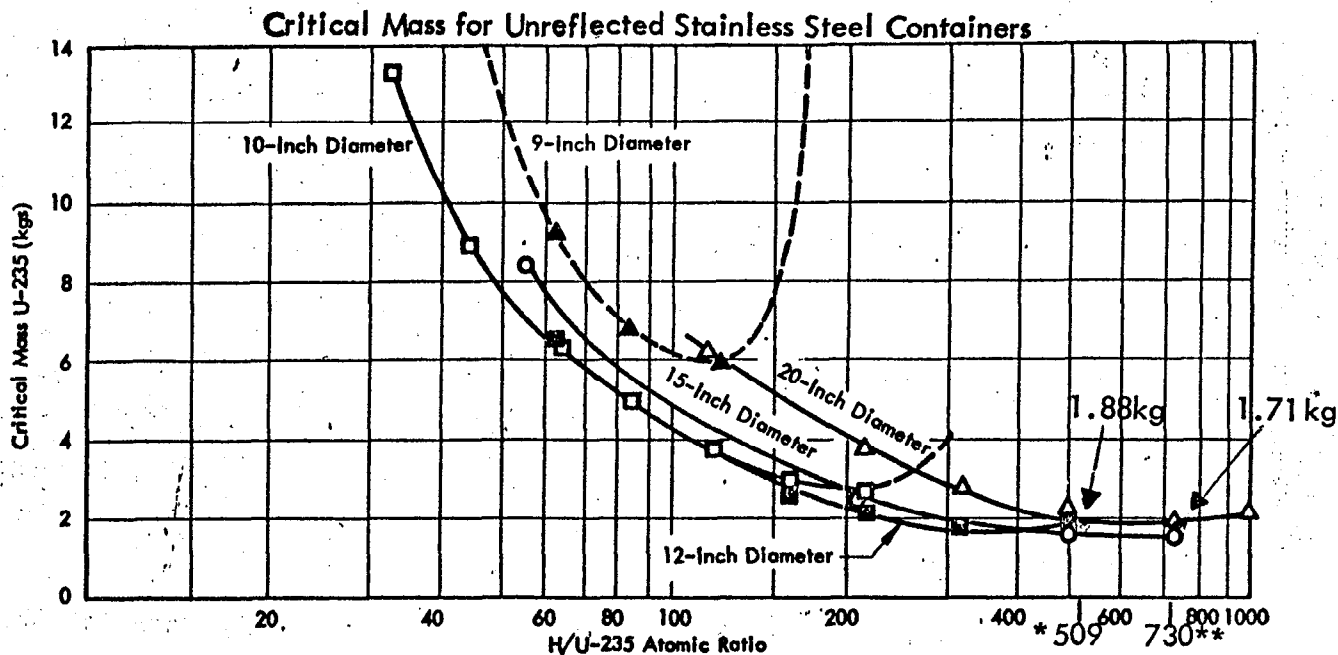


FIGURE B-1-C



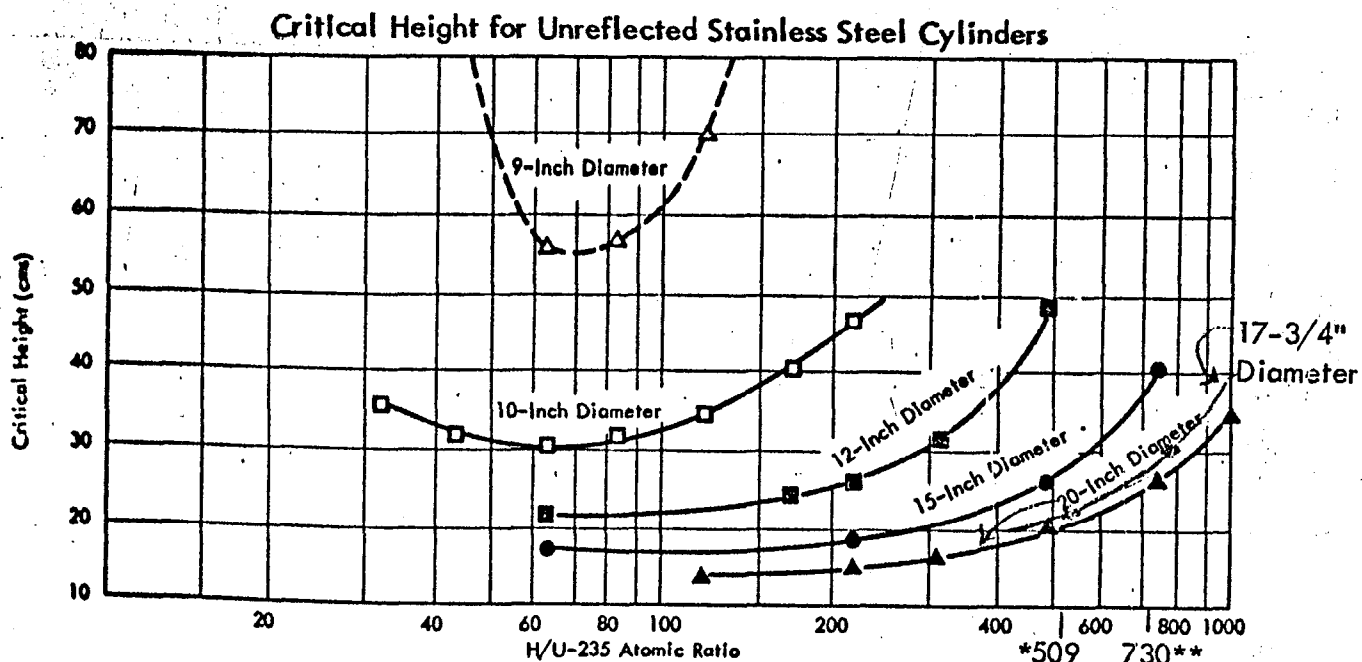
Critical Mass as a Function of the Moderation for Stainless Steel Reactors. (The Various Diameter Cylinders Contained Uranyl Fluoride Solutions Enriched to 93.4% U-235. Beck, et al, K-343.)

Figure B-1-C extracted from Y-1272, Y-12 Plant Safety Handbook, March 1963.

Note: \* Final Configuration

\*\* Continuous Pouring

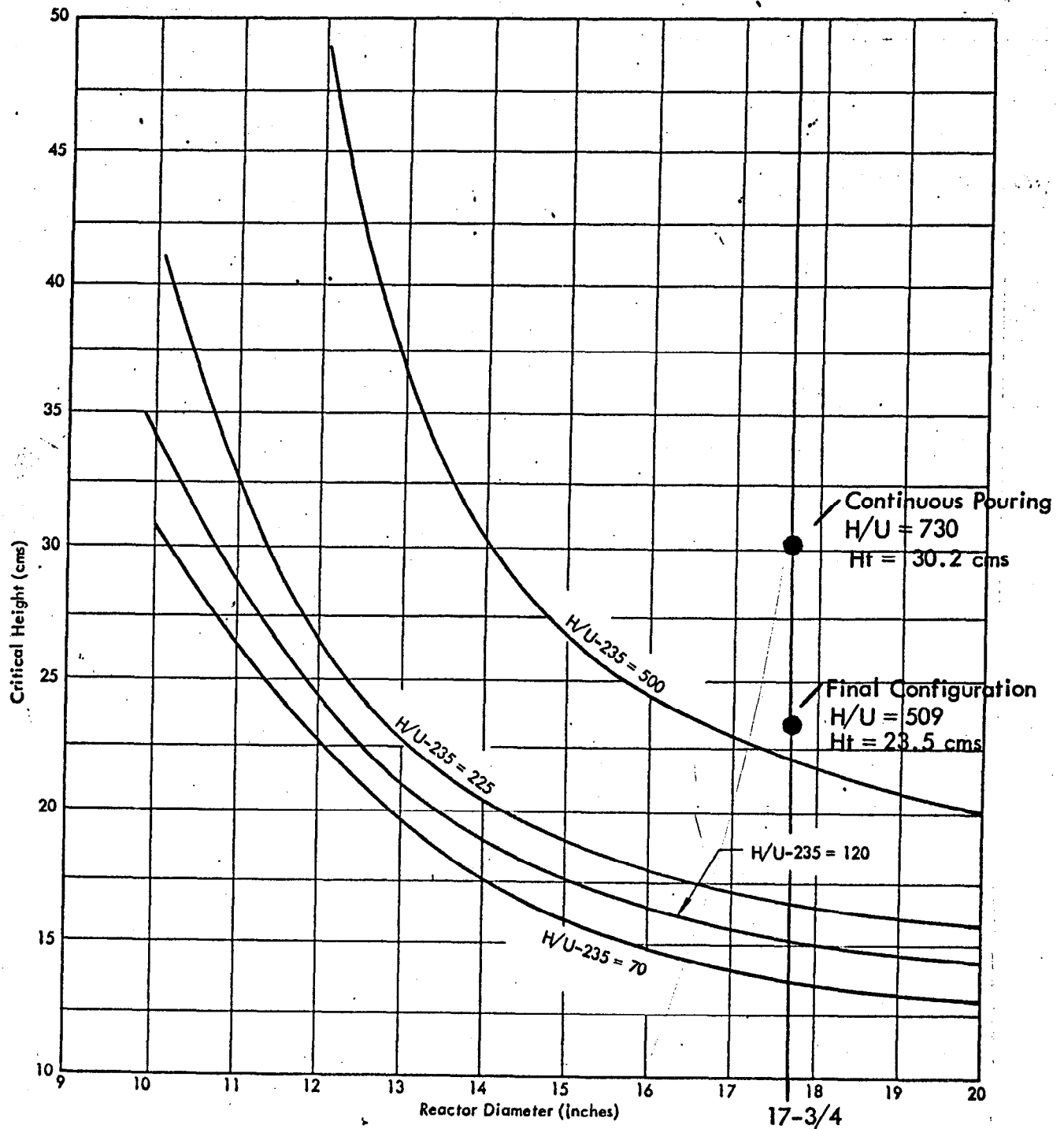
FIGURE B-1-D



Critical Height as a Function of the Moderation for Stainless Steel Reactors. (The Various Diameter Cylinders Contained Uranyl Fluoride Solutions Enriched to 93.4% U-235. Beck, et al, K-343.)

Figure B-1-D extracted from Y-1272, Y-12 Plant Safety Handbook, March 1963.

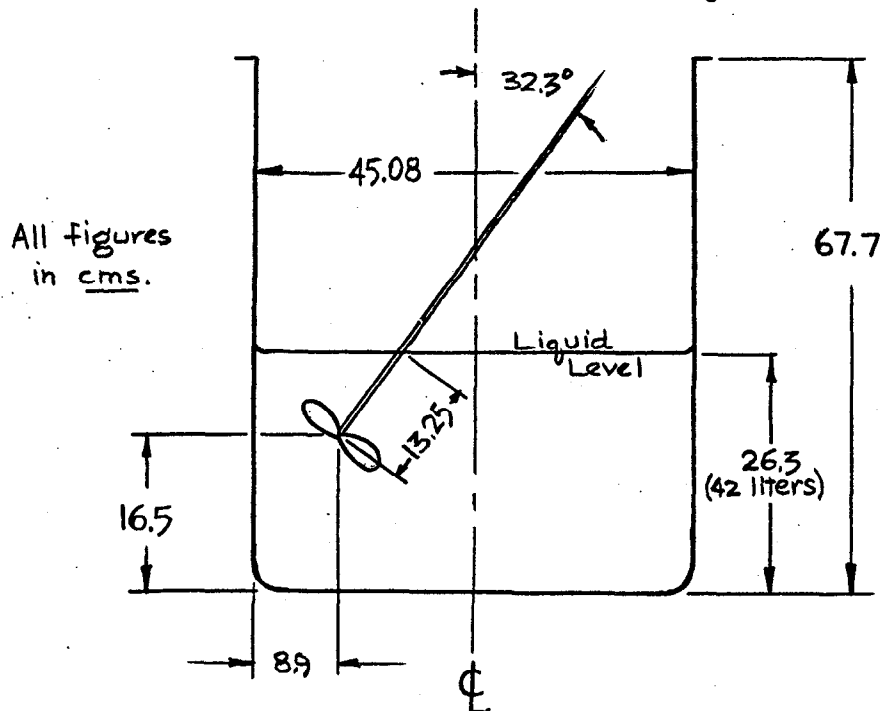
FIGURE B-1-E

Critical Height as a Function of the Diameter for Unreflected Stainless Steel Reactors

(The Various Diameter Cylinders Contained Uranyl Fluoride Solutions at Various Moderations. Uranium was Enriched to 93.4% U-235. Beck, et al, K.343.)

d. Peripheral Problems - (Continued)(3) Effect of the Stainless Steel Stirrer

The stainless steel stirrer position in the tank is shown in the rough sketch of the tank in the 42 liter final configuration.



The mass in solution is estimated from data of Appendix A-1.

$$\text{Mass of stainless steel in blades} = 200.9 \text{ g.}$$

$$\text{Mass of stainless steel rod} = \underline{134.5 \text{ g.}}$$

$$\text{Total mass of stainless steel in solution} = 335.4 \text{ g.}$$

Five replacement calculations (stainless steel replacing its volume of liquid) were performed in spherical geometry corresponding to the 42 liter cylindrical case. In all cases the core masses have been conserved and the volumes have been increased to accommodate the inserted stainless steel. As in all previous calculations, volumes of cylinders are increased by height, appropriate equivalent spheres generated and the  $k$ 's calculated.

The starting point of the calculations is the 42 liter final configuration without stainless steel in the core. Five hundred (500) grams of stainless steel are then inserted into this cylindrical configuration increasing the volume to 42.063 liters. The equivalent sphere for



d. Peripheral Problems - (Continued)3. Effect of the Stainless Steel Stirrer - (Continued)

this new cylindrical volume (when compared to the volume of the no-stainless steel sphere case) accomodates 798 grams of stainless steel. The position and manner of inserting these 798 grams, together with their effects is given in Table B-1-1.

The results show that in view of the position of the stirrer in the tank the effect of the stirrer stainless steel on reactivity can be taken as

$$(-.3\text{¢/g}) \times 335 \text{ g} = -100\text{¢} \text{ or } -.4 \text{ cm in solution height.}$$

4. Effect of A "Wave" Formation Due to the Stirrer Action

The problem here is to estimate the effect on reactivity of a "wave" produced on the surface of the 42 liter final configuration. This perturbation is taken as  $\pm 3$  cms about the unperturbed liquid-line as a result of experiments (Appendix A-3).

To estimate this effect, a set of two-dimensional problems were solved using UNC's 2DF code. To avoid excessive machine time, the Hansen-Roach 16 group cross sections were collapsed to four groups using UNC's FAINT-group collapsing code. Results of one and two dimensional, 16 groups and 4 group reactivity calculations are given in Table B-1-2. A rough sketch of the geometry used in the calculations is shown in Figure B-1-F.

The effect of the distortion of the top surface of the liquid is to decrease the reactivity by 2.1% or 2.6 dollars.

## Estimates of Worth of Stainless Steel Stirrer in 42 Liter Final Configuration

| Case | Amount of Stainless Steel (gms) Inserted Into Sphere                | Position of Insertion   | Danger Coeff. + $\phi$ /gram | k with* Stainless Steel in Core |
|------|---|---|------------------------------|---------------------------------|
| a    | 798   | Homogeneous distribution, mixed with core materials                                       | -.134                        | 1.035                           |
| b    | 798   | At center of core (solid stainless steel sphere; 2.89 cms. radius)                        | -.270                        | 1.027                           |
| c    | 798   | At 10 cms; (solid stainless steel shell; .08 cms thick)                                   | -.301                        | 1.025                           |
| d    | Thickness of stainless steel container increased from 1/16" to 1/8" |   | +.012                        | 1/16"; 1.037<br>1/8"; 1.043     |
| e    | 200   | 100 gms., r=0 to r=2.5 cms.<br>100 gms., r=2.5 to r=5.1 cms.<br>Mixed with core materials | -.465                        | 1.036                           |

\* k without stainless steel in core = 1.043

+ 100  $\phi$  = .0075 in k.

(5) Effect of the Presence of A Concrete Wall 15 Inches from the Tank

An estimate of the effect on the reactivity of a concrete wall reflector 15" from the tank surface was made from three criticality calculations. Case 1 is the bare spherical core equivalent to the 42 liter final configuration, Case 2 in the same core with a 30 cm. thick spherical shell of water surrounding the core and Case 3 places the watershell at 30 cm. from the core. It is found that the reactivity decreases approximately proportionally to the inverse square distance. Assuming that the concrete wall thickness (4") is an infinite reflector slab and that half of the neutrons leaking from the core are incident on the wall, gives the following estimate for the positive change in reactivity due to the wall presence:

$$\frac{\Delta k}{k} = +.004 \text{ or } + .50 \text{ dollar or } + .20 \text{ cm in solution height.}$$

This estimate is in good agreement with the 0.3 cm decrease in solution height computed at Los Alamos. (Reference 22, Appendix C)

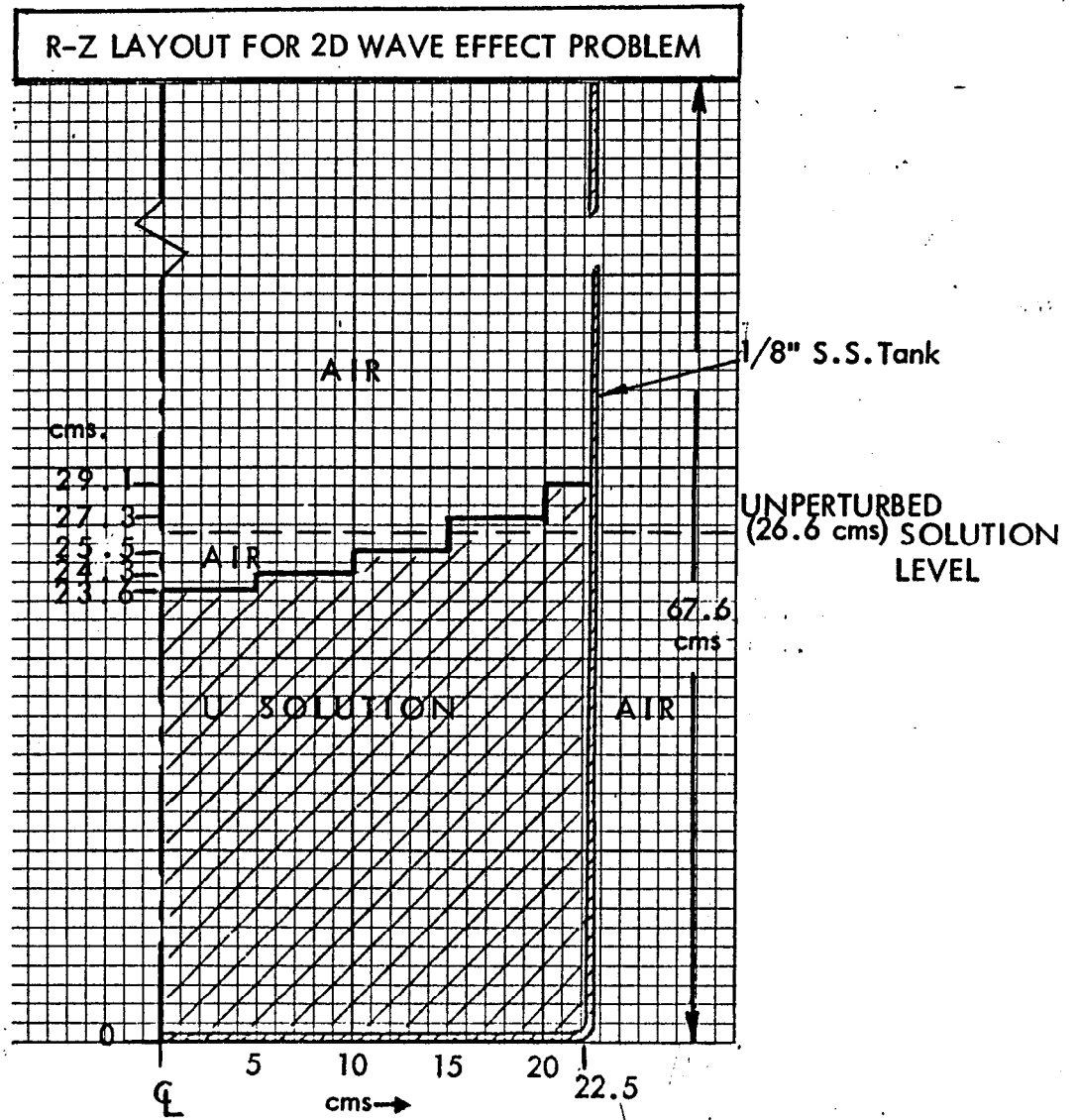
Effect of Surface Distortion

| Number of Groups | Number of Dimensions |       | Remarks           |
|------------------|----------------------|-------|-------------------|
|                  | 1 D                  | 2 D   |                   |
| 16               | 1.043                | 1.028 | Flat surface      |
| 4                | 1.035                | 1.022 | Flat surface      |
| 4                | 0.999*               | 1.001 | Parabolic surface |

\* Estimated by perturbation theory

FIGURE B-1-F

ROUGH SKETCH OF THE WAVE GEOMETRY



d. Peripheral Problems - (Continued)(6) Effect of Self Shielding of Precipitate Molecules

Appendix A-3 concludes that the precipitate consists of particles with a suggested composition  $\text{Na}_4\text{UO}_2(\text{CO}_3)_3 \cdot 2\text{H}_2\text{O}$ , that the individual particles are about 1 micron in size, and that, upon settling, agglomerates are formed with sizes of about 20 microns. Assuming a specific gravity of 5 (it is difficult to see how a value as high as 10 is possible), an absorption cross section of 600 barns leads to a macroscopic thermal absorption cross section of  $3 \text{ cm}^{-1}$ . A sphere 20 microns in diameter then has a radius which is  $3 \times 10^{-3}$  absorption mean free paths, leading to a self-protection factor of .997. Thus, the effect of particle size is to reduce the effective mass of uranium by 0.3%. Combining this with a thermal utilization of 0.8 leads to a  $\delta k/k$  of  $(1 - .8)(0.3\%) = 0.06\%$ . The effect is small.

(7) Effect of Delayed Neutrons in Subcritical Geometries

The final configuration solution was drained through the 1-C-9 solvent recovery column (see Appendix A-1) into one-gallon polyethylene containers. The effect of the delayed neutrons in the container geometry was evaluated using the one-dimensional cylindrical geometry with an axial buckling. Delayed neutrons were introduced with a uniform spatial distribution and energies in the 0.1 to 0.9 Mev range. The results are presented in Table B-1-3.

TABLE B-1-3

| Effect of Delayed Neutrons in Gallon Jug |      |
|--|------|
| Delayed neutrons injected .....          | 13.0 |
| Fission neutrons produced .....          | 2.2  |
| Number neutrons leaked .....             | 12.9 |
| Number neutrons absorbed .....           | 2.3  |

For the 3" column, more neutrons are expected to be leaking out of the system and less neutrons born in the column.

In order to estimate the neutron dose received by the Supervisor while draining the final configuration solution, calculations were performed to estimate the neutron leakage resulting from subcritical multiplication of delayed neutrons of the drain line and the containers into which liquid was poured.

d. Pheripheral Problems - (Continued)(8) Prompt Neutron Lifetime

The prompt neutron lifetime of the 42 liter final configuration was calculated by inserting a "pure"  $\frac{1}{V}$  absorber uniformly throughout the core and reflector of the equivalent sphere to effect approximately a 1% change in  $k$ . This  $\frac{1}{V}$  absorbing nuclide, with 1 barn absorption cross section at thermal, has been averaged over the same group structure and manner of the Hansen-Roach cross sections. The prompt lifetime was computed to be

$$L = 2.7 \times 10^{-5} \text{ sec.}$$

(9) Shutdown Mechanism

Calculations of the transient behavior were made based on KEWB experiments (References 23 and 24, Appendix C). Generally, the calculations show that for stable periods  $\geq 10$  ms ( $\Delta k < 1.25$  dollars), radiolytic gas ( $H_2$  and  $O_2$ ) bubbles are formed at the rate of 5.3 liters/MW-sec., but no large pressures are generated. For periods  $< 5$  ms ( $\Delta k > 2$  dollars), large pressures are generated and solutions are splashed out of open containers.

For the latter case, a digital computer code, KINETICS, based on the Equations of Reference 23 (Appendix C) was prepared. The code was checked by comparing the predicted peak power and energy releases with the calculations of Reference 23 (Appendix C) for the 24 liter bare cylinder KEWB core (core 5, experiment 3041). Calculations were made for a 42 liter (45 cm dia.) core representing the carbonate tank. The results were as follows:

| Reactivity Insertion,<br>Dollars | Energy Release |                       |
|----------------------------------|----------------|-----------------------|
|                                  | MW-sec.        | Fissions              |
| 2.125                            | 5.3            | $1.7 \times 10^{17}$  |
| 3.25                             | 12.1           | $3.8 \times 10^{17}$  |
| 4.38                             | 22.3           | $7.05 \times 10^{17}$ |
| 5.51                             | 32.6           | $10.3 \times 10^{17}$ |

From these results, a step insertion of 1.7 dollars is required to explain the  $10^{17}$  fissions in the initial burst.

For the second excursion of about  $3 \times 10^{16}$  fissions (1 MW-sec), the precipitate particles act as nucleation sites for the radiolytic gas. About 5.3 liters are formed, decreasing the density by  $5.3/42 = 12.6\%$ . From Table B-1-4 this reduces the reactivity by 0.046 if all the gas is present at one time.

4. Summary of Results

Results of the peripheral problems are presented in Table B-1-4 below

TABLE B-1-4

## Reactivity Perturbations on the 42 Liter Configuration

|                                  | Reactivity                                    | Critical Height              |
|----------------------------------|---|------------------------------|
| Temperature coefficient          | $-3.1 \times 10^{-4} \text{ } \circ/\text{C}$ | 0.015 cm/ $^{\circ}\text{C}$ |
| Stainless steel stirrer          | - .0075                                       | 0.4 cm                       |
| No stainless steel reflector top | - .003  | 0.16 cm                      |
| Surface distortion               | - .021  | 1.12 cm                      |
| Wall reflection                  | + .004  | -0.21 cm                     |
| Self-Protection (20 $\mu$ dia.)  | - .0006                                       | +0.03 cm                     |
| Prompt neutron lifetime          | $2.7 \times 10^{-5} \text{ sec.}$             |                              |
| Density effect                   | -.0037/% density decrease                     | 0.19 cm/% density decrease   |

Comparison of these calculated reactivity results with independent calculations performed at Los Alamos (Reference 25, Appendix C) on the final configuration solution gives additional confidence in the criticality results stated in this section as shown in Table B-1-5 below

TABLE B-1-5

## Comparison of Calculated Parameters for Final Configuration Solution

| Parameter  | Calculated                  |                             | Empirical Conversion of Data (LASL) |
|--|-----------------------------|-----------------------------|-------------------------------------|
|  | LASL*                       | UNC                         |                                     |
| Dollar vs. height                                    | 1\$ = 0.48 cm               | 1\$ = 0.43 cm               | -                                   |
| Stainless Steel Stirrer effect                       | increased height by 0.57 cm | increased height by 0.40 cm | -                                   |
| Wall (15" distant effect)                            | decreased height by .3 cm   | decreased height by .2 cm   | -                                   |
| Critical height (including stirrer and wall effects) | 23.8 cm                     | 23.7 cm                     | 23.8 cm                             |

\* See Reference 25, Appendix C

CALCULATIONS OF NEUTRON LEAKAGE SPECTRA

It is necessary, for both dose calculations and activation computations, to obtain a spectrum for the neutrons leaking from the initial and final configurations. Methods of computing neutron leakage which have been used in this work are the multi-group transport programs UNCDTF described in the criticality calculation (Appendix B-1) and the UNC SANE Monte Carlo code (Reference 26, Appendix C). The system configurations which have been considered in these calculations are based on volume and material composition of the core solution obtained at different stages of the study. Generally, an equivalent sphere model of the system is used.

Case 1 is based on preliminary data obtained from the testimonies of the plant personnel.

Case 2 is thought to be the initial configuration determined from chemical and activation measurements.

Case 3 is thought to be the final configuration.

In order to relate the incident neutron current on the human body surface to the back current density from the body, two additional systems were evaluated.

Case 1a is the same core as Case 1 with a 30 cm thick spherical shell model man placed 30 cm from the core.

Case 1b places the same man model in contact with the same core.

Table B-2-1 summarizes characteristics and data for the various configurations. The equivalent sphere method may lead to some errors in interpreting activation measurements on objects located near the cylindrical tank surface. Indeed the out-current density varies along the axial and radial direction on the core outer surface. Further, the average lateral leakage is expected to be different from the average bottom and top leakage in a cylindrical configuration, particularly for low height to diameter ratios. Hence, a second approach was employed. Two dimensional transport calculations of the final configuration for which largest differences are expected have been performed.

Table B-2-2 presents the results obtained for the leakage neutron spectra normalized to one neutron leaking out of the system,  $j_+(E)$ . It can be seen that:

- (1) There are negligible changes in spectrum in all spherical bare cores (Cases 1, 2 and 3). Comparison of calculations at different values of multiplication factor when the uranium content in each of these cases is varied, also indicates negligible changes in the leakage spectrum.
- (2) The two dimensional calculations of the final configuration (Case 3) shows that:
  - (a) Total, side and consequently top and bottom leakage spectra are approximately identical.
  - (b) The equivalent sphere method gives a very good leakage spectrum.
- (3) The presence of man increases the low energy part of the spectrum and has a negligible effect on the non-thermal leakage spectrum.



TABLE B-2-1

## Spherical Calculational Models

| Case | Volume (liters) | Cylindrical Height (cm) | Equivalent Sphere Radius (cm) | SS Reflector Thickness (cm) | U-235 (kg) | Molarity of Na <sub>2</sub> CO <sub>3</sub> | Other Reflector Regions         |
|------|-----------------|-------------------------|-------------------------------|-----------------------------|------------|---|---------------------------------|
| 1    | 67              | 40.81                   | 24.6                          | .36                         | 1.83       | 1   | bare                            |
| 1a   | 67              | 40.81                   | 24.6                          | .36                         | 1.83       | 1   | 30 cm thick tissue at 30 cm     |
| 1b   | 67              | 40.81                   | 24.6                          | .36                         | 1.83       | 1   | 30 cm thick tissue against core |
| 2    | 52              | 32.58                   | 22.14                         | .36                         | 2.61       | .54   | bare                            |
| 3    | 42              | 26.3                    | 20.06                         | .36                         | 2.11       | .54   | bare                            |

TABLE B-2-2

## Leakage Spectra of Neutrons Escaping from Cores

| Energy Group g | Lower Energy E | Spherical Models $j_{+,g}$ * |         |         |        |        | 2 Dimensional Calculations of Core 3 |              |
|----------------|----------------|------------------------------|---------|---------|--------|--------|--------------------------------------|--------------|
|                |                | Case 1                       | Case 1a | Case 1b | Case 2 | Case 3 | Total Leakage                        | Side Leakage |
| 1              | 3 Mev          | .114                         | .092    | .073    | .113   | .113   | .111                                 | .112         |
| 2              | 1.4            | .211                         | .169    | .137    | .206   | .207   | .203                                 | .206         |
| 3              | .9             | .080                         | .066    | .056    | .081   | .082   | .081                                 | .081         |
| 4              | .4             | .108                         | .088    | .076    | .108   | .109   | .109                                 | .108         |
| 5              | .1             | .102                         | .083    | .073    | .101   | .102   | .102                                 | .101         |
| 6              | .017           | .066                         | .054    | .049    | .065   | .065   | .065                                 | .065         |
| 7              | .003           | .043                         | .036    | .035    | .042   | .042   | .043                                 | .043         |
| 8              | 550 ev         | .038                         | .032    | .032    | .037   | .037   | .038                                 | .038         |
| 9              | 100 ev         | .035                         | .030    | .031    | .034   | .034   | .034                                 | .035         |
| 10             | 30             | .024                         | .021    | .022    | .023   | .023   | .023                                 | .024         |
| 11             | 10             | .022                         | .018    | .020    | .021   | .020   | .021                                 | .021         |
| 12             | 3              | .023                         | .020    | .021    | .022   | .021   | .022                                 | .022         |
| 13             | 1              | .020                         | .018    | .019    | .019   | .019   | .019                                 | .020         |
| 14             | .4             | .017                         | .015    | .016    | .016   | .015   | .016                                 | .015         |
| 15             | .1             | .040                         | .037    | .045    | .036   | .035   | .036                                 | .035         |
| 16             | Thermal        | .123                         | .223    | .294    | .076   | .074   | .075                                 | .072         |

$$* \sum_{\text{all } g} j_{+,g} = 1$$

In conclusion, spectral differences will be neglected in the remainder of these calculations when only leakage from a bare reactor is considered.

It is interesting to plot the total neutron current density escaping from the core normalized to one neutron born in the core,  $J_+$ , versus the height or volume of the tank solution. In Figure B-2-A,  $J_+$  is shown to be approximately a linear function of the core volume and therefore of the solution height, since for both the initial and final configuration the core composition is the same.

The change of reactivity due to the distortion of the solution top surface is estimated to 2.1% in  $k$ . If we assume that most of this change is due to increased leakage, the number of neutrons leaking out of the core per neutron born is increased by about 2%. The neutron leakage to fission conversion ratios that are used in the subsequent calculations correspond approximately to the prompt critical state of the tank in the initial and final excursions respectively. They are evaluated at the outer surface of the core.

Initial Excursion: Case 2

$$J_+ = 1.21 \times 10^{-4} \text{ n/cm}^2 \text{ per core fission.}$$

Second Excursion: Case 3

$$J_+ = 1.63 \times 10^{-4} \text{ n/cm}^2 \text{ per core fission}$$

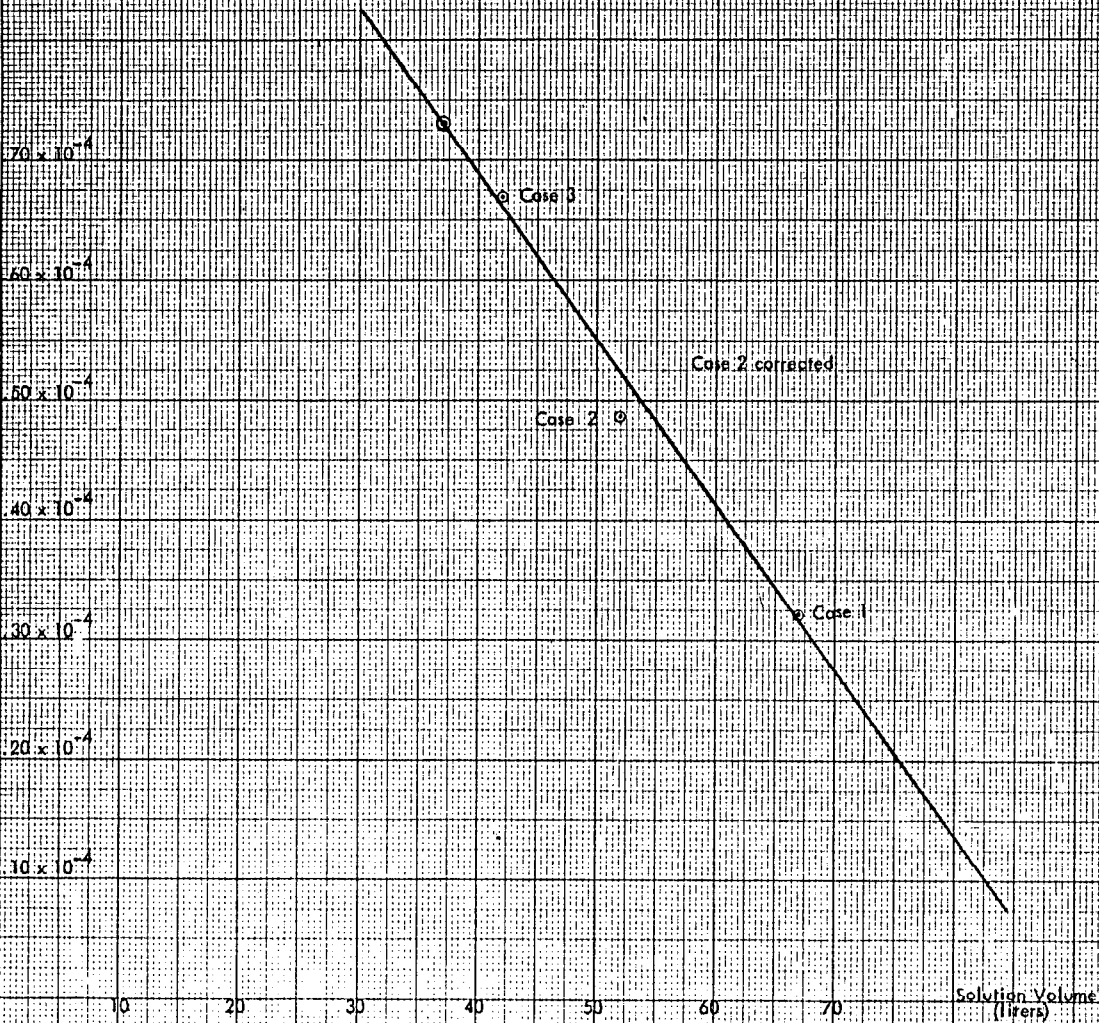
(using 2.43 neutrons born per fission)

Comparison with two dimensional calculations of the final configuration show that 48% of the neutrons escape from the lateral cylinder surface in contact with the solution and the total number of neutrons leaking per fission is equal to that obtained from the equivalent sphere calculations. Of course, the number of neutrons per  $\text{cm}^2$  escaping from the core differs since the sphere surface is minimum.

FIGURE B-2-A

Neutron Current Density Out of Spherical Cores Versus  
Solution Volumes for Various Configurations

Neutron current density out of  
core per neutron born in core,  
( $\mu\text{v}/\text{cm}^2/\text{core neutron}$ ),  $J_0$



The SANE Monte Carlo code was used to calculate the flux leakage spectra at the outer surface of the equivalent sphere obtained for Cases 1 and 2. The 32 energy group structure of the SANE code is presented in Table B-2-3, along with the 16 energy group structure of the transport code, denoted by "DTF". It can be seen that SANE gives a more detailed flux picture, particularly in the high energy range. However, there is no thermal group in the SANE code; neutrons slowing down below 0.037 eV are "killed".

When compared with "DTF", the difference in the fluxes was well within the standard deviation (15%) on the fluxes computed by SANE. Due to different group structure, the values tabulated in Table B-2-4 are summations over the appropriate groups, to permit comparison. The lower leakage at thermal energies for SANE versus DTF is expected.

Figure B-2-B gives a plot of the normalized flux spectrum at the outer core surface for the initial configuration (Case 2) along with the normalized fission spectrum. It can be seen that the use of effective fast reaction cross sections averaged over a fission spectrum is not a valid approximation.

TABLE B-2-3

| Energy Group Structure (ev) |             |            |            |
|-----------------------------|-------------|------------|------------|
| SANE                        |             | DTF Groups |            |
|                             | 1.8017 (7)* |            | 1.800 (7)* |
| 1                           | 1.4032      | 1          | 3.000 (6)  |
| 2                           | 1.0928      | 2          | 1.400      |
| 3                           | 8.5108 (6)  | 3          | 9.000 (5)  |
| 4                           | 6.6282      | 4          | 4.000      |
| 5                           | 5.1621      | 5          | 1.000      |
| 6                           | 4.0202      | 6          | 1.700 (4)  |
| 7                           | 3.1310      | 7          | 3.000 (3)  |
| 8                           | 2.4384      | 8          | 5.500 (2)  |
| 9                           | 1.8990      | 9          | 1.000      |
| 10                          | 1.4790      | 10         | 3.000 (1)  |
| 11                          | 1.1518      | 11         | 1.000      |
| 12                          | 0.89703     | 12         | 3.000 (0)  |
| 13                          | 0.69861     | 13         | 1.000      |
| 14                          | 0.54408     | 14         | 4.000 (-1) |
| 15                          | 0.42373     | 15         | 1.000 (-1) |
| 16                          | 0.3300      | 16         | Thermal    |
| 17                          | 0.12140     |            |            |
| 18                          | 0.44661 (5) |            |            |
| 19                          | 0.16430     |            |            |
| 20                          | 0.60442 (4) |            |            |
| 21                          | 0.22235     |            |            |
| 22                          | 0.81799     |            |            |
| 23                          | 0.30092     |            |            |
| 24                          | 0.11070     |            |            |
| 25                          | 0.40725 (2) |            |            |
| 26                          | 0.14982     |            |            |
| 27                          | 0.55116 (1) |            |            |
| 28                          | 0.20276     |            |            |
| 29                          | 0.74591 (0) |            |            |
| 30                          | 0.27440     |            |            |
| 31                          | 0.10095     |            |            |
| 32                          | 0.037137    |            |            |

\* Note: (N) =  $\times 10^N$

Comparison of "SANE" and "DTF" Fluxes at the Outer Core Surface

|               | DTF<br>Groups | <sup>4</sup> DTF <sup>3</sup> Flux<br>n/cm <sup>2</sup> -n | SANE<br>Groups | <sup>4</sup> SANE <sup>3</sup> Flux<br>n/cm <sup>2</sup> -n |
|---------------|---------------|--|----------------|---|
| <u>Case 2</u> | 1             | 8.49 (-6)  | 1-7            | 8.59 (-6)   |
|               | 2             | 1.56 (-5)  | 8-10           | 1.44 (-5)   |
|               | 3             | 6.58 (-6)  | 11-12          | 7.61 (-6)   |
|               | 4             | 8.97 (-6)  | 13-15          | 8.42 (-6)   |
|               | 5             | 8.59 (-6)  | 16-17          | 7.62 (-6)   |
|               | 6             | 5.59 (-6)  | 18-19          | 7.05 (-6)   |
|               | 7 - 9         | 1.06 (-5)  | 20-24          | 1.12 (-5)   |
|               | 10 - 15       | 1.31 (-5)  | 25-31          | 1.23 (-5)   |
|               | 16            | 7.35 (-6)  | 32             | 4.61 (-7)   |
|               | Total         | 8.49 x 10 <sup>-5</sup>                                    |                | 7.76 x 10 <sup>-5</sup> (± 15%)                             |
| <u>Case 1</u> | 1             | 5.46 (-6)  | 1-7            | 4.69 (-6)   |
|               | 2             | 1.04 (-5)  | 8-10           | 9.28 (-6)   |
|               | 3             | 4.21 (-6)  | 11-12          | 4.27 (-6)   |
|               | 4             | 5.73 (-6)  | 13-15          | 5.69 (-6)   |
|               | 5             | 5.49 (-6)  | 16-17          | 4.62 (-6)   |
|               | 6             | 3.60 (-6)  | 18-19          | 3.23 (-6)   |
|               | 7 - 9         | 6.40 (-6)  | 20-24          | 7.35 (-6)   |
|               | 10 - 15       | 8.01 (-6)  | 25-31          | 6.33 (-6)   |
|               | 16            | 6.67 (-6)  | 32             | 1.01 (-7)   |

FIGURE B-2-B  
 Comparison of SANE Flux Leakage Spectrum and Fission Flux Spectrum

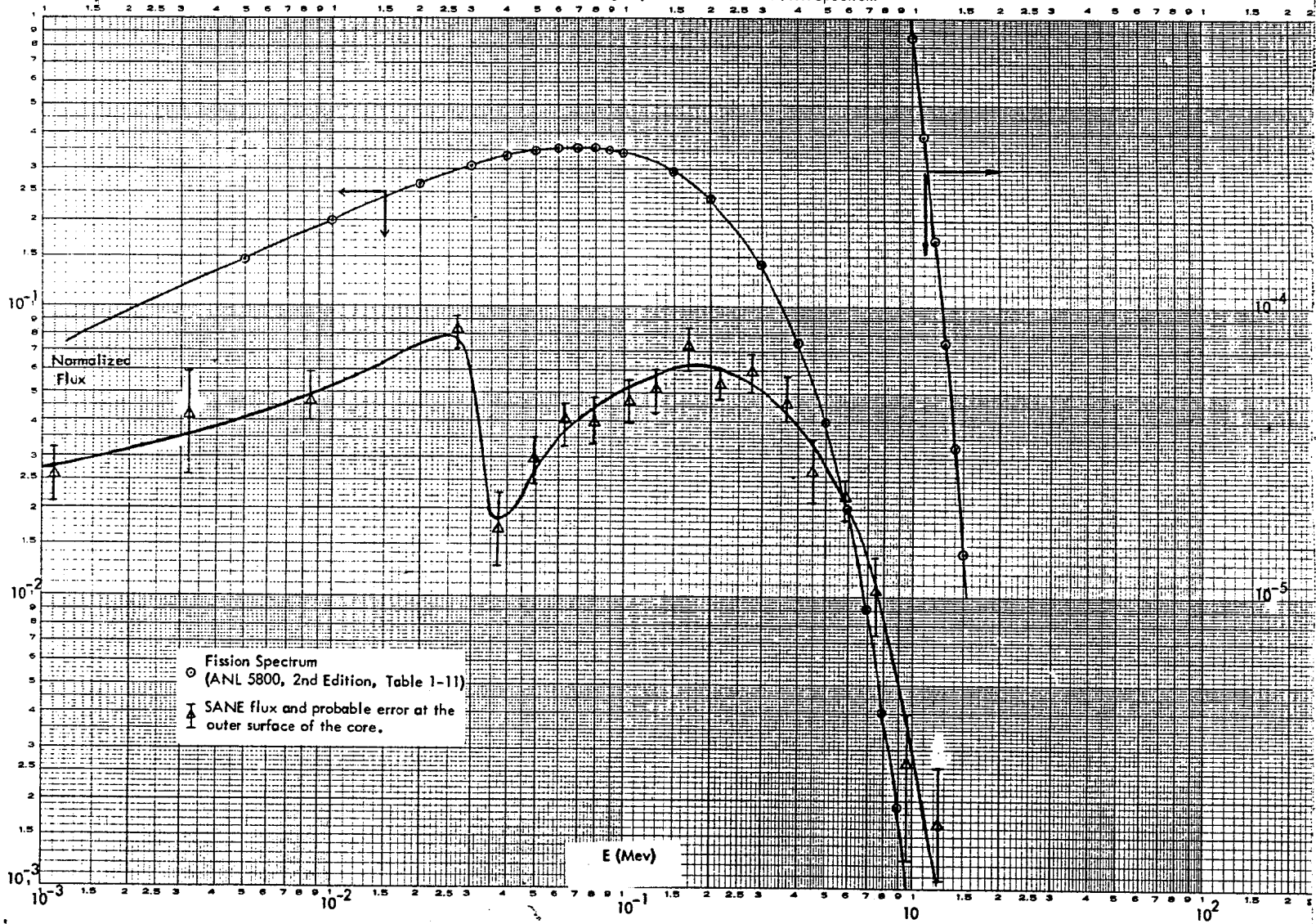


FIGURE B-2-B

NEUTRON DOSE TO INCIDENT NEUTRON FLUX CONVERSION RATIOS

## 1. Overall average "first collision" neutron dose per unit incident neutron flux

It is usual to compute a first collision neutron dose which is the absorbed dose received by a small amount of tissue. The first collision neutron dose includes all the energy imparted to tissue by the first collision of neutrons. This excludes the energy deposited in the body by the hydrogen capture gamma rays and multiple neutron scattering.

A curve of the conversion factor as a function of energy,  $D_o^{(1)}(E)$ , is given in NBS Handbook 63. Table B-3-1 lists average values of the conversion ratio in each of the 16-groups used in the transport calculations.

The overall average first collision neutron dose per neutron incident on the tissue then evaluated

$$\bar{D}_o^{(1)} = \int_0^{\infty} D_o^{(1)}(E) j_+(E) = \sum_{g=1}^{16} D_{o,g}^{(1)} \times j_{+,g} \quad (B-3-1)$$

where  $j_+(E)$  is the normalized leakage spectrum evaluated in Appendix B-1 and  $D_{o,g}$  is the average conversion ratio in group g.

Since the spectral differences for the configurations thought to be close to the actual ones are negligible, the overall average first collision neutron dose per unit incident neutron current is

$$\bar{D}_o^{(1)} = 1.50 \times 10^9 \frac{\text{rad}}{(\text{n/cm}^2)}$$



Group Values for First Collision Neutron Dose for Unit  
Incident Neutron Flux

| Group<br>Number, g | Lower Energy<br>in Group | $D_{o, g}^{(1)}$ | $\text{rad}/(\text{n}/\text{cm}^2)^+$ |
|--------------------|--------------------------|------------------|---------------------------------------|
| 1                  | 3 Mev                    | 4                | $\times 10^{-9}$                      |
| 2                  | 1.4 Mev                  | 3                | $\times 10^{-9}$                      |
| 3                  | .9 Mev                   | 2                | $\times 10^{-9}$                      |
| 4                  | .4 Mev                   | 1.7              | $\times 10^{-9}$                      |
| 5                  | .1 Mev                   | 1.0              | $\times 10^{-9}$                      |
| 6                  | .017 Mev                 | .3               | $\times 10^{-9}$                      |
| 7                  | .0035 Mev                | .05              | $\times 10^{-9}$                      |
| 8                  | 550 ev                   | .01              | $\times 10^{-9}$                      |
| 9                  | 100 ev                   | .002             | $\times 10^{-9}$                      |
| 10                 | 30 ev                    | .001             | $\times 10^{-9}$                      |
| 11                 | 10 ev                    | .001             | $\times 10^{-9}$                      |
| 12                 | 3 ev                     | .0017            | $\times 10^{-9}$                      |
| 13                 | 1 ev                     | .0026            | $\times 10^{-9}$                      |
| 14                 | .4 ev                    | .005             | $\times 10^{-9}$                      |
| 15                 | .1 ev                    | .006             | $\times 10^{-9}$                      |
| 16                 | Thermal                  | .024             | $\times 10^{-9}$                      |

+ Extracted from Figure 1, NBS 63.

2. Overall average maximum neutron dose<sup>+</sup> per unit incident neutron flux

It is also of interest to evaluate an overall average "maximum" neutron dose which the dose absorbed in a 30-cm thick infinite slab of tissue. The conversion factors have been computed by Neufeld and Snyder (Reference 27, Appendix C).

Table B-3-2 lists the values of the group average of maximum dose conversion ratios used in the calculations.

The overall average "maximum" neutron dose per unit incident neutron flux is then evaluated

$$\bar{D}_o^{\text{max}} = \sum_{g=1}^{16} D_{o,g}^{(\text{max})} \times j_{t,g}$$

It is found that

$$\bar{D}_o^{(\text{max})} = 2.45 \times 10^{-9} \text{ rad}/(\text{n}/\text{cm}^2)$$

+ Often called "whole body dose".

TABLE B-3-2

Group Values for "Maximum" Neutron Dose for Unit Incident Neutron Flux

| Group Number<br>g | Energy Range           | $\bar{D}_o^{(max)} / \bar{D}_o^{(1)}$ (rad/n/cm <sup>2</sup> )* |
|-------------------|------------------------|---|
| 1 - 3             | .9 Mev                 | 5 x 10 <sup>-9</sup>  |
| 4 - 6             | .9 Mev < E < .017 Mev. | 1 x 10 <sup>-9</sup>  |
| 7 - 15            | 17 Kev < E < 1 ev      | 0.6 x 10 <sup>-9</sup>  |
| 16                | Thermal                | 0.32 x 10 <sup>-9</sup>   |

\* Extracted from Figure 2-3 and Table 2-2, p. 18-19, H. Goldstein, "Fundamental Aspects of Reactor Shielding", 1959, Addison, Wesley.

It is of interest to note that

$$\bar{D}_o^{(max)} / \bar{D}_o^{(1)} = 1.63$$

which is in good agreement with the NBS plot of this ratio as a function of energy.<sup>+</sup>

The fast neutron contribution to the neutron dose is preponderant as shown below:

| Neutron Energy Range | Fraction of Neutrons in that Range | Contribution to the Neutron Dose |
|----------------------|------------------------------------|----------------------------------|
| E > 3 Mev            | .113                               | .30                              |
| 3 Mev > E > 1.4 Mev  | .206                               | .41                              |
| 1.4 Mev > E > .9 Mev | .081                               | .11                              |

Hence 80% of the neutron dose is due to neutrons of energy higher than 1 Mev.

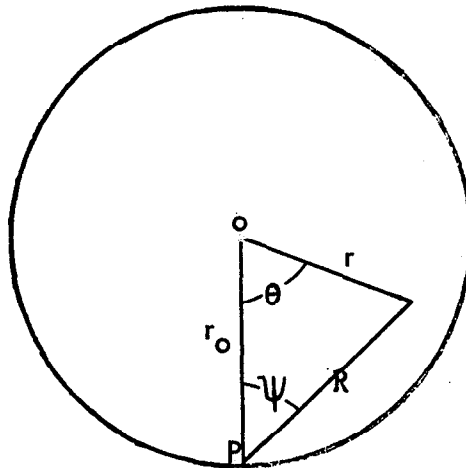
+ NBS Handbook 63, Figure 15, p. 64.

GAMMA RAY DOSE and GAMMA RAY-TO-NEUTRON DOSE RATIO CALCULATIONS

The gamma dose at the surface of the tank was computed as follows:

1. The prompt fission gammas were divided into six energy groups as shown in Table 8.1 of ANL 5800.
2. Capture gammas in materials other than U and H were shown to be negligible.
3. The U capture gamma spectrum was assumed to be the same as the prompt fission spectrum and H was assumed to yield 1.1 two Mev gammas per capture.
4. The tank was treated as a sphere of radius  $r_0$  having the correct volume, and the gamma source distribution was taken as proportional to  $1 - \frac{r^2}{r_0^2}$ .
5. Buildup in leaking from the sphere was taken into account by using the buildup factors for water (Reference 28, Appendix C)

The leakage from the sphere was computed as follows:



$$\text{Source density} = 1 - \frac{r^2}{r_0^2}$$

$$\text{Build-up: } A_1 e^{-\alpha_1 \mu r} + A_2 e^{-\alpha_2 \mu r}$$

Current density at point P due to source in  $r \sin \theta dr 2\pi d\theta$  is then given by

$$dI = r_0^2 \left(1 - \frac{r^2}{r_0^2}\right) \frac{e^{-\mu R}}{4\pi R^2} (A_1 e^{-\alpha_1 \mu r} + A_2 e^{-\alpha_2 \mu r}) r^2 \sin \theta 2\pi d\theta \cos \psi$$

The total gamma ray source in the sphere is

$$S = 2 \int_0^\pi \int_0^{r_0} \left(1 - \frac{r^2}{r_0^2}\right) r^2 \sin \theta \, dr \, d\theta$$

The fraction of gamma rays which leaks from the sphere is then given by

$$\frac{\int_0^\pi \int_0^{r_0} dI}{S} = \frac{15}{l_0^2} A_1 \left[ \frac{2}{3} l_0^3 - 2 l_0^2 + 8 - e^{-l_0} (2 l_0^2 + 8 l_0 + 8) \right] \\ + \frac{15}{L_0^2} A_2 \left[ \frac{2}{3} L_0^3 - 2 L_0^2 + 8 - e^{-L_0} (2 L_0^2 + 8 L_0 + 8) \right]$$

where

$$l_0 = 2 (\mu + \alpha_1) r_0$$

$$L_0 = 2 (\mu + \alpha_2) r_0$$

The gamma ray dose at the surface of the equivalent sphere was computed to be

$$D\gamma = 3.28 \times 10^{-13} \text{ rad/fission for Case 3}$$

$$D\gamma = 3.17 \times 10^{-13} \text{ rad/fission for Case 2}$$

$$D\gamma = 3.07 \times 10^{-13} \text{ rad/fission for Case 1}$$

(See Appendix B-2 for definitions of cases)

Fission product gamma rays in the first two seconds after excursion are negligible compared with prompt and capture gamma. The emission rate at short times after excursion is given as  $\frac{62 \text{ Mev}}{1+t \text{ Sec}}$  per fission ( $t$  in sec). (Reference 29, Appendix C). This is compared to a computed value of approximately 10 Mev fission for the prompt gammas and 1.18 Mev fission for the uranium-capture gamma rays.

In the cases of bare reactors, the fission distribution at the core boundary is approximately 1/40 of the central value. Thus the assumption of a parabolic distribution should be reasonably accurate. However, in cases where the effect of tissue is approximated by a spherical layer of water at 30 cm from the tank, the boundary value is 1/11 of the central value. Thus, the gamma density distribution may perhaps be regarded as the superposition of a parabolic distribution and a uniform distribution.

The gamma dose per core fission at the tank surface in the presence of a 30 cm thick spherical layer of tissue placed at 30 cm from the surface (Case 1a) was computed to be

$$\bar{D}_\gamma = 3.28 \times 10^{-13} \frac{\text{rad}}{\text{fission}}$$

Hence, comparison between Cases 1 and 1a shows that the presence of the spherical layer of tissue increases the gamma ray dose by approximately 7% and the neutron dose by about 20%. The effect on the gamma to neutron dose ratio is less than 10%. However, the real effect of the human body can be considered negligible since the fraction of neutrons leaking from the core and incident on the body placed against the tank is less than 13% when the body is assumed to be a right cylinder of 15 cm. in radius. This fraction decreases as the distance from the body to the tank increases.

The gamma ray to neutron dose ratio that will be used in subsequent calculations is evaluated as follows:

In the initial configuration (Case 2), the first collision neutron dose at the surface of the equivalent sphere is estimated to be (using the results presented in Appendix B-2)

$$\bar{D}_n^{(1)} = 1.50 \times 10^{-9} \frac{\text{rad}}{(\text{n/cm}^2)} \times 1.21 \times 10^{-4} \frac{\text{n/cm}^2}{\text{core fission}} = 1.81 \times 10^{-13} \frac{\text{rad}}{\text{fission}}$$

and therefore,

$$\frac{D_\gamma}{D_n^{(1)}} = 1.75 \text{ (initial configuration).}$$

Similarly, for the final configuration (Case 3),

$$\bar{D}_n^{(1)} = 1.50 \times 10^{-9} \frac{\text{rad}}{\text{n/cm}^2} \times 1.63 \times 10^{-4} \frac{\text{n/cm}^2}{\text{core fission}}$$

$$\bar{D}_n^{(1)} = 2.45 \times 10^{-13} \frac{\text{rad}}{\text{fission}}$$

and therefore,

$$\frac{D_\gamma}{D_n^{(1)}} = 1.34 \text{ (final configuration)}$$

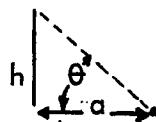
Gamma Dose From Fission Products in Drain Line

The Supervisor and Superintendent drained the mixture from the carbonate tank into gallon bottles. The radiation levels in the vicinity of the column are estimated below. The extraction column from which the liquid was drained, on the first floor, has a length of 250 cm and a diameter of 7.62 cm. It contained 11.4 liters. Assuming that this was filled with solution from the tank, it contained a fraction equal to  $11.4/52 = 0.22$  of the original reacting liquid and, it is assumed, of the fission products from the original burst. Using the fission product emission data given in Goldstein (Figure 8.10) at  $1-3/4$  hr. = 6300 seconds one obtains  $5 \times 10^{-5}$  Mev/sec.-fission. Thus, for an initial excursion of  $10^{17}$  fissions, 6300 seconds prior, the activity in the column is

$$S_L = \frac{10^{17} \times 5 \times 10^{-5} \times .22}{250} = 4.4 \times 10^9 \text{ Mev/cm-sec.}$$

Rockwell (Reference 30, Appendix C) presents an equation for the flux from a line source assuming no absorption of gammas

$$\bar{\Phi} = \frac{S_L}{4\pi a} F(\theta, 0)$$



where "a" is the distance from the base of the line source to the detector and  $\theta = \arctan \frac{h}{a}$  where "h" is the height of the line source.

For  $a = 305$  cm (10') using the graph on page 385 of Reference 30, Appendix C., one obtains

$F(40^\circ, 0) = 0.7$ . Then  $\bar{\Phi} = 8 \times 10^5$  Mev/cm<sup>2</sup>-sec. and the dose, using the conversion factor

1 R/hr =  $5.854 \times 10^5$  Mev/cm<sup>2</sup>-sec. is

$$D\dot{\gamma} = 1.41 \text{ rad/hr.}$$

At 1 foot from the column the dose will be a factor of 23.2 higher or 32.7 rad/hr. For this position the assumption of a line source with no absorption yields a slightly high dose.

For the second excursion the material in the column represents a fraction of the total fission products equal to  $11.4/41 = 0.27$ . Assuming the second burst had  $2 \times 10^{16}$  fissions and using the fission product emission rate of

$$\frac{.62}{1+t} \text{ Mev/sec.-fission (Reactor Handbook, page 27)}$$

the source strength after 120 seconds would be

$$\frac{2 \times 10^{16} \times .27 \times .62}{121 \times 250} = 1.1 \times 10^{11} \text{ Mev/sec.-cm}$$

and the dose rate at 10', scaling the previous result would be 35 R/hr. At 1' the rate would be 810 R/hr.

Since the draining took place over a period of 20 minutes, the doses from the second excursion should be integrated over the period of time from 2 to 20 minutes. If this is done using a  $1/t$  time dependence, then the total dose received is the initial rate multiplied by 0.128 or

$$\text{at } 10' \quad D_{2-20} = 4.5 \text{ R}$$

$$\text{at } 1' \quad D_{2-20} = 104 \text{ R}$$

It is possible that draining did not start until 6 minutes after the second excursion in which case the integrated dose between 6 and 20 minutes would have been

$$\text{at } 10' \quad D_{6-20} = 1.4 \text{ R}$$

$$\text{at } 1' \quad D_{6-20} = 32 \text{ R}$$

#### Dose at Tank Surface Due to Fission Product after 6300 Seconds (1-3/4 hr)

Calculations have been performed to determine the gamma dose at the center of the side wall of the cylindrical tank at 6300 seconds after  $10^{17}$  fissions. The fission product spectrum due to Perkins and King (Goldstein - Figure 8.10) for this time was used.

| <u>E <math>\gamma</math></u> | <u>Mev/sec.</u>                       |
|------------------------------|---------------------------------------|
| .25                          | $.35 \times 10^{-5}$                  |
| .65                          | $1.7 \times 10^{-5}$                  |
| 1.12                         | .8                                    |
| 1.57                         | 1.2                                   |
| 2.0                          | .5                                    |
| 2.4                          | .4                                    |
| 3.0                          | .18                                   |
|                              | <hr/>                                 |
|                              | $5.1 \times 10^{-5} \text{ Mev/sec.}$ |

Applying the geometrical formula for leakage from a cylinder due to Rockwell (Page 360) (Reference 30, Appendix C) the total dose rate is calculated to be 800 R/hr. when the attenuation in the 1/8" steel wall is accounted for.



## CONVERSION OF ACTIVATION MEASUREMENTS TO TOTAL INCIDENT DENSITY

### 1. General Relations

#### a. Determination of the Neutron Flux at the Sample

Samples are analyzed for activation products and measurements are made on either a given gamma ray or beta radiation emitted by the activated isotope which decays with a half life  $T_{1/2}$ . These measurements may then be converted into the number of atoms produced in the irradiation,  $N_B$ , after use of the appropriate correction factors that are given in Appendix A.

The number of atoms of the isotope,  $N_A$ , which produce a particular activation is obtained by spectrographic analysis of the sample and the knowledge of the abundance of the isotope in the natural element. Hence, one may write that

$$\frac{N_B}{N_A} = \int_0^{\infty} \sigma(E) \varphi(E) dE \quad (\text{B-5-1})$$

where  $\sigma(E)$  is the reaction activation cross section and  $\varphi(E)$  the time integrated flux seen by the sample.

Two types of neutron reactions are considered in the following analysis when the activation is due essentially to thermal neutrons and when the activation is due to fast neutrons above a threshold energy,  $E_T$ .

#### (1) Essentially Thermal Activation Reaction

Then Equation B-5-1 can be written as

$$\frac{N_B}{N_A} = \bar{\varphi}_{th} \sigma_{th} + \int_{non\ th} \varphi(E) \sigma(E) dE \quad (\text{B-5-2})$$

and introducing the thermal self shielding factor through

$$\bar{\varphi}_{th} = f \bar{\varphi}_{oth},$$

may be written as

$$\frac{N_B}{N_A} = \bar{\varphi}_{oth} \sigma_{th} \left[ f + f \frac{\int_{non\ th} \varphi(E) \sigma(E) dE}{\bar{\varphi}_{th} \sigma_{th}} \right] \quad (\text{B-5-3})$$

where  $\bar{\varphi}_{oth}$  is the maxwellian thermal flux at the sample in the absence of thermal neutrons self shielding in the sample and  $\sigma_{th}$  is the maxwellian averaged thermal activation cross section.

In most cases, the non-thermal contribution is negligible and  $\bar{\varphi}_{\text{oth}}$  may be evaluated if  $f$  and  $\sigma_{\text{th}}$  are known. Sometimes the resonance region contribution to the activation is not negligible as in the case of gold. It will be shown, then, that a correction factor can be evaluated.

## (2) Threshold Reactions

For threshold reactions Equation B-5-1 can be written

$$\frac{N_B}{N_A} = \int_{E_T}^{\infty} \sigma(E') \varphi(E') dE' \quad (\text{B-5-4})$$

To determine the flux required to produce a given activation, one desires an effective cross section,  $\bar{\sigma}_E$ , such that

$$\int_E^{\infty} \varphi(E') dE' = \frac{\int_{E_T}^{\infty} \sigma(E') \varphi(E') dE'}{\bar{\sigma}_E} \quad (\text{B-5-5})$$

The usual approach is to assume that, above the threshold energy, the flux spectrum at the sample is similar to a fission spectrum. Hence, if  $X_f(E)$  is the normalized fission spectrum, the effective cross section in Equation B-5-5 is given by

$$\bar{\sigma}_E = \frac{\int_{E_T}^{\infty} \sigma(E) X_f(E) dE}{\int_E^{\infty} X_f(E) dE} \quad (\text{B-5-6})$$

where we assume that  $E \geq E_T$ . The numerator of Equation B-5-6 is obtained directly by activation measurements in a GODIVA-type reactor. It was shown, however, in Appendix B-2, that such an approximation is not valid by comparing the Monte Carlo leakage flux spectra from the accident configuration to a fission spectrum.

Therefore cross section information for the fast reactions of interest (i.e.,  $S^{32}$ ,  $Ni^{58}$  and  $Fe^{54}$  (n, p) reactions) was obtained and the point values were averaged over the calculated leakage flux spectrum. This, however, assumes that the fast leakage flux spectrum has the same shape with and without a body present. It will be shown that this assumption is reasonable. Results on cross sections are presented in Section 2 of this Appendix.

b. Relation of the Neutron Flux to the Total Neutron Uncollided Current Density Incident on the Sample

To translate from neutron fluxes to total neutron current density incident on the sample,  $J_S$ , several methods may be used depending on the type of situation.

- The sample (screwdriver, clamps) is isolated.
- The sample (film badge, hair) is located on the body surface.
- The sample (blood sodium activation, whole body sodium activation) is taken from the human body.

Each of these methods will be treated in the following sections.

(1) Isolated Sample

The incident neutron current is related to the angular flux as follows:

$$J_+(E) = \int_0^1 \omega(E) \varphi(E, \omega) d\omega \quad (B-5-7)$$

or

$$J_+(E) = \bar{\omega}(E) \varphi(E) \quad (B-5-8)$$

where  $\bar{\omega}(E)$  is some appropriately averaged value of the cosine of the angle at which neutrons of energy  $E$  are incident on the sample.

A subsequent average over the energy group,  $g$ , yields

$$J_{+,g} = \bar{\omega} \varphi_g \quad (B-5-9)$$

If  $j_{+,g}$  is the fraction of the leakage current from the core (Appendix B-2) found in energy group  $g$ , and  $J_S$  is the total uncollided current integrated over all energies and incident on the sample,

$$J_S = \frac{\text{number of neutrons leaking}}{4\pi R^2}$$

then

$$J_{+,g} = f_g(R) j_{+,g} J_S \quad (B-5-10)$$

where  $f_g(R)$  is a correction factor for the contribution of neutrons scattered from the walls and floor in energy group  $g$  at distance  $R$  from the center of the tank.

Introducing Equation B-5-9 into Equation B-5-8 yields

$$J_S = \bar{\omega}_g \frac{\varphi_g}{f_g(R) j_{+,g}} \quad (B-5-11)$$

For purposes of the study,  $f_g(R)$  is taken equal to 1 for all non-thermal neutrons. An evaluation of  $f_{th}(R)$  is shown in Table B-5-7.

(2) Sample in Contact with the Human Body

The Equation B-5-9 must be written

$$\phi_g = \frac{J_{+,g}}{\bar{\omega}_g} - \frac{J_{-,g}}{\bar{\omega}'_g} \quad (B-5-12)$$

where  $J_{-,g}$  is the neutron current density in group  $g$  "reflected" from the body.

$\bar{\omega}_g$  is the average value of the cosine of the angle at which neutrons reflected from the body are incident on the sample. It will be assumed that the angular distribution of the neutrons leaving the human body is approximately semi-isotropic.

$$\bar{\omega}'_g = 0.5$$

The reflected current in group  $g$  consists of

- neutrons in group  $g$  incident on the body and reflected in the same group.
- neutrons in group  $g' < g$  (i.e., of higher energy) which slow down in the body and reflected in group  $g$ .

Then, if the albedos

$$\alpha_g = \frac{J_{-,g}}{J_{+,g}} \text{ and } b_{g',g} = \frac{J_{-,g'}}{J_{+,g}} \text{ (} g' < g \text{) are evaluated,}$$

Equation B-5-12 can be written

$$\phi_g = J_{+,g} \left[ \frac{1}{\bar{\omega}_g} + 2\alpha_g \right] + 2 \sum_{g' < g} b_{g',g} J_{+,g'} \quad (B-5-13)$$

Use of the normalized leakage current spectrum given in Appendix B-2 and Equation B-5-10 then yields the relation of the flux with the total uncollided neutron current incident on the sample.

$$\phi_g = J_S \left\{ \frac{f_g(R)}{2} j_{+,g} \left[ \frac{1}{\bar{\omega}_g} + 2\alpha_g \right] + 2 \sum_{g' < g} b_{g',g} j_{+,g'} \right\} \quad (B-5-14)$$

The factor  $f_g(R)/2$  is used because the presence of the body reduces by a factor of approximately two the contribution of room scattered thermal flux.

Hence, for fast threshold reactions, if we evaluate the flux above 3 Mev ( $g=1$ ), then  $b_{g,g} = 0$  and

$$J_S = \frac{\varphi_1}{\left(\frac{1}{\bar{\omega}_1} + 2\alpha_1\right) j_{+,1}} \quad (\text{B-5-15})$$

where

$$\varphi_1 = \int_3^{\infty} \varphi(E) dE \quad (\text{B-5-16})$$

For thermal reactions, we define a non-thermal albedo,  $b$ , and

$$J_S = \frac{\varphi_{\text{oth}}}{\frac{1}{2} f_{\text{th}}(R) j_{+, \text{th}} \left(\frac{1}{\bar{\omega}_{\text{th}}} + 2\alpha_{\text{th}}\right) + 2j_{+, \text{non th}} b} \quad (\text{B-5-17})$$

where  $j_{+, \text{non th}} = 1 - j_{+, \text{th}}$ .

### 3. Sample Taken from the Body Volume

The method is based on the following assumptions:

- the activated isotope is initially uniformly distributed in the body.
- the reaction is essentially thermal.
- the body can be replaced by a cylindrical phantom of radius,  $R_0$ , and the incident neutrons form a beam normal to the cylindrical axis.

Let  $\mu_a$  = Maxwell average thermal cross section of the body, ( $\text{cm}^{-1}$ ).

$V_{\text{man}}$  = Body volume

$A_{\text{man}}$  = Body area projected on a surface normal to the beam.

$\alpha(E)$  = the probability that a neutron of energy  $E$  will be captured as a thermal neutron in the human body.

Then the total number of neutrons incident on the body and captured as thermal neutrons is equal to the total number of thermal neutron absorptions in the body.

$$\int_0^{\infty} \alpha(E) j_+(E) A_{\text{man}} dE = \bar{\psi}_{\text{oth}} \bar{\mu}_a V_{\text{man}} \quad (\text{B-5-18})$$

where  $\bar{\psi}_{\text{oth}}$  is the thermal flux derived from the activation measurements. Using Equation B-5-10

$$\int \alpha(E) j_+(E) dE = \left[ \alpha_{\text{th}} f_{\text{th}} (R) j_{+, \text{th}} + \int \alpha(E) j_+(E) dE \right] J_S \quad (\text{B-5-19})$$

non th

where  $j_+(E)$  is the uncollided normalized incident current. The quantity in brackets is the number of absorptions per uncollided neutron incident on the body. It can be greater than unity because of the contribution of the scattered thermal neutrons. Denoting this quantity by  $\bar{a}$ , then the total uncollided neutron current density incident on man is given by

$$J_S = \frac{\mu_a}{\bar{a}} \frac{V_{\text{man}}}{A_{\text{man}}} \bar{\psi}_{\text{oth}} \quad (\text{B-5-20})$$

Then 2,200 meter cross section assuming unit density for the body and the elemental abundance in the standard man has been calculated by Hurst, et al, (Reference 31, Appendix C) and is equal to  $.02339 \text{ cm}^{-1}$ . Hence

$$\mu_a = \frac{\sqrt{\pi}}{2} \times .02339 = .0206 \text{ cm}^{-1}$$

It is customary to assume  $R_o = 15 \text{ cm}$ . Then

$$\frac{V_{\text{man}}}{A_{\text{man}}} = \frac{\pi R_o^2 h}{2 R_o h} = \frac{\pi}{2} \times R_o = 23.56 \text{ cm}$$

Then Equation (B-5-20) becomes

$$J_S = 0.4853 \frac{\bar{\psi}_{\text{oth}}}{\bar{a}} \quad (\text{B-5-21})$$

b. Conclusions

The preceding analysis shows that the activation measurements can be converted to total uncollided current density incident on the sample if the following factors are evaluated properly.

- Thermal activation cross sections,  $\bar{\sigma}_{th}$ .
- Self shielding correction factors.
- Non thermal contribution to the thermal activation.
- Effective cross sections for fast reactions  $\bar{\sigma}_E$ .
- Average cosine of the neutron incidence angle,  $\bar{\omega}$ .
- Thermal and Fast albedos,  $\alpha_{th}$  and  $\alpha_1$ .
- Non thermal to thermal albedo,  $b$ .
- Average thermal absorption probability for total incident neutrons,  $\bar{a}$ .
- Correction factor for contribution of scattered thermal neutrons,  $f_{th}$ .

The calculations of these factors are described in Section 2 following except for the second and third items (Self-Shielding and Non-Thermal Contribution) which were considered in specific cases.

## 2. Calculations of Various Factors

### a. Thermal Activation Cross Sections

Thermal activation cross sections are taken from BNL 325. Table B-5-1 presents data used in subsequent calculations.

TABLE B-5-1  
Thermal Activation Cross Sections

| Nuclide           | 2,200m Cross Section (barns) | Maxwell Averaged Cross Section $\phi_{th}$ (barns) |
|-------------------|------------------------------|--|
| Na <sup>23</sup>  | 0.536                        | 0.475  |
| Cr <sup>50</sup>  | 13.5                         | 12.0   |
| Fe <sup>58</sup>  | 1.0                          | 0.8865   |
| Ag <sup>109</sup> | 3.2                          | 2.84   |
| In <sup>113</sup> | 56                           | 49.6   |
| Au <sup>197</sup> | 100                          | 88.7   |

### b. Effective Cross Sections Threshold Reactions

The (n, p) reactions in S<sup>32</sup>, Ni<sup>58</sup> and Fe<sup>58</sup> are used in the activation measurements. It was evident from a comparison of the leakage flux spectra evaluated by the SANE Monte Carlo code with a fission flux spectrum that the validity of using fission spectrum averaged cross section was questionable. (See Figure B-2-B). Hence activation cross sections for the accident analysis were computed directly from the basic cross section data using the SANE leakage spectra (See Appendix B-2) and compared to calculated and measured fission spectrum averaged activation cross sections.

Cross section information for the (n, p) reaction in S<sup>32</sup>, Ni<sup>58</sup> and Fe<sup>54</sup> is presented in Figures B-5-A, B-5-B and B-5-C on Pages B-5.10, B-5.11 and B-5.12. In the case of Fe<sup>54</sup>(n, p) Mn<sup>54</sup> reaction, the data is clearly insufficient. However, for S<sup>32</sup> and Ni<sup>58</sup> sufficient cross section data is available to give a good degree of reliability.

Table B-5-2 presents computed effective cross sections,  $\sigma_o$ .

$$\sigma_o = \int_0^{\infty} \sigma(E) \phi_N(E) dE \quad (B-5-22)$$

where  $\phi_N(E)$  is the normalized flux spectrum.



In subsequent calculations, it will be assumed that the incident flux is not perturbed by the presence of the body for fast neutrons ( $E \geq 1$  Mev). Hence, fast neutron flux above energy  $E$  can be computed directly from Equation B-5-5 using the effective cross section

$$\bar{\sigma}_E = \bar{\sigma}_o \times \frac{1}{\int_E^\infty \phi_N(E) dE} \quad (B-5-23)$$

TABLE B-5-2

Activation Cross Section (millibarns),  $\sigma_o$

|                        | 1  | 2   | 3  | 4  |
|------------------------|----|-----|----|----|
| $S^{32}(np), p^{32}$   | 45 | 57  | -- | 65 |
| $Ni^{58}(np), Co^{58}$ | 60 | 115 | 99 | 91 |
| $Fe^{54}(np), Mn^{54}$ | 49 | 101 | 65 | -- |

1. Cross section averaged over spectrum obtained from "SANE".
2. Cross section averaged over fission spectrum ANL 5800, Table 1-11
3. Cross Section used by AEC Idaho Falls in activation calculations. "Radiochemical Analysis of the UNC Incident at Wood River Junction, Rhode Island", D. G. Olson, September 17, 1964.
4. NSE 10, 4, 308 (fission spectrum averaged)

Table B-5-3 presents the effective cross sections for  $E = 3$  Mev, 1.4 Mev and 0.9 Mev.

TABLE B-5-3

Effective Cross Section Averaged Over the Fast Neutron Flux,  $\bar{\sigma}_E$  (in barns)  
(Note 1)

|                         | $\bar{\sigma}_3$ | $\bar{\sigma}_{1.4}$ | $\bar{\sigma}_{0.9}$ |
|-------------------------|------------------|----------------------|----------------------|
| $S^{32}(n,p), p^{32}$   | .398             | .141                 | .113                 |
| $Ni^{58}(n,p), Co^{58}$ | .531             | .188                 | .150                 |
| $Fe^{54}(n,p), Mn^{54}$ | .442             | .157                 | .125                 |

(Note 1)  $\bar{\sigma}_E$  is defined as follows:

$$\bar{\sigma}_E = \frac{\int_0^\infty \bar{\sigma} \phi dE}{\int_E^\infty \phi dE}, \quad E \text{ in Mev}$$

FIGURE B-5-A

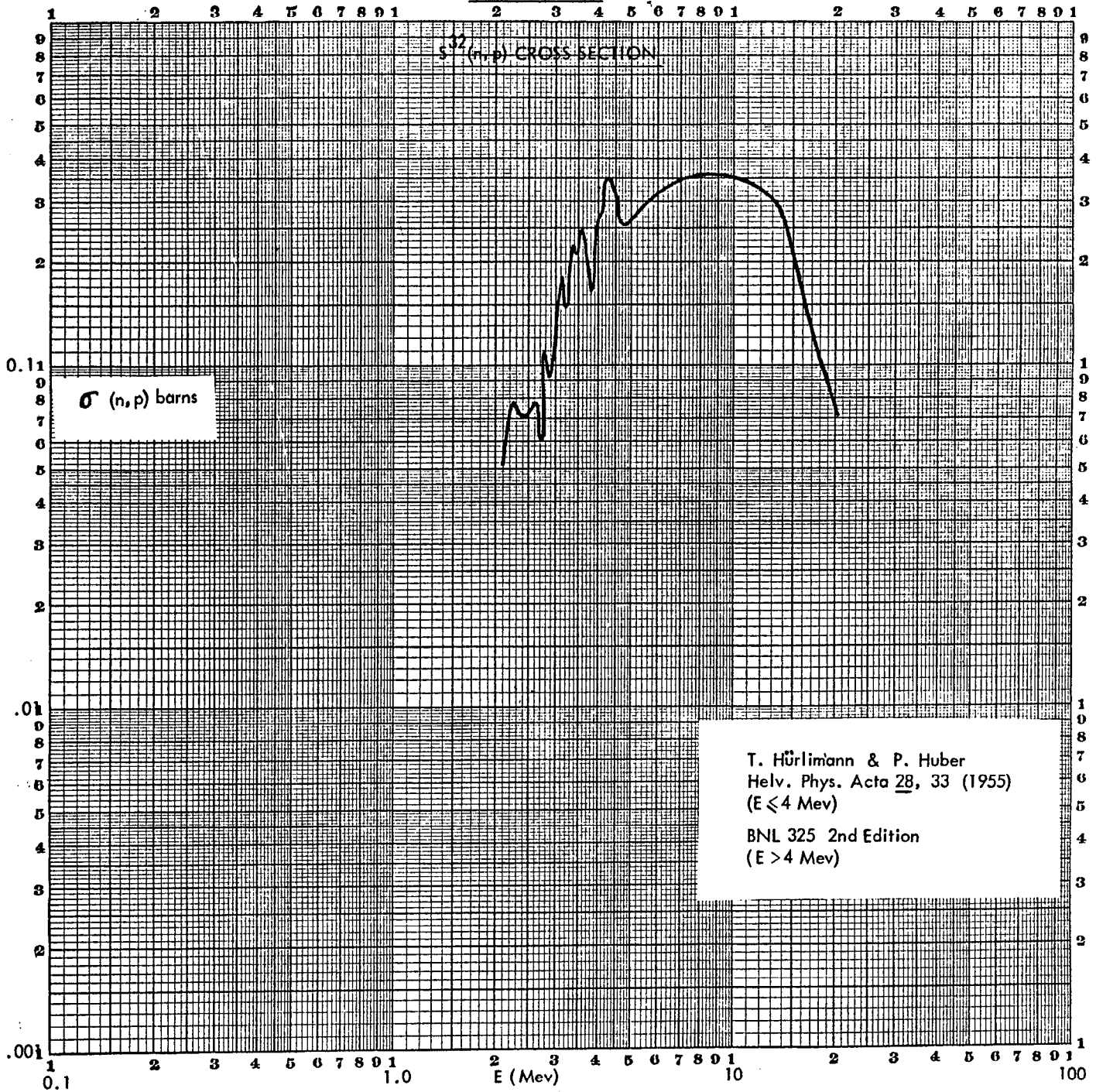


FIGURE B-5-B

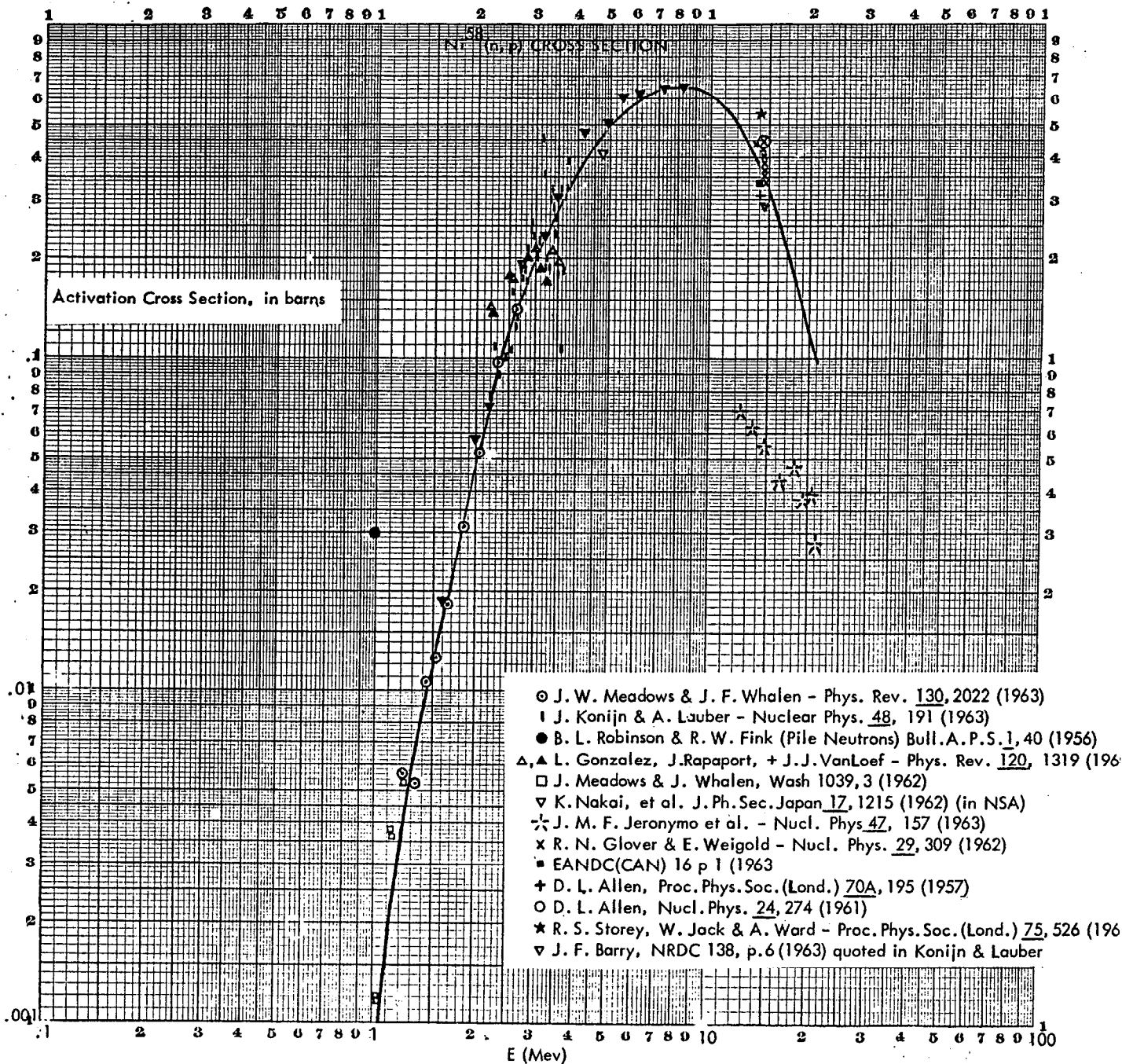
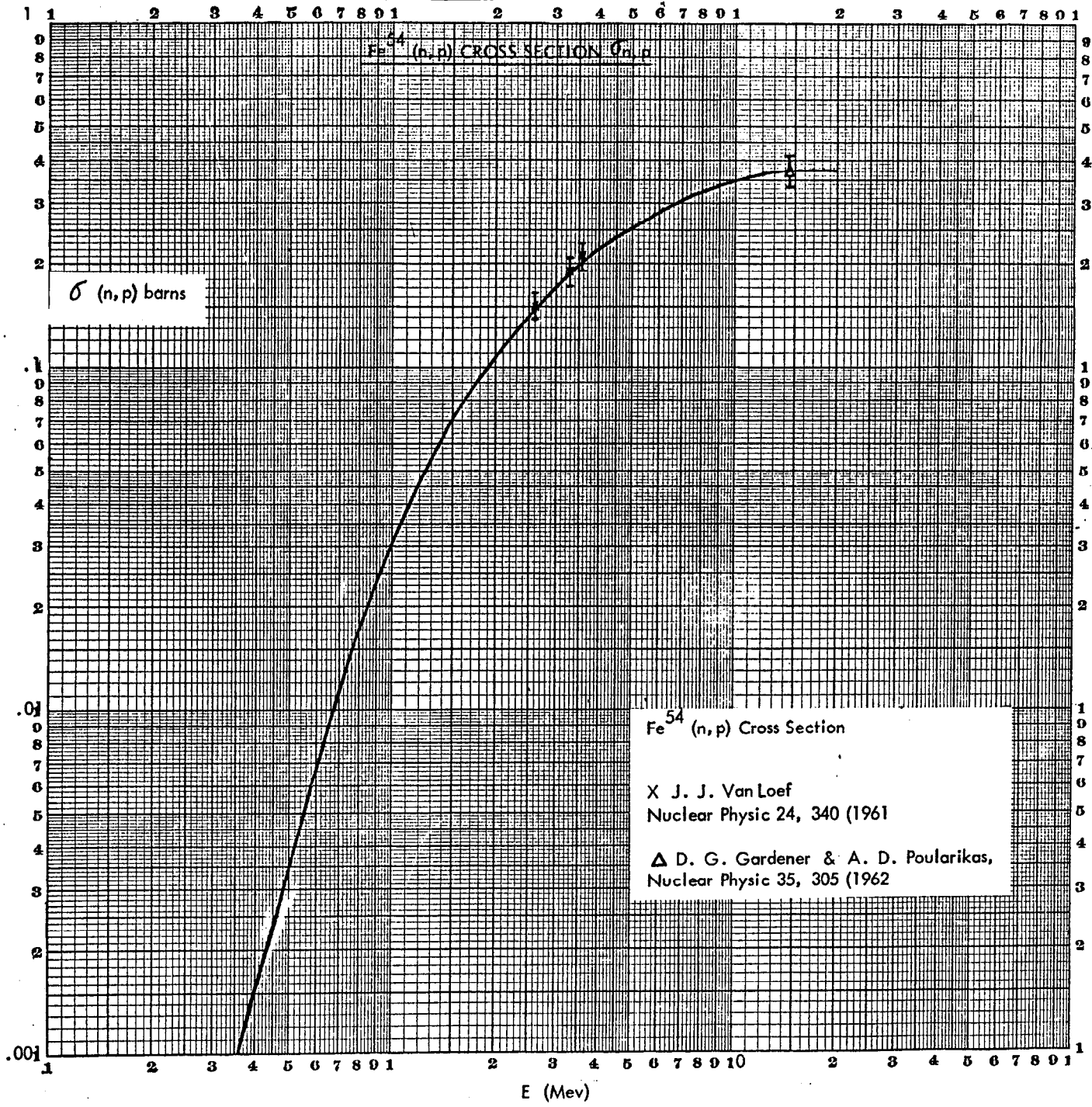


FIGURE B-5-C



c. Evaluation of the Average Cosine of the Neutron Incidence Angles

The output of the 16-group one dimensional transport calculations gives currents and fluxes averaged over the angular distribution in each energy group at the outer surface of a pre-determined region.

Table B-5-4 presents the values of  $\bar{\omega}_g$  at the outer surface of the core and at 10 feet from the core for the fast and thermal energy groups. The value of  $\bar{\omega}_g$  is insensitive to the core model and variations of  $\bar{\omega}_g$  with energy are negligible. In conclusion,  $\bar{\omega}_g$  depends strongly on the location at which flux and current are evaluated. Near the outer surface of the core, the angular distribution is not too far from the semi-isotropic angular distribution ( $\omega = .5$ ). As the distance from the tank increases, the angular distribution tends to become normal.

In calculations concerning the superintendent and the supervisor which are thought to have been standing 15 feet away from the tank, we will assume that the neutrons are normally incident on the body,  $\omega_g = 1$ .

TABLE B-5-4  
Average Cosine of the Neutron Incidence Angles

| Group            | Energy Range<br>(Mev) | $\omega_g = \frac{J_{+,g}}{\varphi'_{,g}}$ |            |
|------------------|-----------------------|--|------------|
|                  |                       | At Core Surface                            | At 10 Feet |
| 1                | $E > 3$               | .67  | .86        |
| 2                | $3 > E < 1.4$         | .66  | .86        |
| 3                | $1.4 > E > .9$        | .62  | .86        |
| $\sum_{g=1,2,3}$ | $E > .9$              | .65  | .86        |
| 16               | Thermal               | .60  | .84        |

d. Fast and Thermal Albedo Calculations

Cases 1a and 1b described in Appendix B-2 were used to evaluate the reflected to incident current ratio at the body surface in a given energy group. In the high neutron energy range, contribution from slowing down neutrons to the reflected current is expected to be negligible and therefore, these ratios give a good estimate of the albedos,  $\alpha_g$ . Fast neutron albedos are given in Table B-5-5 for the neutrons of energy higher than 1 Mev. It can be seen that a small percentage of neutrons are reflected back above 3 Mev. As the energy decreases, the albedo increases, but the calculations become less reliable because of the man model used in the calculations. Indeed, use of a spherical layer of tissue makes it possible to have a high energy neutron be reflected back from some point of the spherical shell of tissue and be incident on another point with its energy in the range considered.

If we note that the albedo  $\alpha$  should not depend on the placement of the spherical shell of tissue with respect to the spherical core, comparison between Case 1a and Case 1b shows that the results obtained in group 3 ( $0.9 < E < 1.4$  Mev) are already not very reliable. Therefore, only albedos in Group 1 and 2 will be used.

TABLE B-5-5  
Evaluation of Fast Neutron Albedos,  $\alpha_g$

| Group | Energy Range (Mev) | $\alpha_g = \frac{J_{-,g}}{J_{+,g}}$ |         |
|-------|--------------------|--------------------------------------|---------|
|       |                    | Case 1a                              | Case 1b |
| 1     | $E > 3$            | .036                                 | .037    |
| 2     | $3 > E > 1.4$      | .051                                 | .059    |
| 3     | $1.4 > E > .9$     | .090                                 | .112    |

The probability that a thermal neutron incident on the body is reflected back is known to be 0.80 (NBS Handbook 63).

$$\alpha_{th} = 0.80$$

e. Evaluation of the Non Thermal to Thermal Neutron Current Albedo-b.

As previously described (Appendix B-5, Section 1) the back thermal current density,  $J_{-,th}$ , is due to direct thermal albedo ( $\alpha_{th} \times J_{+,th}$ ) and to a non-thermal - thermal albedo whereby non thermal neutrons enter the body, become thermal inside the body and leave as thermal neutrons.

By arguments presented below, the non-thermal to thermal albedo, b, is estimated to be about 0.14,

$$b \approx 0.14$$

The argument runs as follows. The albedo b depends only on the spectrum of non-thermal neutrons incident on the body. Further, the non-thermal incident spectrum should be close to the non-thermal leakage spectrum from a bare reactor; in other words, the presence of the man is assumed to have a negligible effect on the non-thermal spectrum incident on him.

Thus, what is desired is the fast-thermal albedo of a thick water layer for a leakage spectrum corresponding to the bare core Case 1 calculation of Appendix B-2. But the albedo for this case cannot be obtained from the UND DTF calculations because there is no water reflector present. However, the fast-thermal albedo can be obtained from the UND DTF printouts for Cases 1a and 1b. Case 1a has a 30 cm. thick spherical water shell placed 30 cm. from the core. Case 1b places

the same man model in contact with the core. The non-thermal spectrum incident on the man are given in Table B-5-6. In Case 1, it is simply the leakage spectrum. In Cases 1a and 1b, it is the spectrum incident on the man model.

It is seen from the table that the appropriate spectra form closely an arithmetic progression proceeding from Case 1a to Case 1b to 1. The albedo values,  $b$ , are therefore assumed to form an arithmetic progression. The albedos in Cases 1a and 1b are obtained from the equation

$$J_{-th} = 0.80 J_{+th} + b J_{+non\ th}$$

using the printout values for the  $J$ 's at the surface of the 30 cm. thick spherical shell. The results are that

$$b = 0.20 \text{ in Case 1a}$$

$$b = 0.17 \text{ in Case 1b}$$

from which it follows from the above arguments that for Case 1

$$b = 0.14.$$

TABLE B-5-6

Non-Thermal Spectrum Incident in Man in Cases 1, 1a, 1b Values Given Are Normalized to One Non-Thermal Neutron Leaving the Core

| Non-Thermal Group Number, g | Case 1 | Case 1a | Case 1b |
|-----------------------------|--------|---------|---------|
| 1                           | .13    | .09     | .10     |
| 2                           | .24    | .17     | .19     |
| 3                           | .092   | .07     | .079    |
| 4                           | .12    | .10     | .11     |
| 5                           | .12    | .10     | .10     |
| 6                           | .075   | .070    | .070    |
| 7                           | .049   | .053    | .050    |
| 8                           | .043   | .051    | .046    |
| 9                           | .040   | .051    | .044    |
| 10                          | .028   | .036    | .031    |
| 11                          | .025   | .033    | .028    |
| 12                          | .026   | .036    | .030    |
| 13                          | .023   | .033    | .027    |
| 14                          | .019   | .027    | .023    |
| 15                          | .045   | .084    | .063    |

Accurate calculations by stochastic methods (Reference 32, Appendix C) in 30 cm. thick tissue slab show that approximately 70% of the non-thermal neutrons incident on the slab are slowed down to thermal and somewhat under 60% of the non-thermal incident neutrons are captured as thermal neutrons in slab geometry. Hence, one estimates that in the neighborhood of 10% of the non-thermal incident neutrons come out as thermal neutrons.

f. Correction Factor for Scattered Thermal Neutrons

Since the albedo of thermal neutrons in the concrete walls and floor is high, the thermal fluxes fall much less rapidly with the distance from the tank than the non-thermal fluxes. The relative fast-to-thermal fluxes have been evaluated for the isolated sample activation measurements. The activated-to-target atom ratios  $\frac{N^*}{N_T}$  are given in Table A-7-1, Appendix A-7. Thermal cross sections are presented in Table B-5-1. Effective cross sections to evaluate fluxes of neutrons above 3 Mev are given in Table B-5-3. Using the data, thermal and above-3-Mev fluxes are calculated and given in Tables B-5-7 and B-5-8. Ratios of thermal to fast fluxes appear in Table B-5-9.

TABLE B-5-7

Maxwell Average - Thermal Fluxes

| Item   | Analysis  | Laboratory | $\bar{\phi}_{th}$ (n/cm <sup>2</sup> ) |
|--|---|------------|--|
| Screwdriver<br>(Tank Surface)                      | $\frac{Fe^{58}(n,\gamma)Fe^{59}}{(chem. Sep.)}$ | AEC-ID     | $5.40 \times 10^{12}$                  |
|  | (scanned)                                       | AEC-ID     | $5.35 \times 10^{12}$                  |
|  | (scanned)                                       | UNC-P      | $7.72 \times 10^{12}$                  |
| Stainless Steel<br>Clamp<br>(9" From<br>Surface)   | $\frac{Fe^{58}(n,\gamma)Fe^{59}}{(chem. sep.)}$ | AEC-ID     | $3.68 \times 10^{12}$                  |
|  | $\frac{Cr^{50}(n,\gamma)Cr^{51}}{(chem. sep.)}$ | AEC-ID     | $2.43 \times 10^{12}$                  |
|  | (scanned)                                       | UNC-P      | $1.59 \times 10^{12}$                  |
| Stainless Steel<br>Clamp<br>(174" From<br>Surface) | $\frac{Fe^{58}(n,p)Fe^{59}}{(scanned)}$         | AEC-ID     | $2.75 \times 10^{11}$                  |
|  | $\frac{Cr^{50}(n,\gamma)Cr^{51}}{(scanned)}$    | AEC-ID     | $1.34 \times 10^{11}$                  |
|  | (scanned)                                       | UNC-P      | $.86 \times 10^{11}$                   |



TABLE B-5-8

## Fast Neutron Fluxes Above 3 Mev

| Item                                      | Analysis  | Laboratory | $\bar{\phi}_1$ (n/cm <sup>2</sup> ) |
|---|---|------------|-------------------------------------|
| Screwdriver (Tank Surface)                | <u>Fe<sup>54</sup>(n, p)Mn<sup>54</sup></u><br>(scanned)    | AEC-ID     | 3.53 x 10 <sup>12</sup>             |
|   | (chem. sep.)  | AEC-ID     | 2.83 x 10 <sup>12</sup>             |
|   | (scanned)   | UNC-P      | 3.80 x 10 <sup>12</sup>             |
| Stainless Steel Clamp<br>(9" From Tank)   | <u>Fe<sup>54</sup>(n, p)Mn<sup>54</sup></u><br>(chem. sep.) | AEC-ID     | 8.24 x 10 <sup>11</sup>             |
|   | <u>Ni<sup>58</sup>(n, p)Co<sup>58</sup></u><br>(chem. sep.) | AEC-ID     | 10.00 x 10 <sup>11</sup>            |
|   | <u>Ni<sup>58</sup>(n, p)Co<sup>58</sup></u><br>(scanned)    | UNC-P      | 8.81 x 10 <sup>11</sup>             |
| Stainless Steel Clamp<br>(174" From Tank) | <u>Fe<sup>54</sup>(n, p)Mn<sup>54</sup></u><br>(scanned)    | AEC-ID     | 2.40 x 10 <sup>10</sup>             |
|   | <u>Ni<sup>58</sup>(n, p)Co<sup>58</sup></u><br>(scanned)    | AEC-ID     | 3.54 x 10 <sup>10</sup>             |
|   | <u>Ni<sup>58</sup>(n, p)Co<sup>58</sup></u><br>(scanned)    | UNC-P      | 1.00 x 10 <sup>10</sup>             |

TABLE B-5-9

Thermal to Above 3 Mev Flux Ratios and Correction Factors,  $f_{th}$ 

| Item  | Laboratory | R    | $\bar{\varphi}_{th}/\bar{\varphi}_1$ | $f_{th}(R)$ | Average $f_{th}(R)$ |
|---|------------|------|--------------------------------------|-------------|---------------------|
| Screwdriver<br>(chem. sep.)<br>(scanned)<br>(scanned) | AEC-ID     | 9"   | 1.91                                 | 2.89        | 2.75                |
|   | AEC-ID     |      | 1.52                                 | 2.30        |                     |
|   | UNC-P      |      | 2.03                                 | 3.07        |                     |
| Stainless Steel Clamp<br>at 9"                        | AEC-ID     | 18"  | 4.47                                 | 6.77        | 4.3                 |
|   | AEC-ID     |      | 2.43                                 | 3.68        |                     |
|   | UNC-P      |      | 1.80                                 | 2.72        |                     |
| Stainless Steel Clamp<br>at 174"                      | AEC-ID     | 183" | 11.46                                | 17.3        | 23.                 |
|   | AEC-ID     |      | 26.42                                | 40.         |                     |
|   | UNC-P      |      | 8.60                                 | 13.         |                     |

By definition, the correction factor  $f_{th}(R)$  is the ratio of the thermal flux at the sample to that from the uncollided radiations. Since no correction is being made for the fast fluxes, we have

$$f_{th}(R) = \frac{\left[ \frac{\bar{\varphi}_{th}}{\bar{\varphi}_1} \right]_{\text{measured}}}{\left[ \frac{\bar{\varphi}_{th}}{\bar{\varphi}_1} \right]_{\text{calculated}}}$$

$\left[ \frac{\bar{\varphi}_{th}}{\bar{\varphi}_1} \right]_{\text{calculated}}$  is evaluated from the leakage flux spectra given in Appendix B-2. It is approximately equal to 0.66. Values for  $f_{th}(R)$  are also tabulated in Table B-5-9.

However, when the sample is not isolated or inside the man but on the body surface, it sees approximately half of the thermal scattered neutrons. Therefore, the calculated factors in Table B-5-9 will be reduced by a factor of 2 when used for such samples.

g. Average Thermal Absorption Probability for Total Incident Neutrons on Body

Letting  $a(E)$  be the probability that a neutron of energy  $E$  will be captured as a thermal neutron in the human body, the spectral average absorption probability,  $\bar{a}$ , is defined as the probability that a neutron incident on the body will be absorbed thermally per uncollided neutron incident on the body.

$$\bar{a} = \int a(E) j_+(E) f(E, R) dE \quad (\text{B-5-25})$$

or

$$\bar{a} = a_{th} f_{th}(R) j_{+th} + \int_{non\ th} a(E) j_+(E) dE \quad (\text{B-5-26})$$

where  $f_{th}(R)$  is the correction factor for thermal scattered neutrons evaluated above and  $j_+(E)$  is the normalized incident current spectra given in Appendix B-2.

The table below presents values for  $a(E)$  estimated by Hurst, Ritchie and Emmerson for the case of a right cylinder of radius 15 cm. and tissue equivalent composition.

| Neutron Energy | $a(E)$ |
|----------------|--------|
| Thermal        | 0.18   |
| 5 kev          | 0.40   |
| 0.5 Mev        | 0.51   |
| 2.5 Mev        | 0.50   |
| 5 Mev          | 0.42   |
| 10 Mev         | 0.33   |

For the configurations of interest here,

$$\bar{a} = .377 + .0135 f_{th}(R)$$

If  $f_{th}(R) = 1$ ,  $\bar{a} = .39$

Table B-5-10 presents the values of  $a$  versus the distance  $R$ .

TABLE B-5-10Estimates of  $\bar{a}$ 

| R    | $f_{th}(R)$ | $\bar{a}$ |
|------|-------------|-----------|
| 9"   | 2.75        | 0.414     |
| 18"  | 4.3         | 0.435     |
| 183" | 23.         | 1.245     |

## BIBLIOGRAPHY

- | Reference | Description   |
|-----------|---|
| 1         | G. S. Hurst, et al., "Accidental Radiation Excursion of the Oak Ridge Y-12 Plant III", Health Physics, Pergamon Press 1959, Vol. 2, pp. 121-123.  |
| 2         | J. A. Auxier, "Dosimetric Considerations in Criticality Exposures", Diagnosis and Treatment of Acute Radiation Injury, 1961, Geneva, World Health Organization, pp. 141-150.                      |
| 3         | J. A. Auxier, et al., " $\text{Na}^{24}$ Activation in the Dosimetry of Nuclear Accidents", Radioactivity in Man, C. C. Thomas, Editor, 1961.   |
| 4         | F. W. Sanders and J. A. Auxier, "Neutron Activation in Anthropomorphic Phantoms", Health Physics, Pergamon Press, Vol. 8, pp. 371-379.  |
| 5         | W. L. Allison, et al., "Nuclear Incident at United Nuclear Corporation, Wood River Junction, Rhode Island, September 14, 1964.  |
| 6         | Letter from John M. McGreevy, Director, State Council of Defense, Scituate, Rhode Island, September 14, 1964.   |
| 7         | Letter from Carl R. Wilson, NSEC, to F. R. Nakache, UNC, September 14, 1964.  |
| 8         | Letter from Carl R. Wilson, NSEC 22-11-4012, to F. R. Nakache, UNC, August 28, 1964.  |
| 9         | Verbal communication Fred F. Haywood, Health Physics Division, ORNL.  |
| 10        | W. L. Ginkel, et al., "Nuclear Incident at Idaho Chemical Processing Plant on October 16, 1959". IDO 10035, February 1960.  |
| 11        | Dale G. Olson and Claude W. Sill, "Radiochemical Analysis of the UNC Incident at Wood River Junction, Rhode Island, USAEC, Idaho Falls, September 17, 1964.                                       |
| 12        | H. Soodak, Editor: "Reactor Handbook, Vol. III, Part A, Physics", 1962. Interscience Publishers.  |
| 13        | "Accidental Radiation Excursion at the Y-12 Plant", Y-1234, June 16, 1958, Final Report.  |
| 14        | D. F. Peterson, V. E. Mitchell and W. H. Langham, "Estimation of Fast Neutron Doses in May by $\text{S}^{32}$ (n,p) $\text{P}^{32}$ Reaction in Body Hair", Health Physics 1961, Vol. 6, pp. 1-5. |
| 15        | R. D. Schamberger, "Activity of Materials from Rhode Island Accident", UNC Memoranda. Phys/Math 3634 (8/8/64), Phys/Math 3663 (8/31/64), Phys/Math 3740 (9/28/64) and Phys/Math 3797 (10/19/64).  |
| 16        | Dale G. Olson and Claude W. Sill, "Radiochemical Analysis of the UNC Incident at Wood River Junction, Rhode Island", (9/1/64).  |

| Reference | Description   |
|-----------|---|
| 17        | Carl R. Wilson, Report Letters. Re: Phys/Math 3660, Nuclear Science and Engineering Corporation 22-11-4012 (8/25/64 and 8/28/64).   |
| 18        | F. Peterson: "Sulfur Neutron Dose Estimates in the UNC Criticality Accident". LASL Phys/Math 3709. D. F. Peterson: Letter to F. R. Nakache, October 12, 1964.   |
| 19        | G. S. Hurst, R. H. Ritchie and L. C. Emerson; "Accidental Radiation Excursion Doses", Health Physics, Pergamon Press 1959, Vol. 2, pp. 121-133.   |
| 20        | "Medical Body Burden and Radiation Data in Connection with the United Nuclear Corporation Criticality Accident of July 24, 1964", October 8, 1964.  |
| 21        | NBS Handbook 63, Table 1 "Atomic Composition of the Standard Man".  |
| 22        | W. R. Stratton, LASL, Private Communication, Memo N-2, 10/28/64 to M. M. Shapiro, United Nuclear Corporation.   |
| 23        | "Production of Void and Pressure by Fission Track Nucleation of Radiolytic Gas Bubbles during Power Bursts in a Solution Reactor", P. Spiegler et al, NAA-SR-7086, December 30, 1962.                       |
| 24        | "Summary Review of the Kinetics Experiments on Water Boilers", M. S. Dunnefeld and R. K. Stitt, NAA-SR-7087, February 11, 1963.   |
| 25        | Private Communication, W. R. Stratton, Memo N-2 LASL, October 28, 1964 to M. M. Shapiro, United Nuclear Corporation.  |
| 26        | M. R. Fleishman, "A Sane-Sage Users Guide". Advanced Shield Computational Techniques, Vol. IV, UNUCOR-634, 3/18-19/63.  |
| 27        | W. S. Snyder and J. Neufeld, "On the Passage of Heavy Particles Through Tissue", Radiation Research 6, 67 (1957).   |
| 28        | TID 7004, p. 419  |
| 29        | Reactor Handbook, Second Edition, Vol. III, Part B, p. 27.  |
| 30        | Reactor Shielding Handbook TID-7004, Page 348.  |
| 31        | G. S. Hurst, R. H. Ritchie and L. C. Emerson, "Accidental Radiation Excursion of the Oak Ridge Y-12 Plant 111 - Determination of Radiation Doses", Health Physics, Pergamon Press 1959, Vol. 2, p. 121-133. |
| 32        | W. S. Snyder and J. Neufeld, ORNL (1955).   |

**UNITED NUCLEAR**  
C O R P O R A T I O N

March 31, 1965

P. O. BOX 1883  
365 WINCHESTER AVENUE  
NEW HAVEN, CONN. 06508  
777-5361

Director of Regulations  
U. S. Atomic Energy Commission  
Washington 25, D. C.

Attention: Mr. Harold L. Price

SUBJECT: Supplemental Report of the Accidental Criticality at  
Wood River Junction, Rhode Island, July 1964

Reference: United Nuclear Corporation Report Dated August 21, 1964


Gentlemen:

My transmittal letter to the referenced report which was UNC's first report of the July 24, 1964 incident mentioned that at a later date UNC planned to submit a supplemental report. The supplemental report was to concentrate on the nuclear physics investigation which we hoped would be of some interest to the nuclear community.

The attached report has now been completed and includes a significant amount of original work. Copies of this report are being sent to all recipients of the original report and we trust the contents will be of general interest.

Appreciation is again expressed to the Atomic Energy Commission personnel who have consulted and assisted in several phases of this work.

Very truly yours,

  
J. A. Lindberg  
Vice President

JAL/b